Fakultät für Medizin

Institut für Virologie

Therapeutic vaccination using MVA-vectors in a murine model of chronic HBV infection

Clemens Jäger

Vollständiger Abdruck der von der Fakultät für Medizin der Technischen Universität München zur Erlangung des akademischen Grades eines

Doktors der Naturwissenschaften

genehmigten Dissertation.

Vorsitzende(r): Univ.-Prof. Dr. P. Knolle

Prüfer der Dissertation:

1. Univ.-Prof. Dr. U. Protzer
2. Univ.-Prof. Dr. J. Durner

Die Dissertation wurde am 3. März 2015 bei der Technischen Universität München eingereicht und durch die Fakultät für Medizin am 15. Juli 2015 angenommen.

Index

Abstract

Chronic infection with the Hepatitis B virus (HBV) remains a major global health threat, which currently affects approximately 240 million individuals. Chronic Hepatitis B (CHB) patients are at risk of premature death from cirrhosis with liver failure or hepatocellular carcinoma, which causes more than 0.6 million deaths annually. Due to unsatisfactory current treatment options with interferon or nucleos(t)ide analogues, novel approaches for the treatment of CHB patients are required. CHB patients show only weak or undetectable T cell responses, whereas acutely infected patients show strong polyclonal and multispecific T cell responses that result in clearance of HBV. Therefore, the aim of the present work was to develop a therapeutic vaccination which might mount broad and strong virus-specific T cell responses in CHB patients and additionally induces specific neutralizing antibodies for viral control and clearance.

In order to develop a powerful vaccination strategy, different adjuvants (CpG, PCEP, aluminum hydroxide) were tested in protein-vaccine formulations combined with recombinant Modified Vaccinia virus Ankara (MVA) expressing the HBV antigens HBsAg or HBcAg in C57BL/6 wildtype mice in a prime-boost vaccination scheme. Recombinant MVA were previously generated by Dr. Simone Backes and further improved during this thesis. The most promising strategy was identified in a prime immunization with a protein-vaccine consisting of HBsAg and HBcAg including the adjuvants PCEP and CpG, followed by a boost immunization with MVA expressing HBcAg or HBsAg, which resulted in the successful induction of strong T cell responses against HBsAg and HBcAg as well as high amounts of the HBV-specific antibodies anti-HBs and anti-HBc. This vaccination strategy was further shown to be successful in HHDII mice, which were used as a model of human MHC-dependent antigen-presentation.

Further studies were performed in the CHB model of HBV1.3.32 transgenic (tg) mice that present peripheral immunological tolerance to HBV upon predominantly hepatic replication of HBV with the subtype ayw (HBV_{ayw}) starting around birth. This model was used to identify the most suitable combination of HBV antigens, promoters for expression of recombinant HBV-proteins by MVA as well as the vaccination scheme that induces broad immune responses against HBV. Furthermore, it was used for comparing different subtypes of HBsAg (ayw and adw) used in vaccinations. The hereby induced immune responses were examined at day 6, 14 and 56 days post final immunization. In general, the vaccination scheme including $HBsAg_{adw}$ induced higher frequencies of polyfunctional T cells against $HBsAg_{ayw}$, indicating the induction of cross-reactive T cells. HBcAg-specific T cells were mostly induced at lower frequencies. The vaccination strategy including $HBsAg_{adw}$ further induced neutralization of HBV_{ayw} by anti-HBs antibodies shown *in vitro*, supporting the hypothesis of an induction of a

cross-reactive immune response in case of HBsAg. On T cell level, the induced immune responses were detected until day 14 post boost immunization. On 56 days post boost immunization, HBsAg-levels remained significantly reduced and high levels of anti-HBs as well as anti-HBc antibodies were detected, suggesting that the established vaccination strategy had a sustained effect on humoral level in HBVtg mice. Moreover, histological analysis of liver sections showed a higher influx of B and T cells as well as proliferation of hepatocytes in HBV-vaccinated mice compared to mock-vaccinated mice.

In addition to T cell responses determined by intracellular cytokine staining, the cytolytic properties of HBV-specific T cells that were induced by vaccination were tested by *in vivo* killing assays. Eradication of splenocytes loaded with HBcAg-derived peptide in wildtype mice, which were immunized specifically against HBcAg with the established vaccination strategy, suggested that the induced T cells were not only polyfunctional in terms of secreting cytokines but were furthermore able to kill effectively their target cells.

In conclusion, the vaccination strategy established in this work was able to overcome tolerance in a mouse model of CHB and provides a promising scheme for therapeutic vaccination in future clinical trials.

Zusammenfassung

Die chronische Infektion mit dem Hepatitis B Virus (chronische Hepatitis B) stellt eine globale Bedrohung der Gesundheit dar, von der 240 Millionen Menschen derzeit betroffen sind. Patienten mit chronischer Hepatitis B haben ein erhöhtes Risiko für die Entwicklung einer Leberzirrhose oder hepatozellulärem Karzinom, welches zum Tod durch Leberversagen führen kann. Jährlich sterben etwa 600 000 Menschen an den Folgen einer chronischen Hepatitis B. Patienten werden derzeit entweder mit Nukleosid/Nukleotid-Analoga oder Interferon behandelt. Diese Therapien sind allerdings nicht zufriedenstellend, da sie das Virus nicht eliminieren und starke Nebenwirkungen haben können. Daher ist es wichtig neue Therapieansätze zu entwickeln. In den vergangenen Jahren wurde beschrieben, dass in chronischen Hepatitis B Patienten nur schwache oder keine T Zellantworten detektiert werden konnten. Im Gegensatz dazu wurde in Patienten, die eine akute Hepatitis B überstanden haben, eine starke, multispezifische T Zellantwort gefunden. Aufgrund dieser Erkenntnisse ist die Entwicklung einer therapeutischen Impfstrategie, die sowohl spezifische T Zellantworten als auch Antikörper induzieren kann, eine erfolgsversprechende Therapiemöglichkeit.

In der vorliegenden Arbeit wurden verschiedene Adjuvantien (CpG, PCEP und Aluminiumhydroxid) in Kombination mit den Hepatitis B Virus (HBV) Antigenen HBs und HBc in einer „prime-boost“ Impfstrategie mit rekombinanten „Modified Vaccinia virus Ankara“ (MVA) getestet, um eine effektive Vakzinierungsstrategie zu entwickeln. Die rekombinanten MVAs exprimierten hierbei entweder das HBsAg oder HBcAg des HBV äquivalent zu den Antigenen, die bei der „prime“-Immunisierung verwendet und von Dr. Simone Backes oder im Rahmen dieser Arbeit generiert wurden. Etabliert wurde die Impfstrategie in C57BL/6 Wildtyp-Mäusen. Als aussichtsreichste Kombination stellte sich die Verwendung von PCEP, CpG sowie HBsAg und HBcAg in der „prime“-Immunisierung sowie die Injektion von MVA-S und MVA-C in der „boost“-Immunisierung heraus, da diese Impfstrategie sowohl eine multispezifische HBV-spezifische T Zellantwort als auch eine starke Antikörperproduktion induzierte. Diese Strategie wurde zusätzlich erfolgreich in HHDII-Mäusen getestet, die als Modell für humane MHC-Antigenpräsentation verwendet wurden.

Weitere Tests wurden in HBV1.3.32-transgenen Mäusen durchgeführt, einem Modell für chronische HBV Infektion. Diese Mäuse replizieren HBV des Subtyps ayw (HBV_{ayw}) ab der Geburt hauptsächlich in ihren Lebern und entwickeln daher eine periphere Toleranz gegen HBV. Da HBV nicht in der Lage ist Mäuse zu infizieren, ist dieses transgene Modell das verlässlichste um chronische Hepatitis B im Kleintiermodell zu simulieren. Dies wurde herangezogen um die optimale Kombination von HBV-Antigenen, die Promotoren für die Expression der rekombinanten HBV-Proteine in MVA sowie das Impfschema, welches eine

breite Immunantwort induziert, zu ermitteln. Des Weiteren konnten in diesem Modell die Subtypen ayw und adw des HBsAg verglichen werden. Die im Zuge der Impfung induzierten Immunantworten wurden an Tag 6, 14 und 56 nach der finalen Immunisierung analysiert. Grundsätzlich wurden die höchsten Frequenzen an polyfunktionalen T Zellen gegen $HBsAg_{ayw}$ durch das Impfschema hervorgerufen, das $HBsAg_{adw}$ enthielt, was auf die Induktion von kreuzreaktiven T Zellen hinwies. Gegen HBcAg konnten T Zellantworten mit vergleichsweise niedrigeren Frequenzen detektiert werden. Die Impfstrategie mit $HBsAg_{adw}$ induzierte zusätzlich HBV_{ayw}-neutralisierende anti-HBs Antikörper. Dies unterstützt die Annahme, dass es sich um eine kreuzreaktive Immunantwort im Falle des HBsAg handelte. Während auf T Zellebene die Immunantworten bis Tag 14 detektiert wurden, konnten HBV-spezifische Antikörper und signifikant reduzierte HBsAg Levels bis zu Tag 56 nach finaler Immunisierung nachgewiesen werden. Dies lässt auf einen länger anhaltenden Effekt der Impfstrategie auf humoraler Ebene schließen. Ferner zeigten die histologischen Analysen in HBV-vakzinierten im Vergleich zu Mock-geimpften Mäusen einen tendenziell verstärkten Influx von B und T Zellen sowie eine erhöhte Proliferation von Hepatozyten. Zusätzlich zur intrazellulären Zytokinfärbung wurden die zytotoxischen Eigenschaften der Vakzine-induzierten HBV-spezifischen T Zellen mit Hilfe eines *in vivo* killing Assays untersucht. Hierbei konnte beobachtet werden, dass die mit einem HBcAg-spezifischen Peptid beladenen Milzzellen in Wildtyp-Mäusen, die zuvor mit der etablierten Impfstrategie gegen HBcAg behandelt wurden, effektiv reduziert wurden. Dies zeigte, dass die Vakzine-induzierten T Zellen nicht nur polyfunktional bezüglich der Zytokinexpression sondern zusätzlich effektive zytotoxische Eigenschaften besaßen.

Zusammenfassend konnte mit der in dieser Arbeit etablierten Impfstrategie die Toleranz gegen HBV in einem Modell für chronische Hepatitis B Virus Infektion überwunden werden, was einen vielversprechenden Ansatz für eine therapeutische Impfung für zukünftige klinische Studien darstellt.

I. List of Abbreviations

aa	amino acid
Ab	antibodies
Ad	adenoviral vector
ADP	adenosine diphosphate
ALT	alanine aminotransferase
APC (fluorescent dye)	Allophycocyanin
APC	antigen presenting cell
APS	ammonium persulfate
ATP	adenosine triphosphate
BCR	B cell receptor
BFA	Brefeldin A
BMDC	bone marrow derived dendritic cell
bp	base pairs
BPB	Bromphenol blue
BSA	bovine serum albumin
cccDNA	covalently closed circular DNA
CFSE	Carboxy fluorescein succinimidyl ester
CHB	chronic hepatitis B
CsCl	cesium chloride
CTAB	cetyl trimethylammonium
CTL	cytotoxic T lymphocyte
Cy7	Cyanin 7
d	day
DC	dendritic cell
ddH_2O	double-distilled water
DHBV	duck hepatitis B virus
DC	dendritic cell
DMSO	simethylsulfoxid
DNA	deoxyribonucleic acid
dsDNA	double-stranded DNA

ECL	enhanced chemiluminescence
EDTA	ethylenediaminetetraacetic acid
EMA	ethidium monoazide bromide
EtOH	ethanol
e.g.	for example
ER	endoplasmic reticulum
FACS	fluorescence-activated cell sorting
FBS	fetal bovine serum
FCS	fetal calf serum
FITC	Fluoresceinisothiocyanate
FSC	forward scatter channel
GM-CSF	granulocyte macrophage colony-stimulating factor
h	hours
HBc	hepatitis B virus core protein
HBcAg	hepatitis B core antigen
HBeAg	hepatitis B e antigen
HLA	human leucocyte antigen
HBs	hepatitis B virus surface protein
HBsAg	hepatitis B surface antigen
HBV	hepatitis B virus
HCC	hepatocellular carcinoma
HRP	horseradish peroxidase
ICS	intracellular cytokine staining
IFN	interferon
IL-	interleukine
i.p.	intraperitoneal
IU	international units
IU (virus titer)	infectious units
i.v.	intravenously
kb	kilo base

KOH	potassium hydroxide
L	ligand
LAL	liver associated lymphocyte
LSEC	liver sinusoidal endothelial cells
MACS	magnetic cell seperation
µg	microgram
MeOH	methanol
MFI	mean fluorescence intensity
MHC	major histocompatibility complex
ml	milliliter
mM	millimolar
MOI	multiplicity of infectious units
mRNA	messenger ribonucleic acid
MVA	modified vaccinia virus Ankara
NK	natural killer
OD	optical density
ORF	open reading frame
OVA	ovalbumin
PBS	phosphate buffered saline
PCEP	poly[di(sodium carboxylatethylphenoxy)phosphazene]
PCPP	poly[di(sodium carboxylatophenoxy)phosphazne]
PCR	polymerase chain reaction
PE	Phycoerythrin
PEG	polythyleneglycol
PerCP	Peridininchlorophyll protein
PFA	Paraformaldehyde
pgRNA	pregenomic RNA
qPCR	quantitative PCR
rcDNA	relaxed circular DNA

RNA	ribonucleic acid
s.c.	sub cutaneous
SCC	sideward scatter channel
SDS	sodium dodecyl sulfate
SVP	subviral particle
TAE	tris-acetat-EDTA buffer
TCR	T cell receptor
TEMED	N, N, N', N'-tetramethyllethylenediamine
TGF	transforming growth factor
T_H	T helper cell
TLR	Toll-like receptor
TNFα	tumor necrosis factor alpha
Tris	N-tris(Hydroxymethyl)-methylglycine
v/v	volume per volume
w/v	weight per volume
WHV	woodchuck hepatitis virus
wt	wild-type

1. Introduction

1.1 Hepatitis B Virus

One of the most important infectious diseases worldwide is hepatitis B which is caused by hepatitis B virus (HBV). There are approximately 2 billion people infected and currently more than 240 million people are chronic carriers and thus at high risk to develop liver cirrhosis or hepatocellular carcinoma (HCC). It is assumed that 30% of all cases of cirrhosis and 53% of HCC worldwide are caused by HBV (Robert-Koch-Institut, Germany). According to the World Health Organization 600 000 deaths per year are related to infection with HBV (WHO, July 2013).

1.1.1 Classification

HBV belongs to the family "hepadnaviridae" that contains two genera, *orthohepadnaviruses* which are found in mammals and *avihepadnaviruses* that are found in birds. The name "hepadnavirus" contains the **hepa**trophic tropism of the virus and its genomic structure which is partially double stranded **DNA**. Compared to other viruses, its genome is one of the smallest. 8 genotypes are described for HBV (A-H) based on more than 8% difference in genome sequences. These genotypes can be further subdivided into subgenotypes that differ by at least 4% in genome sequences (Schaefer 2007). Several related viruses, woodchuck hepatitis virus (WHB), chimpanzee hepatitis B virus (HBVcpz), duck hepatitis B virus (DHBV) and others have been discovered since the sequence of the HBV genome is known.

1.1.2 Structure of the virus particle and genomic organization

In the serum of HBV infected patients three different structures of viral particles can be detected by electron microscopy (Fig. 1.1.2.1). There are non-infectious long filaments and small spheres that contain only hepatitis surface proteins (Gerlich 2013) and infectious particles which are the so-called Dane particles (Dane 1970).

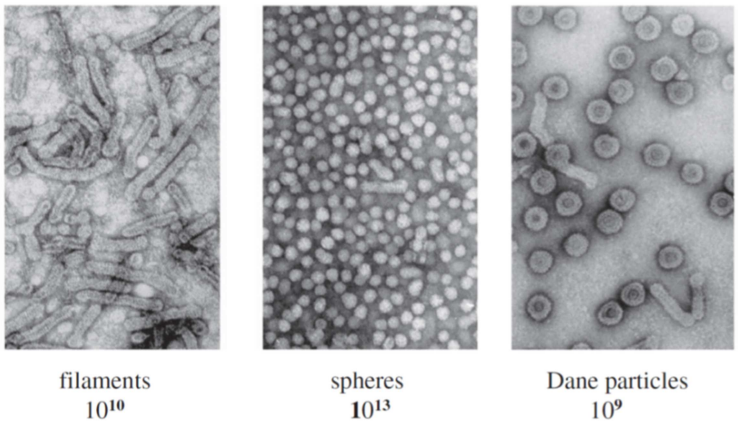

Fig. 1.1.2.1: Electron microscopy images of the three different viral particle structures. Numbers indicate the observed frequency of the structures in 1 ml serum of a high-viremic chronic HBV carrier (Gerlich 2013).

The Dane particle (Fig 1.1.2.2 A) is a spherical enveloped nucleocapsid structure with a diameter of 42-44 nm that contains the partially double stranded relaxed circular DNA (rcDNA) genome. It has a size of about 3200 nucleotides, but the number of nucleotides varies between genotypes and subgenotypes (Schaefer 2007). The nucleocapsid that encloses the genome consists of core proteins (HBcAg) and forms its structure via self-assembly. The complete genetic information is present in the negative strand of the viral DNA that is covalently bound to the viral polymerase and contains small redundancies of 8-9 nucleotides at the 5'- and 3' end which are called R region and are essential for viral replication (Nassal 2008, Seeger 1986, Seeger 2000). The positive strand covers only about 2/3 of the genome length with a 3' end that is variable in size (Lutwick 1977, Summers 1988). A short RNA oligomer originating from the pre-genomic RNA (pgRNA) remains covalently bound to the 5' end of the positive strand after viral DNA synthesis.

The HBV genome (Fig. 1.1.2.2 B) consists of four open reading frames (ORFs). Due to its identical orientation and partial overlap they are organized in a characteristic and highly condensed way (Block 2007). It contains six start codons, four promoters and two transcription-enhancing elements.

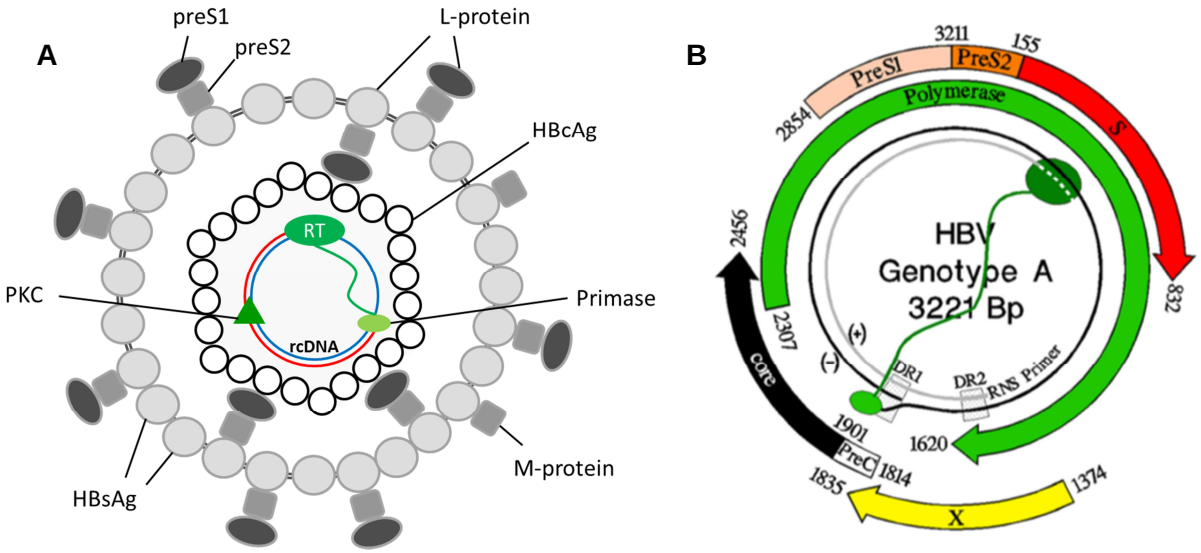

Fig. 1.1.2.2: Schematic illustration of a Dane particle (A). The nucleocapsid consisting of 120 dimers of HBcAg contains the viral genome, the HBV polymerase with the primase, the reverse transcription domain and the cellular protein kinase C alpha (PKC). (B) Open reading frames for encoding proteins of the HBV genome (adapted from (Gerlich 2013, Rehermann 2005).

The viral surface proteins are encoded in the first ORF called preS1/preS2/S. It contains three start codons but only two mRNAs of 2.4 kb and 2.1 kb called preS and S are transcribed (Glebe 2007). These two mRNAs are translated into the small (S), the middle (M) and the large (L) surface proteins. The S-protein is also called HBsAg which can be detected with standardized diagnostic methods. The stoichiometric ratio of the produced S, M and L is 4:1:1. Subviral particles that are secreted in much higher numbers compared to Dane-particles contain mainly S-protein and only traces of L-protein (Bruss 2007). The structure containing S, M and L forms the envelope of the virus. The infectivity of the virion is established by glycosylation of the surface proteins (Glebe 2005, Nassal 2008, Schildgen 2004, Schmitt 2004, Schulze 2010).

HBcAg and HBeAg which is also known as precore protein are encoded in the ORF preC/C. The HBcAg has a size of 183 amino acids and forms the icosahedral nucleocapsid via self-assembly in the cytoplasm. In addition it contains a nucleic acid-binding domain which is crucial for packaging of the pgRNA together with the viral polymerase. The reverse transcription takes place in newly formed capsids where the pgRNA is converted into the partially double stranded DNA genome (Daub 2002, Kann 1994, Kann 2007, Kann 1999). The HBeAg is a non-structural protein that has no function in viral infection or replication, but is important in promoting viral persistence through its tolerogenic functions (Chen 2005, Visvanathan 2006). In the hepatocyte it may interfere with TLR signaling pathways and thereby inhibit innate immune responses of the host

(Lang 2011). Like HBsAg, it is also secreted into the bloodstream and therefore used in molecular diagnostics as marker for viral replication (Chen 2005, Hadziyannis 2006).
The pol ORF encodes the viral polymerase which possesses the activities of the reverse transcriptase, the DNA polymerase and the RNAse H. It is the only enzymatic protein that is encoded in the viral genome. The polymerase domain is located at the N-terminus of the protein and includes the terminal protein that serves as a primer for the reverse transcriptase that transcribes the pgRNA into the negative-strand DNA (Nassal 2008, Zoulim 1994). The RNAase H domain is located at the C-terminus of the viral polymerase and it cleaves the RNA strand of the RNA/DNA complex during reverse transcription. The DNA polymerase synthesizes the positive-strand DNA after reverse transcription during maturation of the nucleocapsid.
The fourth ORF is called X and encodes the regulatory non-structural X protein. It was shown that the X protein is essential for viral replication *in vivo* (Lucifora 2011, Zoulim 1994) and it is able to transactivate cellular and viral genes.
All ORFs have a common polyadenylation signal motif and all transcripts are capped and polyadenylated (Nassal 2008).

1.1.4 Replication cycle of HBV

The first step of HBV infection is a cell type unspecific binding to heparin sulfate proteoglycans that are present on the surface of cell membranes (Schulze 2007). This step is reversible and if the virus is attached by chance to a hepatocyte it binds to a cell type specific receptor (Glebe 2007, Urban 2010) with a region in the preS1 domain of the L-protein and a region in the S-protein (Engelke 2006, Gripon 2005). The cell type specific receptor is a sodium taurocholate cotransporting polypeptide (NTCP) which is predominantly expressed in the liver of mammalians but has a high diversity between species in the protein sequence and thus is responsible for the species tropism of the virus (Yan 2012). Since NTCP is localized on the sinusoidal basolateral side of the plasma membrane (Stieger 1994) and is mostly expressed in differentiated hepatocytes (Liang 1993, Rippin 2001), a successful infection requires polarized and differentiated hepatocytes (Schulze 2012).
After initial binding to the receptors of the hepatocyte it is believed that the virus can enter the cell by 2 ways: It can either pass the cell membrane via endocytosis which is followed by a release of nucleocapsids from endocytotic vesicles or via fusion with the plasma membrane of the hepatocyte. Both pathways lead to release of the viral capsid containing the circular partially double stranded DNA genome.

To establish a persistent infection the viral genome needs to be transported into the nucleus. Therefore, the viral capsid is transported via microtubules to the nuclear periphery (Rabe 2006). The capsid then interacts with nuclear transport receptors and adaptor proteins of the nuclear pore complex which leads to trapping of the nucleocapsid in the nuclear basket and release of viral DNA into the nucleus (Kann 2007, Schmitz 2010). The plus strand of the rcDNA is completed by the viral polymerase. The viral polymerase and the short RNA primer are removed and the persistent genomic structure called covalently closed circular (ccc) DNA is formed. Enzymes involved in DNA repair of the host cell convert the relaxed circular form into a minichromosome consisting of cccDNA molecules with histone and non-histone proteins (Bock 1994, Bock 2001, Levrero 2009, Seeger 2000). It serves as a template for all viral mRNAs. Up to 50 cccDNA molecules can be accumulated in one cell. Integration of cccDNA into the host genome can occur particularly in the presence of DNA damage (Dandri 2002) but is not a regular step in the replication cycle of HBV. The viral genome is transcribed by the cellular transcription machinery and is regulated by host transcription factors and the viral proteins core and X (Levrero 2009). The four mRNAs preS1/preS2/S, preC/C, pol and X are produced, encoding all viral proteins with the largest encoding for the capsid, the polymerase and the pgRNA. Translation of the viral RNAs takes place in the cytoplasm and is performed by enzymes of the host. Once the core proteins and the polymerase are generated the complex formation starts with attachment of the polymerase to the pgRNA. The pgRNA has a secondary structure called ε which is present at the 5' and at the 3' end. At the 5' end it forms a hairpin structure which is recognized by the viral polymerase and serves as initial packaging signal (Bartenschlager 1992). The nucleocapsid is formed by self-assembly of core proteins. During maturation of the nucleocapsid, the pgRNA is converted into rcDNA with the incomplete positive strand by the reverse transcriptase and DNA polymerase activity of the viral polymerase. The mature nucleocapsids can either be re-imported into the nucleus or enveloped to form Dane particles. The envelopment is not fully understood. It requires a balanced co-expression of S- and L-proteins which are co-translationally inserted into the ER membrane. Binding of the nucleocapsid to the L-protein initiates budding into the ER lumen and formation of viral particles that are secreted (Beck 2007, Bruss 2007). In the absence of L-protein subviral particles are secreted to a 10^3 to 10^6 higher rate compared to Dane particles (Fig. 1.1.4).

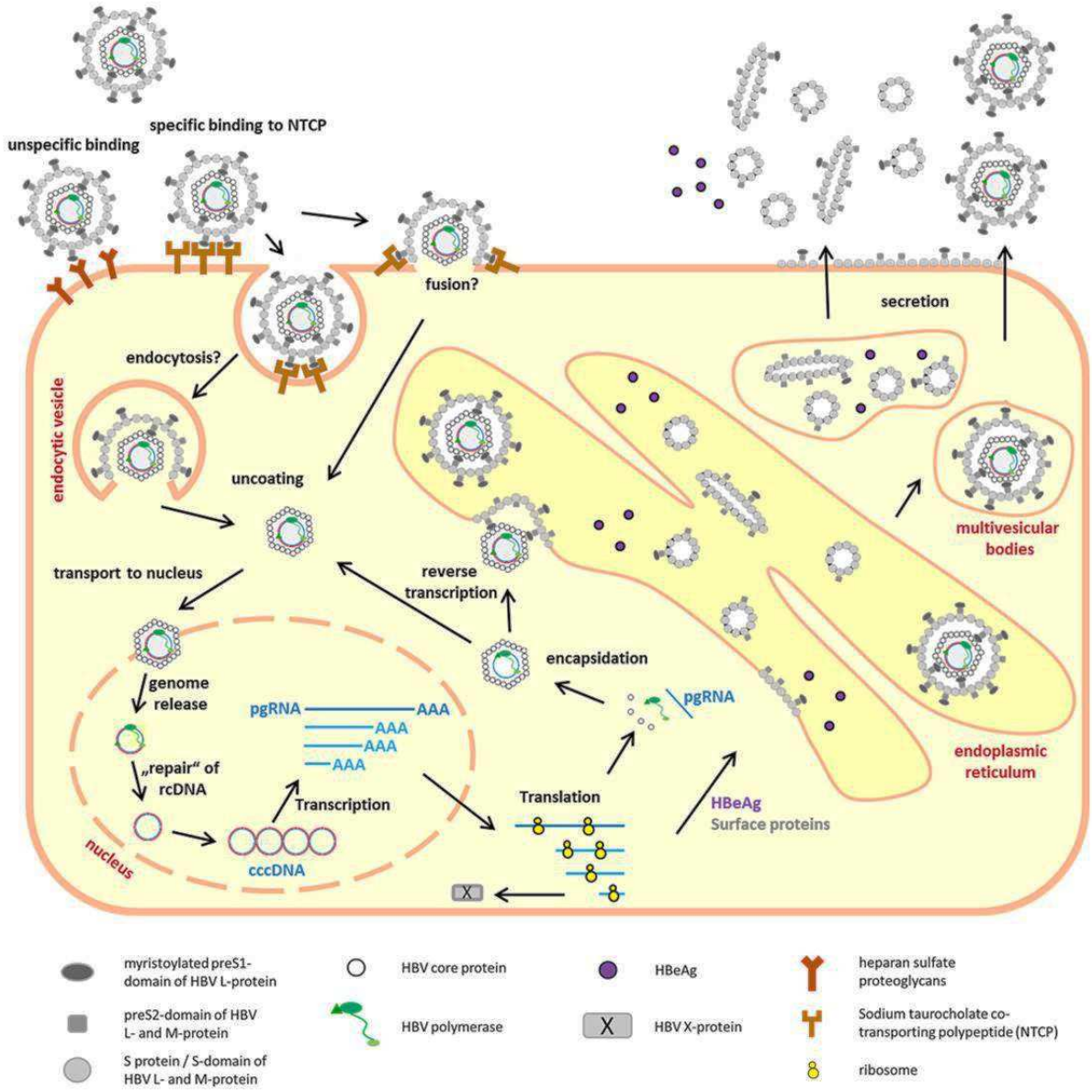

Fig. 1.1.4: Schematic illustration of the replication cycle of HBV. rcDNA = relaxed circular DNA, cccDNA = covalently closed circular DNA, pgRNA = pregenomic RNA, AAA = polyadenylation of RNA.

1.2 HBV infection

1.2.1 Epidemiology

The prevalence of HBV infections varies from below 2% in Western Europe, Central- and North-America, Australia and New Zealand to more than 8% up to 20% in Southeast Asia, China and most parts of Africa (Fig. 1.2.1.1).

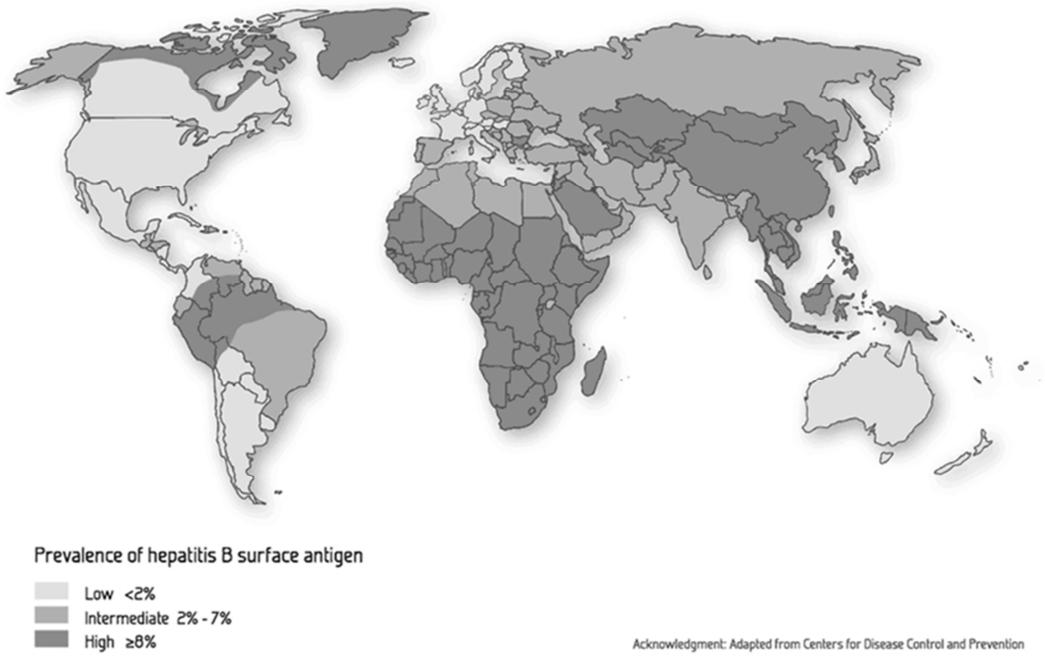

Fig. 1.2.1.1: Prevalence of chronic HBV infection from 2006 (adapted from Centers for Disease Control and Prevention).

Since effective prophylactic vaccination strategies were introduced in developed countries in 1982 (Francis 1982) the number of newly detected infections decreased (Rantala 2008). However, it is difficult to generate exact data due to the asymptomatic course of disease. In contrast to a decrease of new infections, the number of HBV-related diseases like cancers and deaths increased (Gooma 2008, Hatzakis 2011). The reasons might be improved diagnosis and documentation of HBV infections.

Not only HBV infection rates differ among countries but also the prevalence of genotypes of the virus. As described above there are 8 different genotypes (A-H). The most common genotypes in Europe and North-Africa are A2 and D, whereas in China and Southeast Asia genotypes B and C are predominant (Fig. 1.2.1.2).

Fig. 1.2.1.2: Geographic distribution of HBV genotypes and subgenotypes (modified from (Schaefer 2007) with information of JHSPH 2011).

1.2.2 Transmission routes

In general HBV is transmitted via blood. However, HBV can survive outside the human body for several days and can be transmitted from contaminations (WHO).

In low prevalence areas like in Western Europe and North America most of the patients get infected through unprotected sexual intercourse and intravenous drug use. In high prevalence areas the main route is vertical through perinatal infection. Here, the transmission from an HBV-infected mother to her neonate occurs *in utero*, at time of birth or after birth. The infection rate in this case is about 90% depending on the HBV replication rate in the mother (Burk 1994, Li 2004, Zhang 2012). Transmission routes like transfusions or organ transplantation play a minor role.

1.2.3 Courses of HBV infection

Vertical transmission from mothers to neonates or infection during the first year of life results in chronic infection in more than 90% of cases. In adults the chronicity rate is about 5% whereas infection between the age of 1 and 5 years leads in 20-50% of the cases to chronic infection (Ganem 2004, Kutscher 2012, McMahon 1985) (WHO).

1.2.3.1 Course of acute hepatitis B infection

According to the WHO, HBV is 50 to 100 times more infectious than the human immunodeficiency virus (HIV). Studies in chimpanzees showed that one HBV particle is sufficient to establish an infection (S. Wieland, F. Chisari personal communication 2007). In figure 1.2.3.1 the course of disease of an acute hepatitis B is shown.

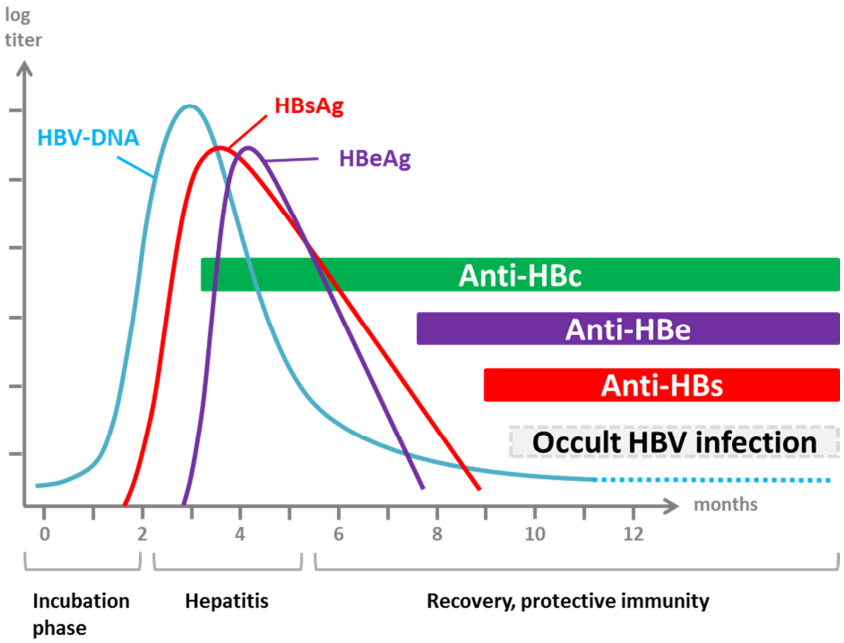

Fig. 1.2.3.1: Course of disease of an acute HBV infection (modified from (Gerlich 2013, Rehermann 2005)).

In general, an infection with HBV starts with an incubation phase that lasts for 1 up to 2 months. During the first months of infection, HBV-DNA and HBsAg-levels increase exponentially in the serum. The peak of those markers is reached before the outbreak of hepatitis B. About 70% of patients with an acute infection have a subclinical hepatitis and only 30% develop an icteric hepatitis with constitutional symptoms like nausea and jaundice. The alanine and aspartate aminotransferase levels (ALT and AST) can rise to 1000-2000 IU/L in an acute phase. The elevated ALT-, HBV-DNA- and HBsAg-levels normalize in recovering patients within 1 to 4 months. The first HBV-specific antibodies that can be detected are directed against the HBcAg whereas the neutralizing antibodies against HBsAg appear 9 months post infection (Gerlich 2013). Although the course of disease in adults is in 95% acute and the patients recover with detectable seroconversion from HBsAg positive to anti-HBs positive, the virus can still persist lifelong in form of cccDNA in hepatocytes. This occult infection is controlled by a T cell response that controls the virus but does not lead to inflammation (Guner 2011, Yotsuyanagi 1998). Therefore, a reactivation of HBV during immunosuppression after organ transplantation or

during chemotherapy is possible. Total clearance of the virus is observed rarely (Gerlich 2013, Michalak 1994).

1.2.3.2 Course of chronic hepatitis B infection

In most patients a chronic course of disease is clinically asymptomatic. Chronic infection is divided into three phases of variable length (Fig. 1.2.3.2).

The first phase is characterized by high levels of HBV-DNA, HBsAg and HBeAg that are detected in the serum of a patient. The ALT levels are not elevated at this stage. This phase can last for decades and is also characterized by the absence of an immune response. The second phase is the immune elimination or immunoactive phase where levels of HBV-DNA, HBsAg and HBeAg decrease and antibodies against HBcAg are detectable. ALT-levels increase during that period due to an immune response which results in a more severe liver disease and can progress to liver cirrhosis and hepatocellular carcinoma. Alternatively it can progress to a low-viremic phase where HBeAg-levels are below detection limit, antibodies against HBeAg are detectable and ALT-levels restored. This low replicative phase can last for life, but in patients that undergo immunosuppressive therapy, the virus replication can elevate to high levels again (Gerlich 2013).

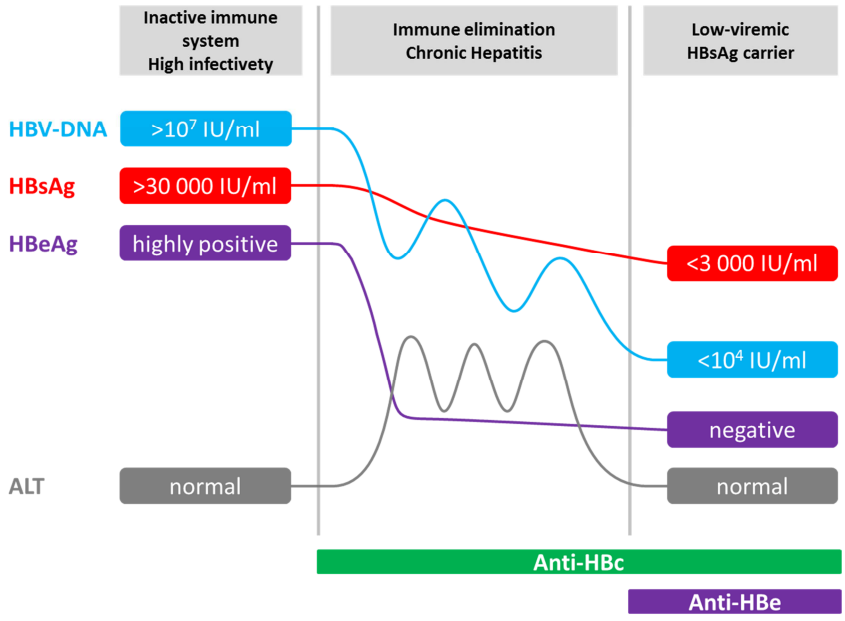

Fig. 1.2.3.2: Course of disease of chronic hepatitis B (Gerlich 2013, Rehermann 2005).

1.3 Standard of care and its limitations

The two standard options to treat HBV infection are: interferon α (IFNα) in standard or pegylated form or nucleos(t)ide analogs. In an acute hepatitis B infection treatment is generally not advised due to a clearance of the virus in 95-99% of cases (Liaw 2009, McMahon 1985). However, recent studies showed that patients with fulminant hepatitis B benefit from treatment with the nucleoside analog Lamivudine (Kumar 2007, Yu 2010). Therefore, treatment with Lamivudine is recommended by the "European Association for the Study of the Liver" (EASL 2012). In contrast, treatment with IFNα is not recommended since it increases the risk of hepatitis (Tassopoulos 1997). Endpoints of treatment are suppression of HBV replication, induction of HBeAg seroconversion and most importantly HBsAg clearance (EASL 2012, (Cornberg 2011, Lok 2009).

Treatment of chronic HBV carriers aims to control virus replication and lower the risk to develop liver cirrhosis and hepatocellular carcinoma through liver damage (EASL 2012, (Cornberg 2011, Lok 2009). According to guidelines of national and international societies, treatment should be performed if HBV-DNA levels are higher than 2000 IU/ml and elevated ALT-levels are detected independent of the presence or absence of HBeAg. Combination of treatments with nucleos(t)ide analogs or IFNα together with nucleos(t)ide analogs are not recommended (Mauss 2013).

IFNα is an immune modulator and belongs to the type I IFNs that are also known as viral IFNs. It is produced by precursor dendritic cells (Foster 2000) but can also be produced by other cell types like leukocytes, fibroblasts and endothelial cells. It leads to the activation of interferon stimulate genes (ISGs) that encode antiviral proteins like Myxoma resistance protein 1 (MxA) (Li 2012) and Apolipoprotein B mRNA-editing enzyme-catalytic polypeptide-like (APOBEC) (Harper 2013) that are known to have antiviral effects against HBV (Bonvin 2006, Bonvin 2008, Lucifora 2014, Suspene 2005, Turelli 2008, Vartanian 2010, Xu 2007). However, if IFNα is applied over a long period of time, only about 20% of patients still respond to the treatment (Wong 1993). Other disadvantages are side effects of the drug like fever, headache, fatigue, arthralgais and myalgais. However, these side effects do not lead to a change in the dosage of the drug. More severe side effects especially of neuropsychiatric nature and irritability are more problematic. Since IFNα has strong immunomodulatory properties, it can induce autoimmune diseases like hypothyroidism or hyperthyroidism. Up to 1% of patients treated with IFNα suffer from severe or even life-threatening side effects like thyroid, visual, auditory, renal and cardiac impairment and pulmonary interstitial fibrosis. Overall, these side effects lead to limitation of dose or duration of the therapy (Dusheiko 1997). Another limitation of IFNα is its dependency on the viral genotype. Patients infected with HBV genotypes A and B

respond better than those infected with genotypes C or D (Kao 2000, Zhang 1996). Due to the limited tolerability the treatment period is restricted to usually 6-12 months.

Nucleos(t)ide analogs are inhibiting the reverse transcription of the viral polymerase leading to reduced viral replication and decrease of HBV-DNA levels in serum of treated patients. In contrast to IFNα, nucleos(t)ides are well tolerated and the responsiveness is independent of viral genotypes (Nafa 2000, Pichoud 1999, Seigneres 2000, Westland 2003). A prolonged antiviral treatment is needed which can lead to cell curing by inhibiting the intracellular recycling of cccDNA. It was shown that viral persistence is linked to the half-life of cccDNA in woodchuck models (Fourel 1994, Mason 1998, Moraleda 1997). Although nucleos(t)ide treatment is very promising, long-term application can induce resistant viral mutants. These mutants emerge because the HBV polymerase has no proof reading function and thus nucleotides can be exchanged by accident (Park 2003).

To prevent disease progression and complications treatment with the available drugs needs to be introduced early after HBV infection which is hard to realize in most cases. Due to the fact that nucleos(t)ide analogs and IFNα do not target the formation of cccDNA or cccDNA itself, there is a high risk of renewed viral replication, clinical reactivation and loss of viral control (Zoulim 2004). Therefore, it is necessary to find new treatment strategies that can eradicate the virus and cure the patient.

1.4 Immune system and liver

1.4.1 Innate immune system

The innate immune system is the first line of host defense which acts immediately and leads to acute inflammation induced by microbial infection or tissue damage (Akira 2006, Beutler 2006). Importantly, it is also required for the activation and modulation of the adaptive immune system. Its components are epithelial barriers, cytokines, complement, the cell-autonomous defense system and cells like macrophages, dendritic cells (DC), granulocytes and natural killer cells. Also nonprofessional immune cells contribute to innate immunity such as epithelial cells, endothelial cells and fibroblasts. Both the professional and nonprofessional immune cells can be activated via direct recognition of microbes by germline-encoded pattern recognition receptors (PRR) that detect pathogen-associated molecular patterns (PAMP). There is evidence that they can also recognize endogenous molecules that are released from damaged cells that are called damage-associated molecular patterns (DAMP) (Takeuchi 2010).

The members of the PRR family are transmembrane proteins such as Toll-like receptors (TLR) and C-type lectin receptors, as well as cytoplasmic proteins Retinoic acid-inducible gene (RIG)-I-like receptors (RLR) and NOD-like receptors (NLR). The sensing of PAMPs or DAMPs leads to an upregulation of proinflammatory cytokines like tumor necrosis factor (TNF), interleukin (IL)-1 and IL-6, type I interferons, chemokines and antimicrobial proteins dependent on the activated PRR. The induction of TNF, IL-1 and IL-6 leads to cell death of inflammatory tissues, increase of vascular endothelial permeability, recruitment of blood cells to inflamed tissue and production of acute-phase proteins (Takeuchi 2010).

In an immune-privileged organ like the liver, specific cells play important roles in innate immunity. First of all there are hepatocytes that represent the most predominant cell population of the organ. On the one hand, they play an important part in immunity by activating T cells and producing proteolytic plasma proteins that belong to the complement system and acute-phase response. On the other hand, they play a major role in the tolerogenicity of the liver by ectopic expression of auto-antigens and B7-H1 which leads to inhibition of cytotoxic T cell effector functions. Liver sinusoidal endothelial cells (LSEC) are covering the hepatic sinusoid, separating hepatocytes and stellate cells from circulating leukocytes and build the space of Dissé. LSECs, hepatocytes and stellate cells can all function as antigen presenting cells (APC). Another cell type which has an APC function is the Kupffer cell. Kupffer cells represent the macrophages of the liver which patrol through the sinus and have a strong impact on tolerance by producing anti-inflammatory cytokines such as IL-10 and transforming growth factor (TGF) β. Natural killer (NK) cells, natural killer T (NKT) cells, DCs and T cells the latter from the adaptive immune system, belong to the liver associated lymphocytes (LAL) which are located in the liver interstitium (Thomson 2010).

Effective activation of the innate immune system is important to elicit a strong adaptive immune response, especially in immune-privileged organs like the liver.

1.4.2 Adaptive immune system

Antigen-specific immune responses are mediated by the acquired or adaptive immune system. It is inducible and can be subdivided into a cellular and a humoral response. The key players of the cellular response are T cells. T cells recognize antigens that are presented on major histocompatibility complex (MHC) class I or II via T cell receptors (TCR). B cells are responsible for the humoral response. B cells recognize antigens via B cell receptors (BCR) and produce antigen-specific antibodies. Since both responses are antigen-specific the immune system needs to adapt to the specific pathogen.

1.4.2.1 Generation of a lymphocyte repertoire

During development of the adaptive immune system the generation of a lymphocyte repertoire is a major task. In this process, central tolerance is established that ensures that the lymphocytes are not reactive to self-antigens. The origin of T and B cells are pluripotent hematopoietic stem cells from the bone marrow.

The proliferation and differentiation of progenitor T cells takes place in the thymus (von Boehmer 1990) where the cells undergo different phenotypic stadiums that can be determined by specific expression patterns of surface markers CD4, CD8, CD3, CD25 and CD44. Gene segments of TCRs undergo a set of rearrangements which result in a huge amount of progenitor T cells each of them with a single specificity. TCRs recognize antigens that are presented on MHCs which are expressed on almost every cell of the organism. MHC class I molecules are present on all nucleated cells and present antigens that are recognized by TCRs accompanied by the coreceptor CD8 of cytotoxic T cells (CD8 T cells). MHC class II molecules are usually expressed on the surface of APCs that present antigens to TCRs accompanied by the coreceptor CD4 of helper T cells (CD4 T cells). During the differentiation process epithelial cells of the thymic cortex present self-antigens on both MHC types for positive selection and co-receptor specificity determination (Anderson 1993). The result is a peripheral repertoire of CD4 or CD8 positive T cells that recognize antigens bound to self MHC class I or class II. To prevent autoreactivity of positively selected T cells there are three mechanisms: clonal deletion, clonal anergy and functional inhibition of autoreactive T cell clones. Clonal deletion is the negative selection process in the thymus that leads to apoptosis of T cells that recognize self-antigens presented on self-MHC by APCs and medullary thymic epithelial cells (Blackman 1990). Cells that survived the selection process are called naïve T cells. Each individual naïve T cell recognizes one specific antigen, but in total the whole population is specific for millions of antigens. This is called clonal diversity. Naïve T cells are circulating through the lymphatic system and the blood (Murphy 2011).

The development of B cells takes place in the bone marrow. The first step is antigen-independent but requires interaction with bone marrow stromal cells which produce cell adhesion molecules (CAM) and cytokines like stem cell factor (SCF) and IL-7 (Osmond 1990). During this phase rearrangements in the antibody gene loci occur which result in expression of mono-specific BCRs on the surface of so called immature B cells. On molecular level BCRs are membrane bound immunoglobulins (Ig) which are also called antibodies. The next phase is the induction of tolerance to self-antigens by clonal deletion which is similar to the negative selection of T cells (Nemazee 1991). B cells that recognize self-antigens which are bound to a cell surface are eliminated via apoptosis. If they bind soluble antigen they migrate to the periphery (lymph nodes and spleen) and become

inactive, a state of anergy and die. B cells that do not bind to self-antigens migrate to the periphery and develop into mature naïve B cells (Murphy 2011).

1.4.2.2 Peripheral Tolerance

As described earlier T and B cells undergo a negative selection during their development. However, in the thymus this process is not complete and some self-reacting T cells are able to migrate to the periphery (Gallegos 2006, Mathis 2010, Mueller 2010, Redmond 2005). Additionally, there are T cells that are specific for antigens from food, commensal bacteria or have a weak avidity against self-antigens (Mowat 2003, Zehn 2006). To control these T cells and inhibit autoimmunity there are several mechanisms leading to peripheral tolerance.

One of the key players in the liver are CD4 and Foxp3 positive regulatory T cells (Treg) and APCs that inhibit activation of effector T cells (Vignali 2008). Tregs can develop either in the thymus as a population or through antigenic stimuli that lead to transformation of naïve effector T cells into adaptive Tregs (Miyara 2007). Tregs suppress the proliferation, cytokine production and cytotoxic activity of T cells (Billerbeck 2007). Additionally, Tregs can inhibit APCs (von Boehmer 2005) and modulate T cells and APCs through expression of molecules like TGFβ, cytotoxic T-lymphocyte antigen 4 (CTLA-4), TLR-2 and -8 and others (Miyara 2007).

Another important factor of peripheral tolerance is the surface protein PD-1 and its ligands PD-L1 and PD-L2. PD-1 can be expressed on activated T-, B- and NKT-cells (Nishimura 1996) as well as activated monocytes and DCs. The two ligands PD-L1 and PD-L2 have different expression patterns. PD-L1 is expressed on murine T and B cells, DCs, macrophages and interestingly nonparenchymal cells of the liver (Yamazaki 2002). PD-L2 is only expressed on DCs, macrophages and bone marrow derived mast cells (Zhong 2007). In a T cell, PD-1 stimulation results in downregulation of IL-2 and IFNγ and is the counterpart of the co-stimulatory signaling via CD28 and thereby inhibits T cell responses (Nurieva 2006).

Another mechanism to induce tolerance in the periphery is depending on APCs. In the absence of inflammation APCs express only low amounts of co-stimulatory molecules which are important for activation of T cells. A T cell recognizing a peptide presented on an APC that is not providing a co-stimulation at the same time does not receive activation- or survival-signals and becomes anerg which is an irreversible state of the cell (Hamilton-Williams 2005, Hernandez 2001, Schietinger 2012, Steinman 2003).

With these mechanisms of peripheral tolerance it is possible to prevent T cell hyperactivation, diminish chronic inflammatory reactions and maintain tolerance to self-

antigens (Rouse 2006). However, peripheral tolerance can prevent immune responses that are necessary to clear pathogens like HBV from the host.

1.4.2.3 T cell response

The most important cells for clearing pathogens from the host are T cells. Cytotoxic CD8 T cells destroy infected cells that present antigens on MHC I, CD4 T cells control cell-mediated-, humoral immune responses and cells like macrophages that produce cytokines to activate other cells.

As mentioned above components of the innate immune system are necessary for the development of an adaptive immune response. Immature professional APCs such as DCs circulate through the body and constantly sample the environment for pathogens through PRRs and endocytosis. Upon detection of a presentable antigen the DC becomes activated and turns into a mature DC. In contrast to an immature DC, the endocytic activity of a mature DC is low but co-stimulatory molecules CD80, CD86 and CD40 that are necessary for T cell activation and MHCs that present antigens to T cells are upregulated. They migrate to lymph nodes and present the antigens to CD4 T cells and via cross-presentation to CD8 T cells (Guermonprez 2002). The specific T cell clones then start to proliferate, a process that is called clonal expansion and differentiate into effector cells which are the basis for an effective primary immune response. There are three kinds of T effector cells: cytotoxic CD8 T cells, T_H1 and T_H2 cells that are CD4 positive. There are also other T helper cells like T_H9 and T_H17 (Jager 2009) which will not be described in more detail. Depending on the pathogen a T cell response can involve predominantly cytotoxic CD8 T, T_H1 or T_H2 cells. In case of intracellular pathogens like HBV CD8 T cells are the most important effector cells because they eliminate infected cells that present antigens that are endogenously expressed on MHC class I by inducing apoptosis, secretion of lytic granula or via induction of apoptosis with the Fas/FasL-system and thereby clear HBV from the host (Russell 2002). But also T_H1 cells contribute in this matter since they detect exogenous antigens that were endocytosed and presented on MHC class II. They activate macrophages that upregulate MHCs and co-stimulatory molecules which leads to enhanced antigen-presentation. T_H2 cells are necessary to activate B cells which play also an important role in successful clearance of the virus (Murphy 2011).

1.4.2.4 B cell response

B cells can be activated by the antigen itself or more commonly in a T_H2 cell dependent manner via their BCRs. For a T_H2 cell dependent activation both cells need to recognize

the same antigen. The B cell itself presents peptides from internalized antigens on MHC class II to a T cell that recognizes the peptide with its TCR. Additionally the T cell binds with its CD40 ligand to CD40 on the surface of the B cell and secretes cytokines that activate the B cell (Parker 1993). The activated B cell in return provides signals via upregulated CD80 and CD86 surface molecules to the T cell and therefore prolongs its activation state. Upon this interaction the activated B cell forms a germinal center where the B cell proliferates and differentiates into antibody-secreting plasma cells or memory B cells. In the germinal center somatic hypermutation (French 1989) and selection for high affinity clones takes place. The highly specific plasma cells migrate to the bone marrow and secrete huge amounts of antibodies. Antibodies can function in three different ways. The first is neutralization by inactivating or blocking binding sites of the pathogen or binding toxins. The second is opsonization by covering the pathogen and promote phagocytosis. The third includes a component of the innate immune system. Antibodies can trigger the activation of the complement system which can kill pathogens directly or enhance opsonization (Klaus 1979). B cell responses that develop without the help of T cells are only including the formation of plasma cells but not memory cells (Murphy 2011).
In case of HBV infection, the neutralizing function of antibodies plays an important role to prevent infection or spread of the virus.

1.5 Therapeutic vaccination

Clearance of pathogens like HBV requires a broad immune response. The induction of potent CD8 T cell responses including cytotoxic killing of infected cells as well as non-cytolytic antiviral responses like secretion of IFNγ and TNFα are necessary. Cell lysis leads to a turnover of hepatocytes and repopulation of the liver. Additionally, B cell responses resulting in secretion of neutralizing antibodies prevent spread of virions. As described above, innate immunity is crucial to trigger adaptive immune responses. Direct effects of NK- and NKT cells are also important for successful clearance (Bertoletti 2003). In chronic infectious diseases the pathogen successfully inhibits these immune responses or tolerizes the immune system. The aim of therapeutic vaccination is to overcome pathogen-specific peripheral tolerance and activate the immune system which eventually leads to elimination of the pathogen. In case of HBV, there are different therapeutic vaccination strategies such as protein- or peptide-based, DNA- and cell-based vaccines that have been investigated in different animal models like woodchucks and transgenic mice (Buchmann 2013, Kosinska 2013, Kosinska 2010). Some vaccination strategies

were also tested in clinical trials with encouraging but not satisfying outcomes (Mancini-Bourgine 2006, Vandepapeliere 2007, Xu 2013).

Protein- or peptide-based vaccines consist of complete proteins or synthetic peptides which are thought to be immunogenic. They can be administered together with adjuvants which give the opportunity to additionally activate specific types of immune responses.

While protein- or peptide-based vaccines need to be taken up by antigen presenting cells, genetic vaccines lead to expression of a polypeptide that is presented on MHCs of transfected cells. Genetic vaccines can be either plasmids (DNA vaccines) or recombinant viral vectors. DNA vaccines have been tested for their efficacy against several viral infections (Liu 2011).

Protein- or peptide-based and also DNA vaccines can be additionally combined with cytokines or recombinant viral vectors in heterologous prime-boost vaccinations to enhance immune responses efficiently (Woodland 2004).

All these options present a wide range of possibilities to develop vaccines that might be capable of curing patients from chronic infections.

1.5.1 Adjuvants

Adjuvants play an important role in vaccination. Due to their different functions they can be grouped into delivery systems and molecules that lead to modulation of the microenvironment and thus to activation of immune cells.

Particle-based delivery systems, such as liposomes and microparticles are suitable for antigen delivery. The antigen is presented on MHC class II upon phagocytosis by macrophages and DCs (Lutsiak 2002, Newman 2002). This process is controlled by TLR ligands and allows DCs to discriminate between self and non-self antigens (Blander 2006). Due to the presence in early and late endosomes various TLRs can be stimulated which leads to a stronger activation of the DC and therefore to an enhanced response to the antigen (Trinchieri 2007). As described earlier, TLRs belong to the pattern recognition receptor family. There are 10 different TLRs in humans and 11 in mice (Murphy 2011). Each of them is specific for one or more microbial molecular pattern. Some of them form heterodimers to be functional like TLR-1/TLR-2 and TLR-2/TLR-6) (Murphy 2011). In case of antigens that are applied in combination with particle-based delivery systems TLR-3, -7 and -9 that are located in endosomes can be activated.

An example for a potent immune modulator are CpG-oligodeoxynucleotides (CpG-ODN) that occur naturally in bacterial DNA and are detected by TLR-9 of B cells and DCs. Used in vaccinations they stimulate B cells (Lipford 1997), NK cells, DCs and macrophages. In these cells CpG-ODNs activate NFκB that leads to upregulation of several other

transcription factors (Krieg 2002). This leads to increased expression of IFNγ, TNFα, IL-1β, IL-6, IL-12, type I interferons, several co-stimulatory molecules such as CD80, CD86, and CD40, and MHC class II (Anitescu 1997, Jakob 1998, Krug 2001, Sparwasser 1998, Stacey 1996, Sun 1998). In general it was shown that CpG-ODNs promote T_H1 type immune responses (Klinman 2006, Klinman 2004) that are crucial for clearance of pathogens like HBV.

Polyphosphazenes can function as immune modulators as well as delivery-vehicles. They are synthetic, water-soluble polymers with a long backbone of alternating nitrogen and phosphorous atoms with two side groups attached to each phosphorous (Andrianov 2006, Andrianov 2004). They can also be formulated as microspheres and are biodegradable. Complexed with antigen by non-covalent binding, it induces the formation of nanopores in the membrane of cells leading to activation of cellular pumps and therefore activation of the whole cell. In case of APCs, MHCs and co-stimulatory molecules are upregulated (Andrianov 2005, Kabanov 2004). The use of polyphosphazenes like poly[di(sodium carboxylatophenoxy)phosphazene] (PCPP) and poly[di(sodium carboxylatethylphenoxy)-phosphazene] (PCEP) in vaccinations show their strong adjuvant activity with several viral and bacterial antigens (McNeal 1999, Payne 1998, Wu 2001). PCEP does not only enhance the magnitude but also the quality of the immune response in case of an influenza antigen (Mutwiri 2007) and leads to higher antibody responses compared to alum in case of HBsAg (Mutwiri 2008). PCEP induces mixed T_H1 /T_H2-type immune responses in a study using HBsAg (Dar 2012). Its adjuvant activity is the consequence of a strong activation of the innate immune system which leads to upregulation of adjuvant core response genes at the site of injection like T_H1-type IL-2 and IFNγ, T_H2 type IL-4, IL-13 and also TNFα and NFκB. Thus, application of PCEP creates a milieu that attracts monocytes to the site of injection and activates them. In DCs this leads to enhanced antigen presentation (Awate 2012). Most interestingly it upregulates the expression of TLR9 and therefore enhances the effect of CpG if combined in a vaccination. Due to their inability to induce systemic cytokine production and their water-soluble nature, polyphosphazenes are considered to be safe compared to adjuvants like mineral oil or alum that induce reactions at the side of injection (Payne 1998). Their immune stimulatory and safety properties make them interesting candidates to include in vaccinations.

1.5.2 MVA

Modified Vaccinia virus Ankara (MVA) is a strain of vaccinia virus originated from Chorioallantois vaccinia virus Ankara (CVA) that was passaged over 570 times in chicken embryo fibroblasts (CEFs) and has a double-stranded DNA genome. Through the

passaging process the virus lost about 15 percent of its parental genome including genes for virus host range regulation and evasion of host immune responses (Antoine 1998, Meyer 1991). The result is a highly attenuated virus which is strongly restricted to avian cells and unable to replicate in most mammalian cell lines (Meyer 1991, Ramirez 2000, Sutter 1992). The cause of this growth deficiency is a defect during the assembly process of the virus that leads to immature viral particles. Thus, translation of early, intermediate and late genes is not disturbed which allows strong expression of recombinant antigens (Kastenmuller 2006, Moss 1996). In recombinant MVAs, genes of interest are placed under transcriptional control of the viral promoters and can be expressed in distinct levels depending on strong or weak promoters with different activity profiles. The packaging capacity is approximately 50 kb (Staib 2003) which allows expression of several antigens in one viral vector. Expressed antigens are presented on MHC class I by the infected cells, but can also be cross-presented on MHC class II by professional APCs which can directly activate CD8 and CD4 T cells. Since it infects and activates efficiently professional APCs, preferentially DCs, it is highly immunogenic and leads to strong activation of the immune system (Drillien 2004, Liu 2008). Because replication of MVA is strictly located in the cytosol of the host cell, there is no possible integration of viral genes in the host genome. This contributes to an excellent safety profile that is also confirmed in studies using immunodeficient animals (Ramirez 2000, Wyatt 2004). Therefore, MVA can be used under bio-safety level (BSL)-1 conditions and its stability allows freeze-thaw cycles which makes it easy to handle.

Due to its safety but still excellent immunogenicity profile and packaging capacity MVA is widely used in many clinical trials dealing with infectious diseases like HBV, HIV, Malaria (Afolabi 2013, Cavenaugh 2011, Dorrell 2006, Dunachie 2006, Goonetilleke 2006) and also cancer like melanoma, prostate cancer, colon cancer, cervical cancer and lung cancer (Acres 2008, Ramlau 2008). MVA is often used in prime-boost vaccination schemes with DNA or protein prime and MVA boost to overcome weak priming abilities and anti-vector immunity in additional MVA vaccinations (Dunachie 2006, Ramshaw 2000).

1.5.3 Animal models for HBV

As described earlier HBV has a strong host tropism and can only infect chimpanzees and humans. However, chimpanzees are not suitable for large scale experiments due to ethical aspects and high costs. Therefore, some research groups use woodchuck and Peking duck as models to investigate HBV-related hepadnaviruses. Both models contributed to basic knowledge about Hepatitis B (Mason 1983, Summers 1978) and are

also used to study treatments for chronic Hepatitis B (Foster 2003, Kosinska 2013). Not only are these animals difficult to keep and expensive, but the main disadvantage is that therapeutic vaccinations established in these models cannot be used against HBV directly and are therefore more difficult to transfer into human clinical trials.

The most convenient animal for large scale studies is the mouse. It is a well-established animal model which is genetically well characterized. Thus, there are many tools and methods established to investigate processes like immune responses *in* or *ex vivo*. To investigate HBV in the context of a mouse, transgenic lineages expressing partial or complete HBV genomes have been generated (Chen 2000, Chisari 1985, Guidotti 1995). These inbred models are especially suitable for testing new therapies against chronic hepatitis B (CHB) because they provide a well-defined immune system. A lot was learned about viral pathobiology, hepatocellular injury and mechanisms of immune cells responding to HBV antigens (Ando 1993, Guidotti 1994, Guidotti 1996, Milich 1998). But being transgenic and not susceptible to HBV infection there are disadvantages that remain. In mice there is no establishment of cccDNA which limits there applicability for understanding mechanisms of the immune system to eradicate the natural template of HBV replication. Another disadvantage is that treatment can never result in clearance of the virus since every hepatocyte expressing HBV antigens that is eliminated will be replaced with a new transgenic hepatocyte. However, they present a suitable model for studying new therapeutic approaches against CHB since they provide an immune system that is peripheral tolerant to HBV antigens and thus mimics the situation of patients that were infected perinatally with HBV.

To solve these problems and to be able to study acute HBV infections in mice, two additional mouse models were established. The first is a genome transfer via adenoviral vectors and the second by hydrodynamic injections (Huang 2012, Sprinzl 2001, von Freyend 2011, Yang 2002). The main advantage is that these models allow observing clearance of the virus upon “acute HBV infection”. They also mimic the generation of a cccDNA because the transfer plasmid stays in an extra-chromosomal organization. But these models do not overcome the problem that it is not a natural HBV infection and therefore not the whole life cycle is performed. With the adenoviral vector it is also possible to generate a model of chronic HBV infection. Here, the titer of recombinant adenovirus is chosen in such a manner that only low titers of antigens are present on cells and in serum of the mice and therefore the immune system does not respond to HBV antigens (Huang 2012). However, this model is difficult to handle and mice are challenged by two different viruses.

To overcome this issue a model with a chimeric mouse with humanized hepatocytes was generated. Here, the full replication cycle from infection to establishment of cccDNA and

the release of infectious particles can be studied. However, this model is very complex and the mice are immunodeficient (Dandri 2001, Katoh 2008, Mercer 2001) and therefore not suitable for addressing immunological questions.
In this study, the HBV1.3tg mouse was used as a model for CHB which is the most challenging model for inducing immune responses against HBV.

1.6 Aim of the study

Up to date treatment of CHB is not sufficient to cure the patient. Antivirals do control but not eliminate HBV and need to be applied for many years. Due to the long treatment with nucleos(t)ide analogs, escape mutants can develop which leads to loss of viral control. Furthermore patients suffer from severe side effects from IFN-treatment. Therapeutic vaccination represents a promising strategy to eradicate HBV and thus end treatment. Previous work performed in the group was successful in establishing a protein prime / MVA boost vaccination strategy to break immune tolerance in low and intermediate, but not in high antigenemic HBV1.3tg mice.
The aim of this study was to further develop the vaccination strategy to break immune tolerance in high antigenemic HBV1.3tg mice. Therefore, the adjuvant PCEP was tested for its potency to induce CD8 T cell and B cell responses in wildtype and HBV1.3tg mice. Additionally a suitable antigen combination was defined and new recombinant MVAs were generated to elicit a polyclonal and multispecific immune response in high antigenemic HBV1.3tg mice.

2. Results

2.1 Construction of plasmids encoding for HBV proteins core (C) and L

For preparation of new recombinant MVAs expressing HBcAg of subtype adw (C_{adw}) and L_{adw} under control of the strong early/late PH5-promoter, the coding sequences of those proteins were amplified by PCRs (described in 4.4.1). The blunt-ended PCR-products were purified and dephosphorylated. The transfer plasmid pIIIΔHR-PH5 (Fig. 2.1.1) which was used for generation of modified MVA genomes by homologous recombination with the wild-type MVA genome was linearized by PmeI-digest and dephosphorylated to exclude self-ligation.

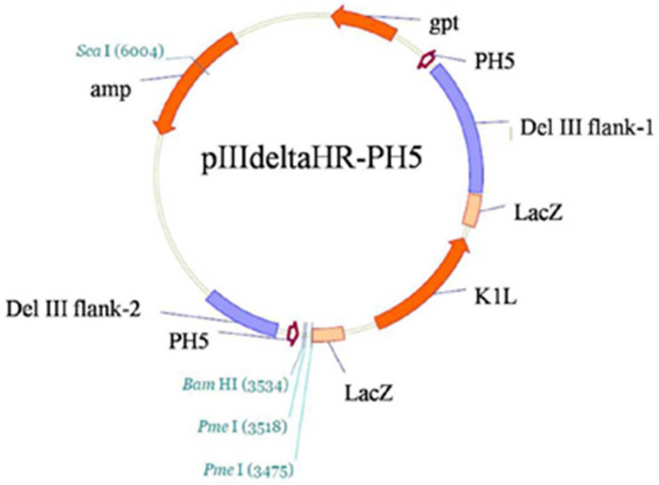

Fig. 2.1.1: Scheme of the transfer plasmid pIIIΔHR-PH5, which was used for generation of modified MVAs by homologous recombination with the MVA genome. The plasmid contains an ampicillin resistance cassette for selection of transformed wild-type bacteria and the K1L gene for selection of recombinant MVA generated in RK-13 cells.

Before ligation was performed, PCR products and linearized plasmid were analyzed by gel-electrophoresis on a 1% agarose gel (Fig. 2.1.2).

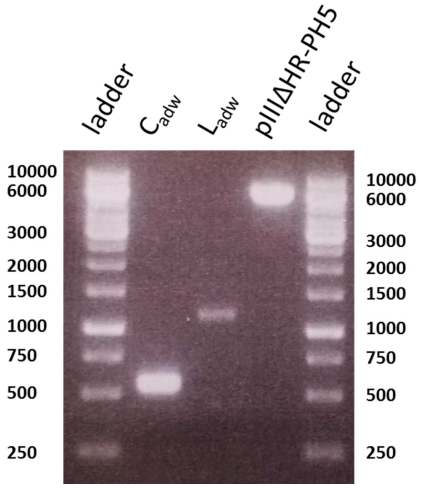

Fig. 2.1.2: Verification of sizes of DNA-fragments used for cloning of MVA-transfer plasmids. 1 % agarose gel of PCR-amplified sequences C_{adw} (552 bp) and L_{adw} (1195 bp) as well as PmeI digested and de-phosphorylated plasmid pIIIΔHR-PH5 (~6000 bp).

After verification of expected sizes of the genes of interest and the cut transfer-plasmid, ligations were performed and subsequently *E. coli* DH10B cells were transformed by electroporation with the respective ligation products.

After selection on LB-agar plates containing ampicillin, eight different clones per construct were picked, plasmid DNA was extracted from respective overnight liquid culture and tested for integration of the genes of interest by control-digestion with PmeI (Fig. 2.1.3).

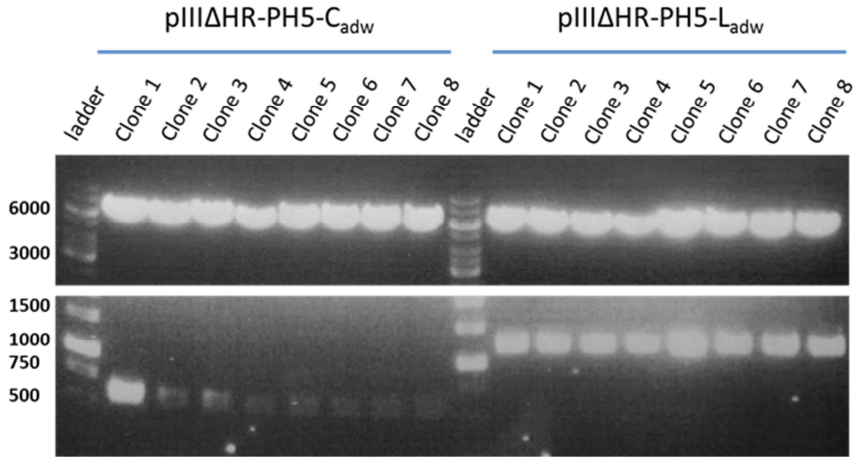

Fig. 2.1.3: Control-digestion of newly constructed transfer plasmids pIIIΔHR-PH5-$Core_{adw}$ and pIIIΔHR-PH5-L_{adw} Plasmid DNA extracted from 8 clones for each construct were digested with PmeI and resulting parts were analyzed by gel-electrophoresis. The upper part shows the digested plasmids and the lower part the inserts of the respective clones.

All clones of each transfer plasmid were positive indicating successful ligations. 4 clones of each construct were sent for sequencing and subsequently clone 3 of pIIIΔHR-PH5-C_{adw} as well as clone 4 of pIIIΔHR-PH5-L_{adw} were chosen for large scale amplification and DNA preparation. The purified plasmids were stored at -20°C.

2.2 Generation of MVA PH5-S_{adw}

To perform vaccination studies in HBVtg mice using the heterologous subtype adw of the HBsAg in protein-prime/MVA-boost immunizations, MVA PH5-S_{adw} was generated by infection of CEF cells with MVA-wt and co-transfection with the transfer plasmid pIIIΔHR-PH5-S_{adw} which was produced by Simone Backes.

Recombinant MVA was selected by plaque picking on RK-13 cells and tested by Del III-specific primers to verify the presence of the inserted gene encoding $HBsAg_{adw}$. After several passages on RK-13 cells with subsequent passaging on CEF cells, a limiting dilution was performed on CEF cells to identify recombinant MVAs that performed a second homologous recombination and thereby lost the K1L marker gene. Clones of the limiting dilution were tested by Del III-PCR and K1L-PCR. As positive control for insertion in deletion III and presence of K1L, a transfer plasmid pIIIΔHR-PH5-C which included K1L was used and the MVA-wt genome was used as negative control.

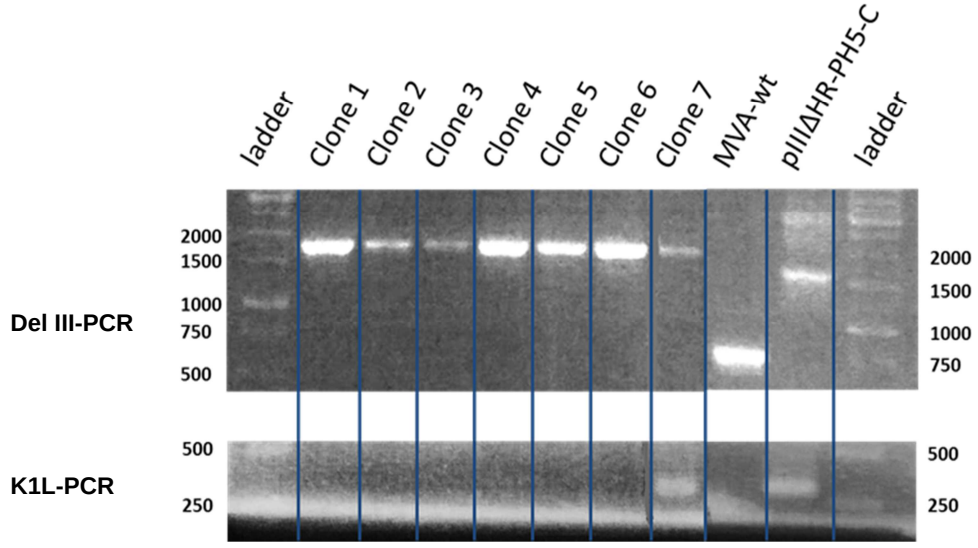

Fig. 2.2.1: PCRs for selecting MVA PH5-S_{adw} clones that lost the marker gene K1L after limiting dilution. The result of the deletion III-specific (Del III) PCR is shown in the upper part and the result of the K1L-PCR is shown in the lower part for respective clones.

As shown in Fig. 2.2.1, MVA clones 1 to 6 were positive for the Del III-PCR and negative for the K1L-PCR indicating that these clones performed the second homologous recombination and lost the K1L-gene. Clone 7 was positive for both PCRs and was therefore not used in further steps.

A 6-well cell culture plate with 90 to 100 % confluent CEF cells was infected with clones 1 to 6. Subsequently, the clone which showed the best infection properties was then amplified in large scale and purified by sucrose gradients.

The prepared MVA PH5-S_{adw} stock was then titrated and tested for HBsAg expression by measuring HBsAg in supernatant of infected HuH 7 cells 48 h post infection with the AxSYM HBsAg (V2) Reagent Pack (Fig. 2.2.2).

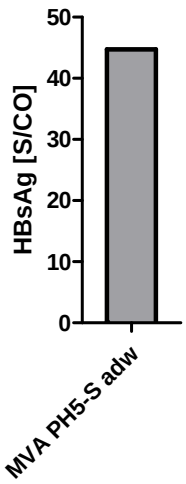

Fig. 2.2.2: HuH 7 cells were infected with MVA PH5-S_{adw} (MOI=100) for 48 h. HBsAg was determined in supernatant of the cell culture in a 1:20 dilution. S/CO = signal to cutoff

As indicated by high HBsAg levels in the supernatant of the infected cell culture, the selected and purified recombinant MVA expressed the protein of interest and was therefore suitable for subsequent *in vivo* vaccination studies.

2.3 Vaccination studies in C57BL/6 (wt) mice

In previous studies by Dr. Simone Backes, it was shown that protein-prime / MVA-boost vaccinations using HBsAg/HBcAg supplemented with adjuvant CpG and MVA-S/MVA-C induced strong HBV-specific CD8 T cell responses in wt mice. Importantly this regimen also induced HBV-specific CTL responses in low (HBeAg = 0 S/CO) and intermediate (HBeAg < 7 S/CO) antigenemic HBVtg mice, which serve as models for CHB. However, it was found that high antigenemia (HBeAg > 7 S/CO) prevented the induction of HBV-specific immune responses. Thus it was necessary to find adjuvants or a combination of adjuvants that would be able to induce a stronger HBV-specific immune response which could overcome tolerizing effects caused by high antigenemia.

2.3.1 Comparison of different adjuvants and their combinations

To test which combination of adjuvants would improve the vaccination strategy, adjuvants CpG and PCEP were tested either individually or in combination in 8 week old female C57BL/6 mice according to the vaccination scheme depicted in Fig. 2.3.1.1 A. The

combination of the two antigens HBs and HBc was expected to induce a broader HBV-specific immune response and also to benefit from the immunogenicity of HBcAg and its effect on B cells which is similar to effects of an adjuvant (Milich 1997).On day 0, the first group of mice (1) received 31.91 µg CpG (which is equivalent to 5 µl of a 1 mM solution of CpG in sterile H_2O), 16 µg HBsAg and 16 µg HBcAg; the second group (2) received 50 µg PCEP, 16 µg HBsAg and 16 µg HBcAg whereas the third group (3) received 31.91 µg CpG, 50 µg PCEP, 16 µg HBsAg and 16 µg HBcAg. All groups of mice were boosted on day 28 with $5x10^7$ IU MVA P7.5-S and $5x10^7$ MVA PH5-C. On day 8, three mice of each group were sacrificed, splenocytes were purified and analyzed by ICS after stimulation with HBV-derived peptides (Kuhober 1996, Schirmbeck 2003, Tscharke 2005). Antibody titers were determined in sera of the remaining mice on day 28 prior to the boost vaccination. On day 34, mice were sacrificed, splenocytes were purified and analyzed by ICS after stimulation with HBV- and MVA-derived peptides and antibody-titers were determined in sera.

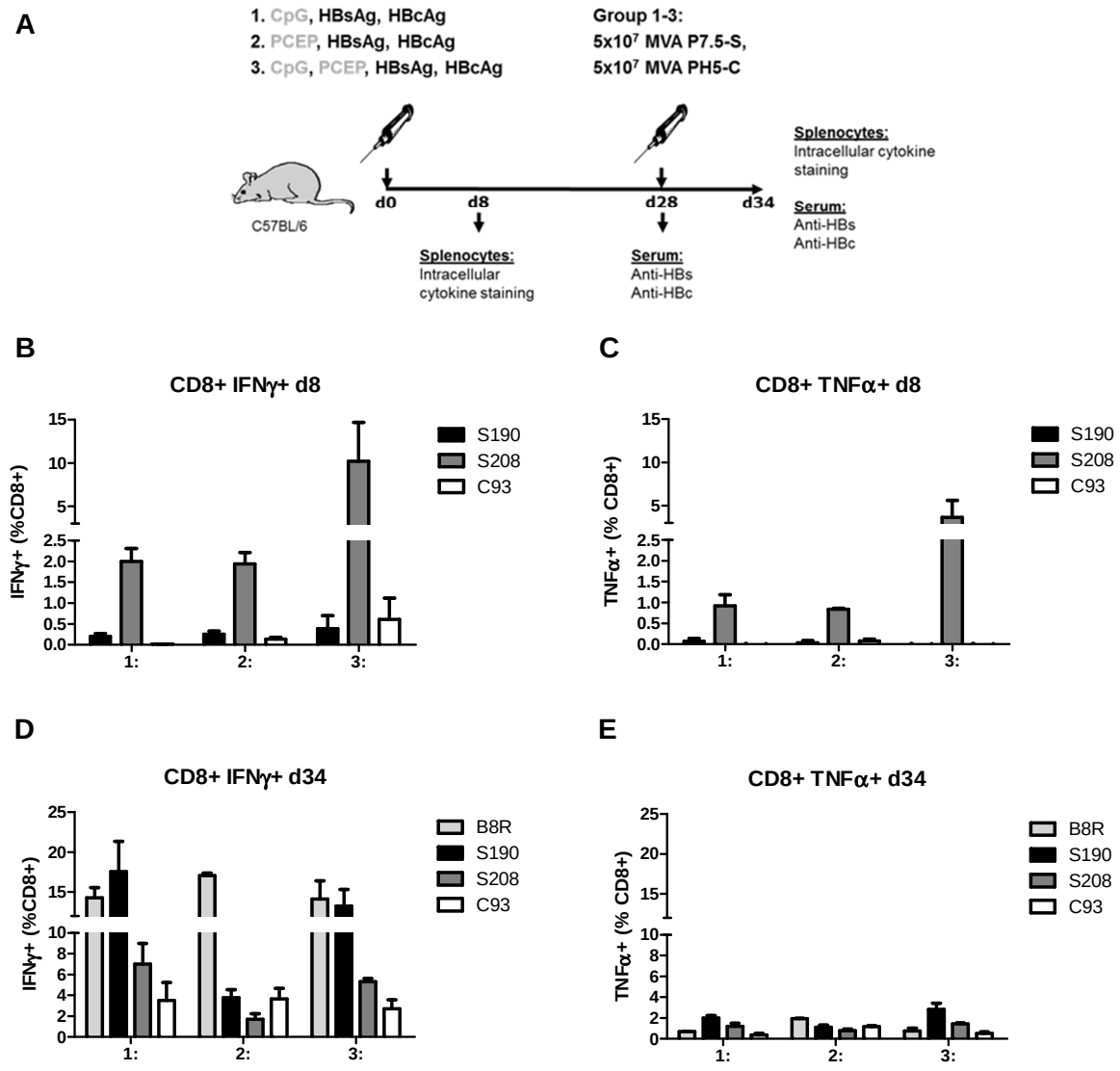

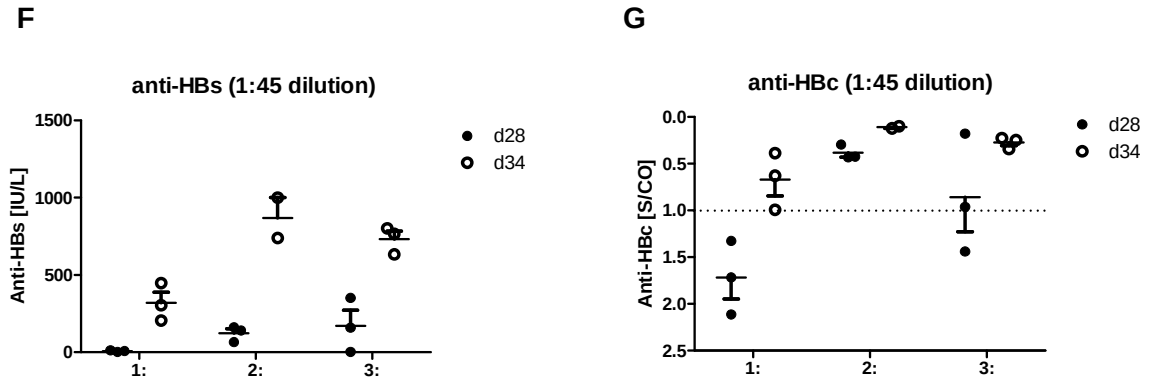

Fig. 2.3.1.1: Comparison of adjuvants CpG, PCEP and the combination of both. Wt mice were vaccinated as shown in (A). On day 8, isolated splenocytes were stimulated with HBV-derived peptides S190, S208 or C93 and analyzed for IFNγ (B) and TNFα (C) expression by ICS. On day 34 post prime, splenocytes were stimulated with HBV-derived peptides S190, S208 or C93 and MVA-derived peptide $B8R_{20}$ and analyzed for IFNγ (D) and TNFα (E) expression by ICS. Titers of anti-HBs (F) and anti-HBc (G) were measured in sera on day 28 and 34. S/CO = signal to cutoff; dashed line = limit of detection; frequencies of IFNγ+ and TNFα+ CD8+ T cells are background subtracted.

As shown in Fig. 2.3.1.1 B and C, HBV-specific CD8 T cells producing IFNγ and TNFα were detected on day 8 post prime immunization. Mice of all groups developed CD8 T cell responses against both HBsAg-epitopes with a stronger response against S208 (Fig. 2.3.1.1 B and C). IFNγ producing T cells against HBcAg-derived peptide C93 were detected in group 2 and 3 (Fig. 2.3.1.1 B), but TNFα-producing T cells were not found (Fig. 2.3.1.1 C). Group 3 which received the combination of PCEP and CpG showed the strongest CD8 T cell responses. At day 34, all groups showed enhanced total HBV-specific CD8 T cell responses (Fig 2.3.1.1 D and E) with the weakest response in group 2. In group 3 a shift in the response directed against the endogenous S190 epitope was observed. Post prime the T cell response against the exogenous S208-epitope was stronger compared to the endogenous S190-epitope. In contrast the T cell response against S190 was stronger than against S208 post boost (Fig. 2.3.1.1 B and D). Similar T cell responses in all groups against $B8R_{20}$ the MVA-derived peptide (Fig. 2.3.1.1 D and E) indicated comparable efficiency of the boost vaccination. 28 days post prime, antibodies against HBs- and HBcAg were detected in groups 2 and 3 which received a vaccine formulation containing PCEP, whereas no antibodies were present in group 1 (Fig. 2.3.1.1 F and G). Due to the MVA boost, the antibody titers were increased on day 34 (Fig. 2.3.1.1 F and G).

In summary, the T cell response of group 1 was slightly stronger compared to group 3 post boost, but anti-HBs titers were twice as high in groups 2 and 3. Therefore, the overall immune response of group 3 was considered stronger than the one of groups 1 and 2.

To investigate whether the adjuvant alum has an additional effect on the induction of immune responses, the commercial vaccine Engerix B containing HBsAg and aluminum hydroxide was tested in 8 week old female C57BL/6 mice within an analog experiment depicted in Fig. 2.3.1.2 A. For priming, the first group of mice (1) received 31.91 µg CpG, 16 µg HBcAg and 10 µl Engerix B containing 0.2 µg HBsAg; the second group (2) received 50 µg PCEP, 16 µg HBcAg and 10 µl Engerix B whereas the third group (3) received 31.91 µg CpG, 50 µg PCEP, 16 µg HBcAg and 10 µl Engerix B. All groups of mice were boosted on day 28 with $5x10^7$ MVA P7.5-S and $5x10^7$ MVA PH5-C. On day 8, three mice of each group were sacrificed; splenocytes were purified and analyzed by ICS after stimulation with HBV-derived peptides. Antibody-titers were determined in sera of the remaining mice on day 28 prior to the boost vaccination. On day 34, mice were sacrificed, splenocytes were purified and analyzed by ICS after stimulation with HBV- and MVA-derived peptides and antibody-titers were determined in sera.

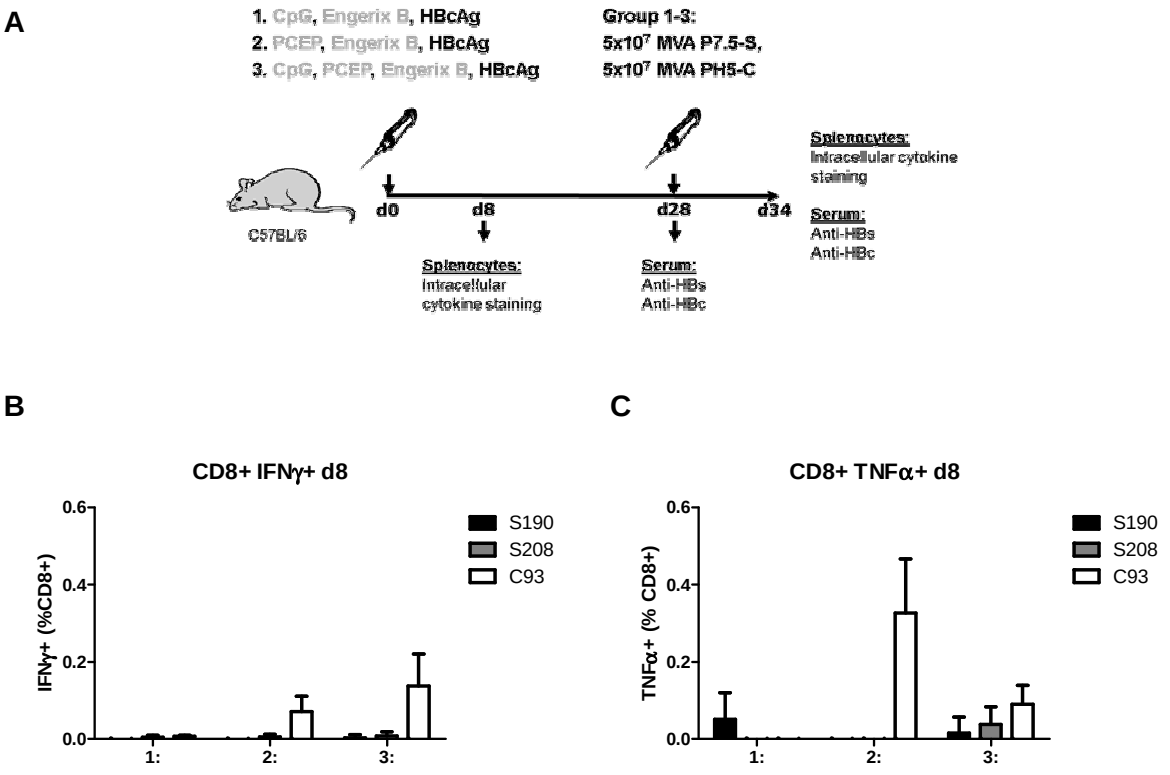

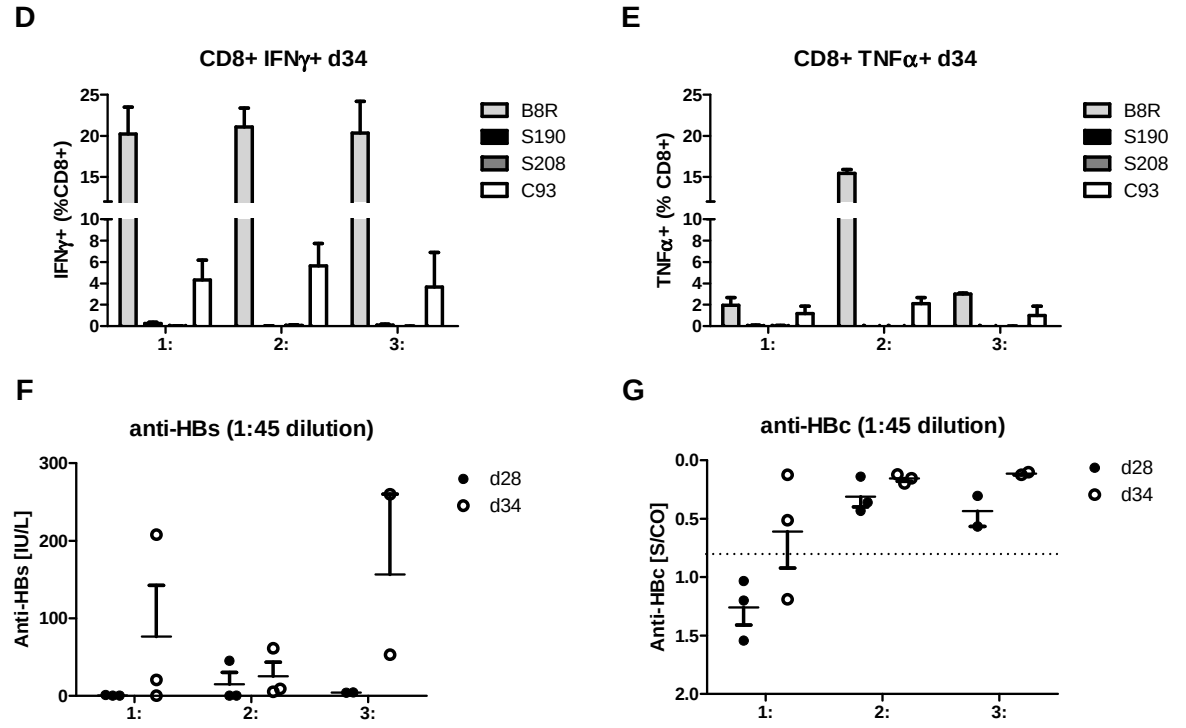

Fig. 2.3.1.2: Comparison of adjuvants aluminum hydroxide, CpG, PCEP and their combinations. Wt mice were vaccinated as shown in in (A). On day 8, splenocytes were stimulated with HBV-derived peptides S190, S208 or C93 and analyzed for IFNγ (B) and TNFα (C) expression by ICS. On day 34 post prime, splenocytes were stimulated with HBV-derived peptides S190, S208 or C93 and MVA-derived peptide $B8R_{20}$ and analyzed for IFNγ (D) and TNFα (E) expression by ICS. Titers of anti-HBs (F) and anti-HBc (G) were measured in sera on day 28 and 34 (F) and (G). S/CO = signal to cutoff; dashed line = limit of detection; frequencies of IFNγ+ CD8+ T cells are background subtracted.

In contrast to vaccinations tested within the first experiment including recombinant HBsAg and HBcAg without the adjuvant alum, the vaccinations containing Engerix B did not result in T cell responses against HBs-specific epitopes. Addition of PCEP induced a weak T cell response against C93 (Fig. 2.3.1.2 B and C). After Engerix B prime, MVA boost was not able to elicit a strong T cell response against HBsAg, but efficiently enhanced the T cell response against C93 (Fig. 2.3.1.2 D and E). The T cell responses against MVA-$B8R_{20}$ were similar in all groups (Fig. 2.3.1.2 D and E) demonstrating similar infection rates of MVA in all groups. Interestingly, while anti-HBs antibody titers in all investigated groups were only slightly above background, anti-HBc antibodies were readily detectable in groups 2 and 3 which received vaccines containing PCEP (Fig. 2.3.1.2 F and G). The titers of anti-HBs and anti-HBc antibodies were increased in all groups post boost (Fig. 2.3.1.2 F and G).

The outcome of above experiments suggested that vaccine formulations containing Engerix B were not suited to elicit T cell responses against HBsAg. Most likely the amount of HBsAg in Engerix B was not sufficient to elicit a T_H1-type T cell response against HBsAg. More interestingly, addition of the adjuvant aluminum hydroxide did not enhance the efficiency of

the vaccine formulation with respect to the induction of HBcAg-specific CD8 T cell responses.

2.3.2 Effects of multiple immunizations with the protein vaccine

To test if multiple immunizations with the protein vaccine would enhance HBV-specific cellular and humoral immune responses to a similar extent like boost vaccinations with recombinant MVA, six 8 week old female wt mice were vaccinated on day 0, 28 and 49 with 31.91 µg CpG, 50 µg PCEP, 16 µg HBsAg and 16 µg HBcAg (Fig. 2.3.2 A). Titers of anti-HBs antibodies were determined on day 21 and 28 before immunization in sera of the mice. Three mice were sacrificed on day 36 and the remaining three mice on day 55. At both time points, splenocytes restimulated *ex vivo* with HBV-derived peptides and CD8 T cell responses were analyzed by ICS.

As shown in Fig. 2.3.2 B, the frequency of HBV-specific CD8 T cells was not increased after three vaccinations. These data indicate that a boost immunization with recombinant MVA is necessary to induce a significantly stronger T cell immune response. In contrast, anti-HBs antibody titers were boosted by factor 2 after the second immunization, and remained stable at high levels after the third protein vaccination (Fig. 2.3.2 C).

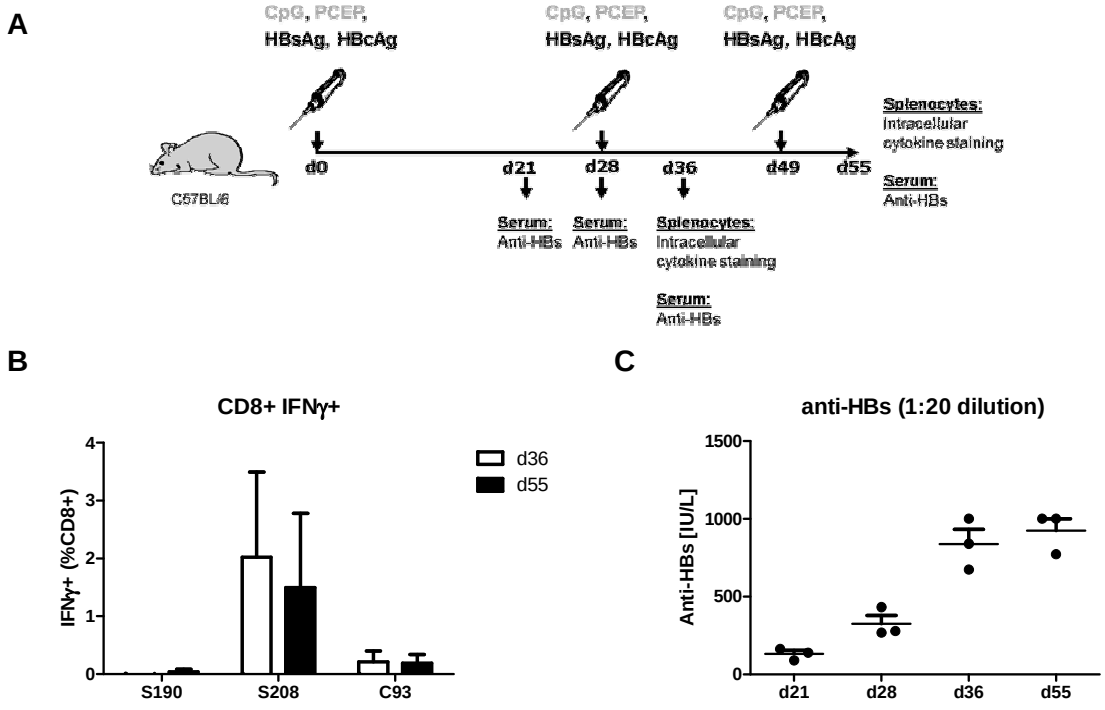

Fig. 2.3.2: Multiple immunization of C57BL/6 mice. (A) Experimental setup for immunizations of mice with the protein vaccine formulation containing 31.91 µg CpG, 50 µg PCEP, 16 µg HBsAg and 16 µg HBcAg. On day 36 and 55, splenocytes were stimulated with HBV-derived peptides S190, S208 or C93 and analyzed for IFNγ expression by ICS (B). Titers of anti-HBs were measured in sera on day 21, 28, 36 and 55 (C). Frequencies of IFNγ+ CD8+ T cells are background subtracted.

Taken together, multiple protein-based immunizations were able to induce strong antibody but rather weak T cell responses. Thus, the heterologous protein-prime / MVA-boost vaccination regimen described above proved to be the superior strategy.

2.3.3 Investigation of effects by endotoxin contamination of HBcAg

The provider of HBcAg that was produced in *E. coli* changed after the first experiments and there was no information available about endotoxin levels of the new HBcAg. Therefore, the new HBcAg as well as the protein vaccine containing CpG, PCEP, HBsAg and the new HBcAg were tested with a Toxinsensor Chromogenic LAL Endotoxin Assay Kit. Both were tested in two dilutions (1:1000 and 1:15000). The calculated value was 134.5 EU (endotoxin units) per vaccine dose. To investigate whether these endotoxin levels might be sufficient to induce an HBcAg-specific T cell response, female 8 week old wt mice were immunized with either (1) 16 µg HBcAg without adjuvants or (2) 16 µg HBcAg adjuvanted with 31.91 µg CpG and 50 µg PCEP. On day 8 post immunization, splenocytes were analyzed for IFNγ, TNFα and IL-2 secretion upon stimulation with $HBcAg_{93}$ peptides or the HBc peptide pool 3 (Fig. 2.3.3 A).

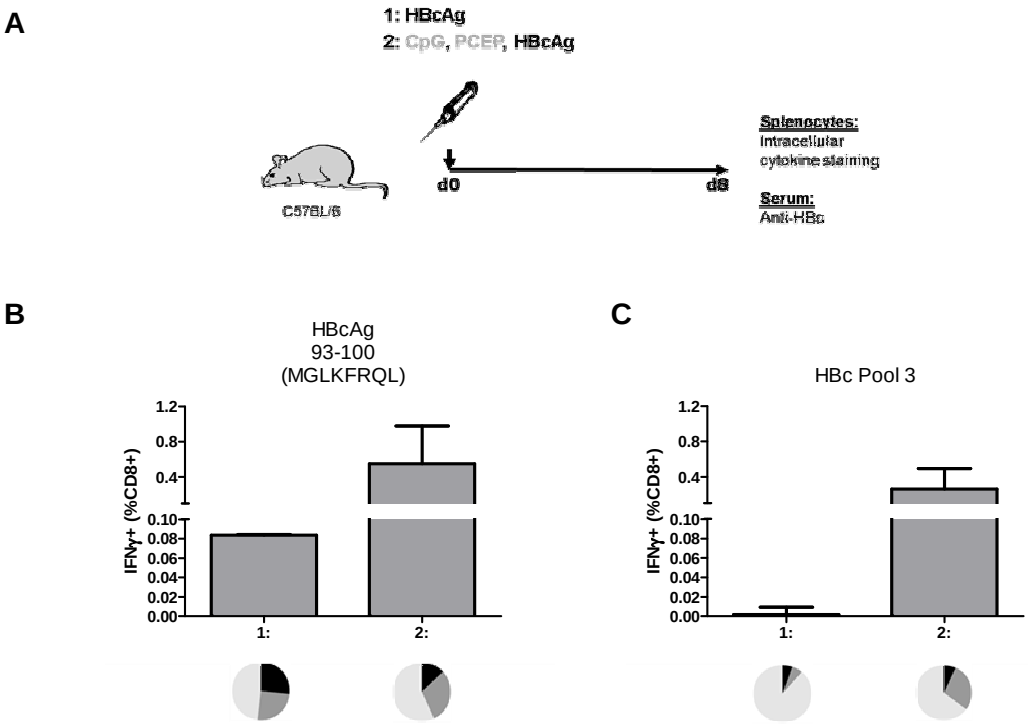

D

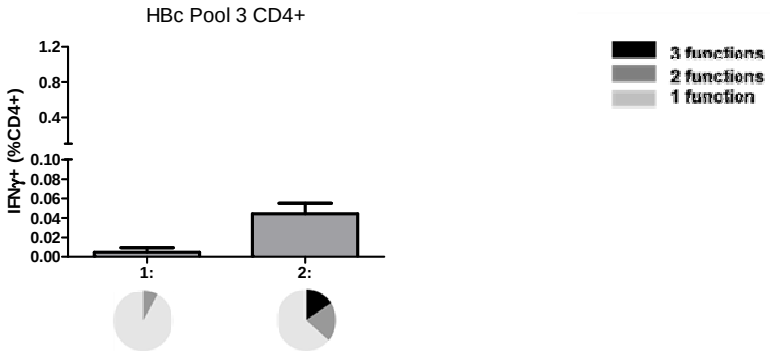

Fig. 2.3.3: Comparison of T cell responses upon immunization with HBcAg without ajuvants and HBcAg adjuvanted with CpG and PCEP in C57BL/6 mice. (A) Vaccination scheme. On day 8, isolated splenocytes were stimulated with HBcAg-derived peptide C93 or HBc Pool 3 containing HBcAg-derived 15mers and CD8 T cells (B and C) as well as CD4 T cells (D) were analyzed for IFNγ, TNFα, IL-2 expression by ICS. Frequencies of IFNγ+ CD8+ and CD4+ T cells are background subtracted.

FACS analysis of ICS (Fig. 2.3.3 B, C and D) showed that HBcAg alone was not sufficient to elicit an HBcAg-specific CD8 T cell response since IFNγ-producing T cells were hardly detected in mice immunized with HBcAg without adjuvants. Pie charts indicating the relative fractions of polyfunctional (black: expression of 3 cytokines), multifunctional (dark grey: expression of 2 cytokines) and monofunctional (light grey: expression of 1 cytokine) CD8 T cells among the total population of responding CD8 T cells showed differences for the cells stimulated with HBc Pool 3, but not with peptide C93. Splenocytes from immunized mice with adjuvanted HBcAg showed a stronger polyfunctionality than those isolated from mice immunized only with HBcAg (Fig. 2.3.3 C and D). The frequency of cytokine producing CD4 T cells was very low overall (Fig. 2.3.3 D).

Taken together, endotoxin present in the HBcAg solution used for vaccinations plays only a minor role in inducing T cell responses.

2.3.4 Test of vaccination strategy in HHDII mice

To test the vaccination strategy in a setting of human MHC molecules, HHDII mice were used as model organisms. HHDII mice are transgenic for human MHC HLA-A2 but are deficient in β2m and H-2D^b expression, which prevents antigen presentation on murine MHC class I molecules. As depicted schematically in Fig. 2.3.4, 6 week old mice were vaccinated on day 0 with 31.91 µg CpG, 50 µg PCEP, 16 µg HBsAg and 16 µg HBcAg and boosted on day 28 with 5x10^7 MVA P7.5-S and 5x10^7 MVA PH5-C. On day 34, mice were sacrificed, splenocytes were isolated and analyzed by ICS after stimulation with HBV- and MVA-derived

peptides (Drexler 2003, Nayersina 1993, Zhang 2007) and antibody-titers were determined in sera.

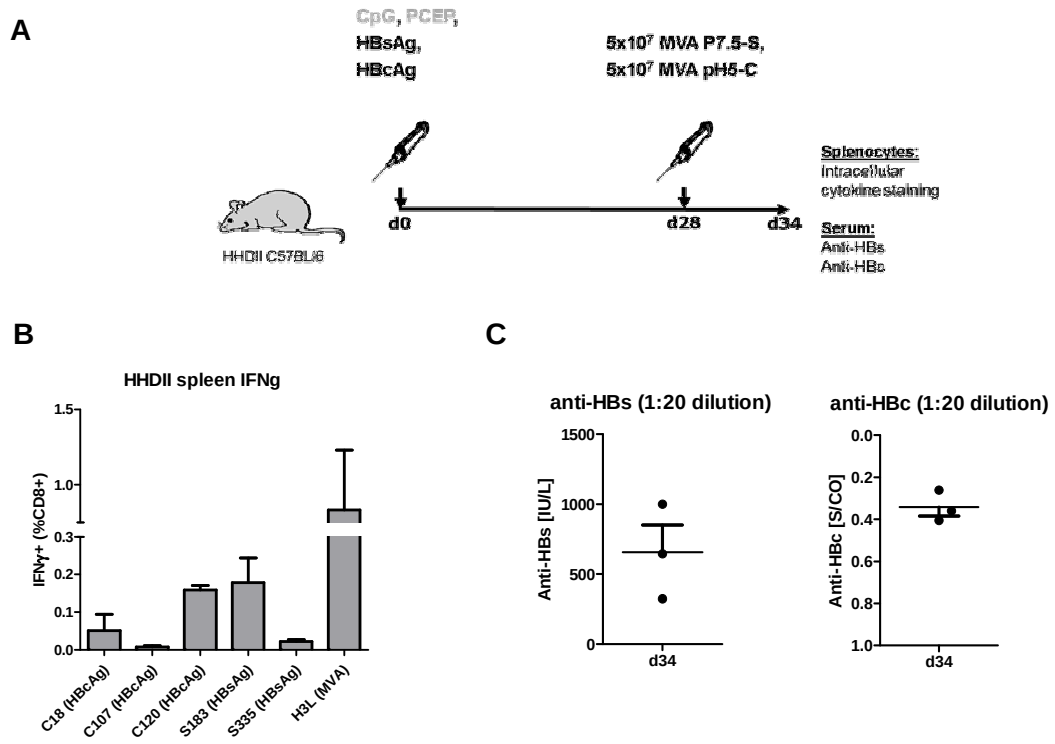

Fig. 2.3.4: Vaccination study in HHDII mice. (A) Vaccination scheme. On day 34, splenocytes were stimulated with indicated HBV-derived peptides and MVA-derived peptide H3L. (B) CD8 T cells were analyzed for IFNγ expression by ICS. (C) Titers of anti-HBs and anti-HBc were measured in sera on day 34 (C). S/CO = signal to cutoff; frequencies of IFNγ+ CD8+ T cells are background subtracted.

As shown in Fig. 2.3.4 B, HBV-specific CD8 T cell responses were induced in this mouse model and T cell responses were strongest upon stimulation with epitopes C120 and S183. Moreover, high titers of anti-HBs antibodies were measured and anti-HBc antibodies were detected (Fig. 2.3.4 C).

Taken together, the results show that the established vaccination protocol was also able to elicit HBV-specific immune responses in a mouse model with human MHC HLA-A2 molecules.

2.4 Vaccination studies in HBVtg mice

Since the aim of this study was to develop a vaccination strategy which is effective against HBV in a setting of chronic infection, the protein-prime, MVA-boost vaccination scheme was tested in our model of chronic HBV infection: the HBVtg mouse.

2.4.1 Comparison of different antigen combinations and MVA promoters

The first step to establish a vaccination protocol that is able to induce cellular and humoral immune responses in high antigenemic HBVtg mice was to test different antigen combinations and different promoters used to express HBV antigens by MVA. Therefore, HBVtg mice with an HBeAg titer higher than 10 S/CO were vaccinated on day 0 with (1) 31.91 µg CpG, 50 µg PCEP, 16 µg $HBsAg_{ayw}$ and 16 µg HBcAg; (2) 31.91 µg CpG, 50 µg PCEP, and 16 µg $HBsAg_{ayw}$; (3) 31.91 µg CpG, 50 µg PCEP and 16 µg HBcAg; (4) 31.91 µg CpG, 50 µg PCEP, 16 µg $HBsAg_{adw}$ and 16 µg HBcAg or (5) 31.91 µg CpG, 50 µg PCEP and 16 µg $HBsAg_{adw}$. On day 28, groups of mice were boosted as follows: (1) $5x10^7$ MVA P7.5-S_{ayw} and $5x10^7$ MVA PH5-C; (2) $1x10^8$ MVA P7.5-S_{ayw}; (3) $1x10^8$ MVA PH5-C; (4) $5x10^7$ MVA PH5-S_{adw} and $5x10^7$ MVA PH5-C or (5) $1x10^8$ MVA PH5-S_{adw} as shown in Fig. 2.4.1 A. An additional group of HBVtg mice (6) was vaccinated with adjuvants PCEP and CpG on day 0 and boosted on day 28 with MVA-wt to study if adjuvants together with MVA-wt and HBV-antigens circulating in the mouse are sufficient to induce an HBV-specific immune response. On day 34, splenocytes and liver-associated lymphocytes (LAL) were purified and stimulated with HBs-derived peptides S190, S208 and the HBc-derived peptide C93. The frequency of IFNγ-producing CD8 T cells was determined by ICS and subsequent FACS analysis. The presence of HBsAg and titers of antibodies against HBs and HBc were measured on day 0 and 34 in sera of vaccinated mice.

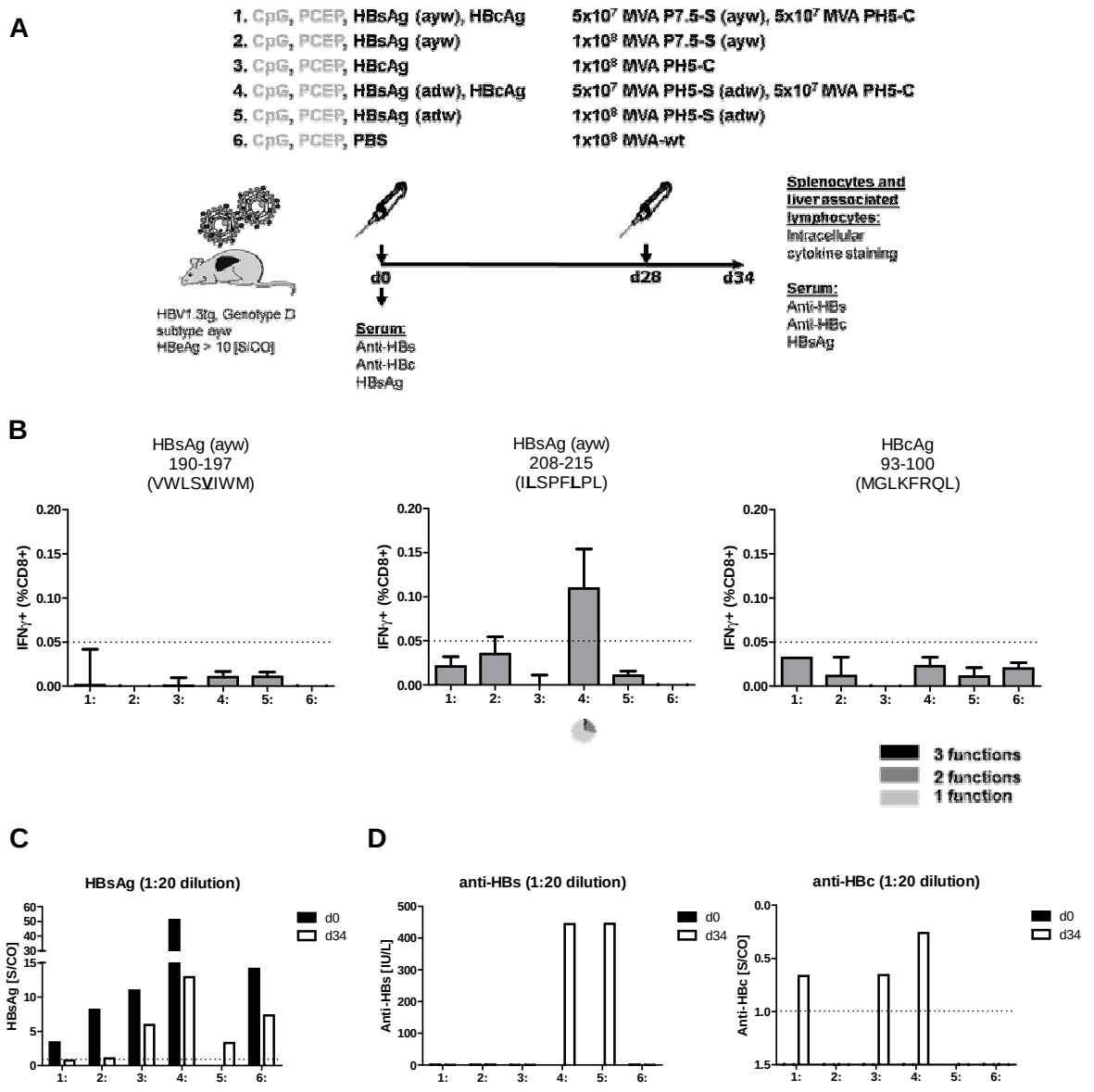

Fig. 2.4.1: Comparison of T cell responses upon immunization with different antigens and recombinant MVA with different promoters. (A) Vaccination scheme. On day 34, splenocytes were stimulated with HBV-derived peptides S190, S208 or C93 and CD8 T cells were analyzed for IFNγ, TNFα and IL-2 (B) expression by ICS. The pie chart indicates T cells that produce 3, 2 and 1 cytokines (B). Titers of HBsAg (C), anti-HBs and anti-HBc in pooled sera were measured on day 0 and 34 (D). dashed line = threshold of T cell responses (B) or detection limit (C and D); S/CO = signal to cutoff; frequencies of IFNγ+ CD8+ T cells are background subtracted.

Group 4 that received CpG, PCEP, $HBsAg_{adw}$ and HBcAg in prime and MVA PH5-S_{adw} together with MVA PH5-C in boost vaccination was the only group that showed a polyfunctional CD8 T cell response in spleen meaning splenocytes produced more than 1 cytokine (Fig. 2.4.1 B) against one of the used HBV-derived peptides upon stimulation. Interestingly, the detected CD8 T cell response was directed against the S208-peptide of subtype ayw which is heterologous to the subtype included in the vaccine formulation but homologous to the subtype that is expressed in the HBVtg mice. HBsAg levels decreased in all groups with the strongest decrease observed in group 4 (Fig. 2.4.1 C). Antibodies against

HBs were detected in mice vaccinated with $HBsAg_{adw}$, whereas antibodies against HBc were detected in all groups that were vaccinated with HBcAg (Fig. 2.4.1 D). Vaccination with adjuvants and MVA-wt did not lead to HBV-specific immune responses.

From these experiments it was concluded that prime immunization with heterologous $HBsAg_{adw}$ protein followed by boosting with recombinant MVA constructs expressing HBsAgadw and HBcAg under control of the strong viral promoter PH5 was most the effective strategy for the induction of HBV-specific immune responses in HBVtg mice.

2.4.1.1 Neutralization of HBV subtype ayw with $HBsAg_{adw}$ induced antibodies

Since the AxSYM kit used for determination of anti-HBs antibodies detects antibodies against the subtypes ayw and adw of HBsAg and anti-HBs antibodies were only detected in groups that were vaccinated with HBsAg subtype adw, sera of mice containing anti-HBs vaccinated on day 0 with 31.91 µg CpG and 50 µg PCEP, 16 µg $HBsAg_{adw}$,16 µg HBcAg and on day 28 with $5x10^7$ MVA PH5-S_{adw} and $5x10^7$ MVA PH5-C of the experiment shown in Fig. 2.4.1.1 were tested for their ability to neutralize HBV subtype ayw in an *in vitro* neutralization assay described in 4.6.13.

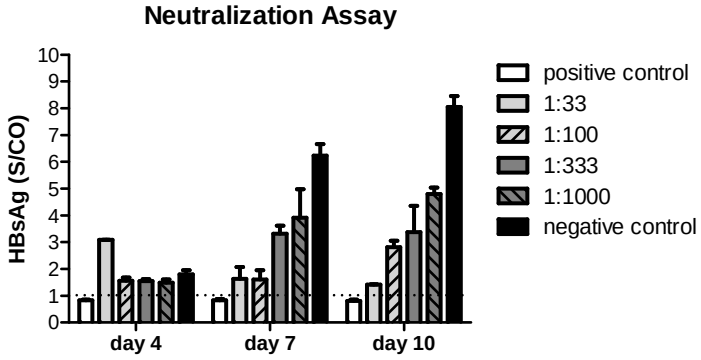

Fig. 2.4.1.1: Produced HBsAg by differentiated HepaRG cells infected with HBV subtype ayw in the presence of serum containing anti-HBs. Titers of HBsAg in supernatants of cultured cells were measured on day 4, 7 and 10. dashed line = detection limit; s/co = signal to cutoff

As shown in Fig. 2.4.1.1, the levels of HBsAg in the supernatant of cultured HepaRG cells that were infected in the presence of 1:33 diluted anti-HBs containing serum decreased over time. HBsAg levels were increased at day 10 if anti-HBs containing serum was diluted further.

This indicated that antibodies secreted upon vaccination with $HBsAg_{adw}$ were able to neutralize HBV subtype ayw. However, the neutralizing capacity of anti-HBs containing sera

derived from $HBsAg_{ayw}$ vaccinated wt mice was found to be three times higher at the same dilution (personal communication with Dr. Claudia Dembek).

2.4.2 Comparison of vaccination schemes with two or three injections

To test if it is beneficial for the induction of HBV specific immunity to have two immunizations with the protein vaccine instead of one, HBVtg mice vaccinated with 31.91 µg CpG, 50 µg PCEP, 16 µg $HBsAg_{adw}$ and 16 µg HBcAg (1) on day 0 and $5x10^7$ MVA PH5-S_{adw} and $5x10^7$ MVA PH5-C on day 28 were compared to HBVtg mice vaccinated on day 0 and day 14 with 31.91 µg CpG, 25 µg PCEP, 16 µg $HBsAg_{adw}$ and 16 µg HBcAg, followed by immunization with $5x10^7$ MVA PH5-S_{adw} and $5x10^7$ MVA PH5-C (2) as shown in Fig. 2.4.2 A. The dosage of PCEP was 50 µg per mouse in total because a small granuloma-like structure was observed at the injection side of the protein vaccine. Mice were sacrificed on day 34; splenocytes and LALs were purified and analyzed for immune responses by ICS after stimulation with HBV- and MVA-derived peptides. HBe- and HBsAg levels as well as HBV-specific antibody titers in sera were determined on day 0 and day 34.

As shown in Fig. 2.4.2 B and C, the vaccination strategy with three immunizations did not enhance HBV-specific immune responses compared to the vaccination strategy with two immunizations. In more detail, one individual immunized two times responded better than the others from the same group upon stimulation with $S208_{ayw}$ and $S208_{adw}$. The response of one individual that received three immunizations was weaker than the response of the other mice of the same group upon stimulation with the MVA-derived peptide $B8R_{20}$ that is considered to be a marker for successful vaccination. Interestingly this individual showed similar responses upon stimulation with HBsAg-derived peptides compared to the rest of the group (Fig. 2.4.2 B and C). The qualities of the T cell responses in both groups were similar as indicated by the pie charts (Fig. 2.4.2 B and C). HBsAg levels decreased in both groups, whereas HBeAg levels were not significantly affected (Fig. 2.4.2 D and E). Titers of HBV-specific antibodies were comparable in both groups (Fig. 2.4.2 F and G).

A

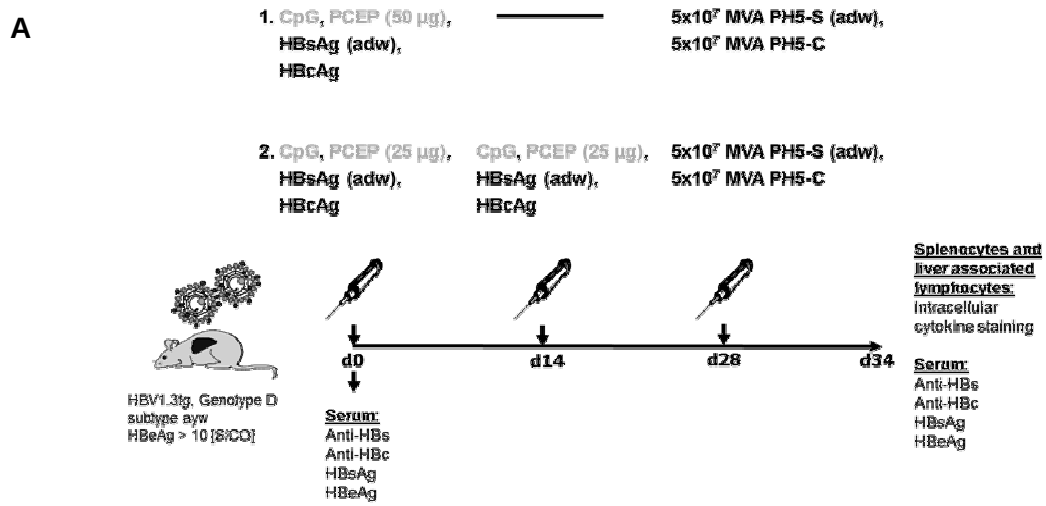
1. CpG, PCEP (50 µg), HBsAg (adw), HBcAg
5x10⁷ MVA PH5-S (adw), 5x10⁷ MVA PH5-C
2. CpG, PCEP (25 µg), HBsAg (adw), HBcAg
CpG, PCEP (25 µg), HBsAg (adw), HBcAg
5x10⁷ MVA PH5-S (adw), 5x10⁷ MVA PH5-C
HBV1.3tg, Genotype D subtype ayw HBeAg > 10 [S/CO]
d0
d14
d28
d34
Serum: Anti-HBs Anti-HBc HBsAg HBeAg
Splenocytes and liver associated lymphocytes: intracellular cytokine staining
Serum: Anti-HBs Anti-HBc HBsAg HBeAg

B

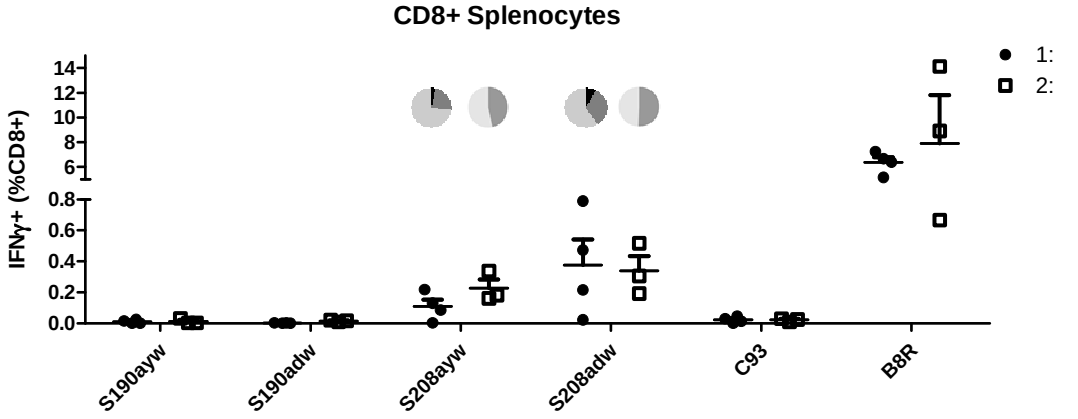
CD8+ Splenocytes
IFNγ+ (%CD8+)
1:
2:
S190ayw
S190adw
S208ayw
S208adw
C93
B8R

C

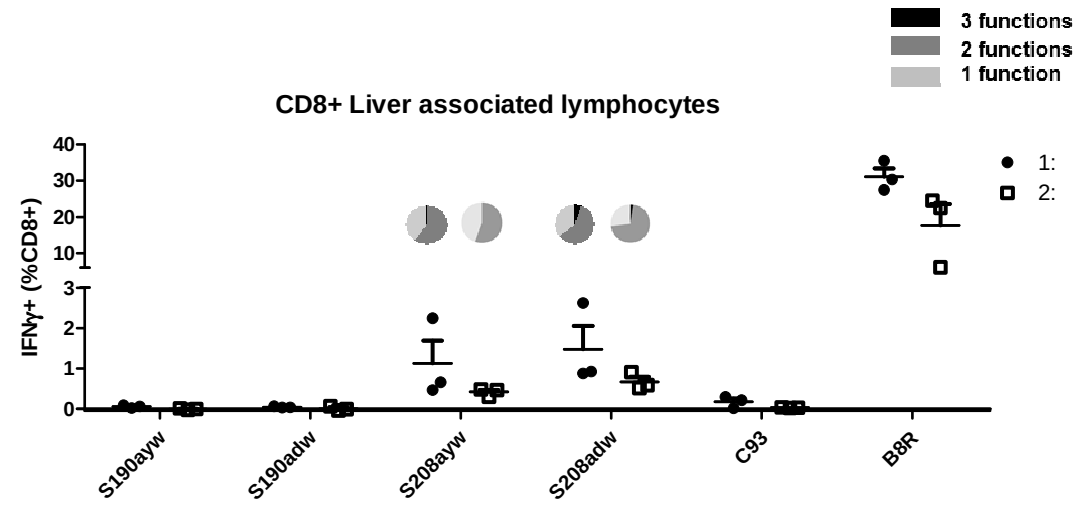
3 functions
2 functions
1 function
CD8+ Liver associated lymphocytes
IFNγ+ (%CD8+)
1:
2:
S190ayw
S190adw
S208ayw
S208adw
C93
B8R

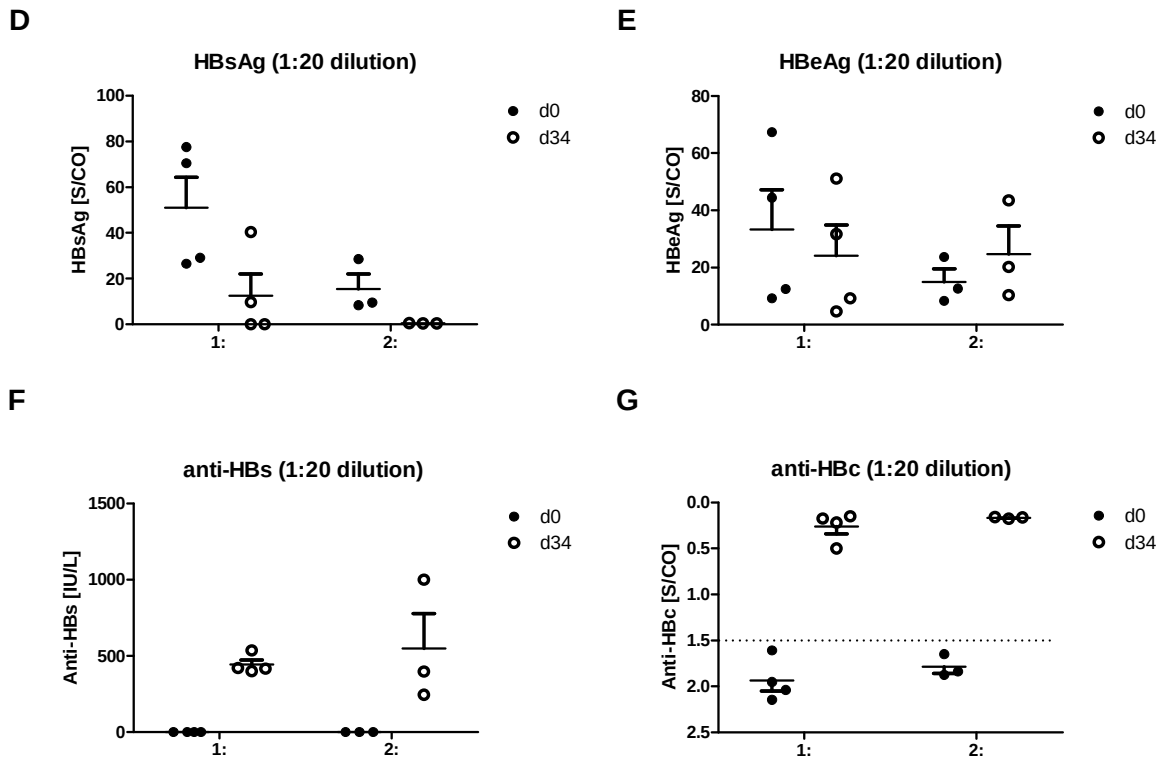

Fig. 2.4.2: Comparison of T cell responses upon immunization with different vaccination schemes shown in (A). On day 34, splenocytes (B) and LALs (C) were stimulated with indicated peptides and CD8 T cells were analyzed for IFNγ, TNFα and IL-2 expression by ICS. Pie charts are shown for immune responses against HBsAg-derived peptides $S208_{ayw}$ and $S208_{adw}$. Titers of HBsAg (D), HBeAg (E), anti-HBs (F) and anti-HBc (G) were measured in sera on day 0 and 34. dashed line = detection limit (G); S/CO = signal to cutoff; frequencies of IFNγ+ CD8+ T cells are background subtracted.

Taken together, the induced HBV-specific immune responses were similar after treatment with both vaccination schemes. The granuloma-like structures were found to be smaller in mice receiving three immunizations after the first, but reached equal size after the second injection.

2.4.3 Comparison of HBsAg subtypes ayw and adw

Since the protein formulation containing $HBsAg_{ayw}$ was boosted with a MVA that expressed $HBsAg_{ayw}$ under the control of the weak early/late promoter P7.5 in HBVtg mice (shown in 2.4.1), I wanted to evaluate the impact of the promoter used for expression in the MVA vector. Therefore, MVA PH5-S_{ayw} was prepared to study whether stronger expression HBsAg might be crucial for eliciting an HBsAg-specific T cell response. Two groups of HBVtg mice were vaccinated on day 0 and day 14 with either 31.91 µg CpG, 25 µg PCEP, 16 µg $HBsAg_{ayw}$ and 16 µg HBcAg (1), or 31.91 µg CpG and 25 µg PCEP, 16 µg $HBsAg_{adw}$ and 16 µg HBcAg (2) followed by an immunization on day 28 with $5x10^7$ MVA PH5-S_{ayw} and $5x10^7$ MVA PH5-C (1) or $5x10^7$ MVA PH5-S_{adw} and $5x10^7$ MVA PH5-C (2). As a control, a third group of mice was immunized with adjuvants on day 0 and 14 and MVA-wt on day 28 (3).

Mice were sacrificed on day 34 and splenocytes as well as LALs were purified and analyzed for T cell responses by ICS after stimulation with HBV-derived peptides. HBe- and HBsAg levels as well as HBV-specific antibody titers in sera were determined on day 0 and 34 (Fig. 2.4.3.1 A).

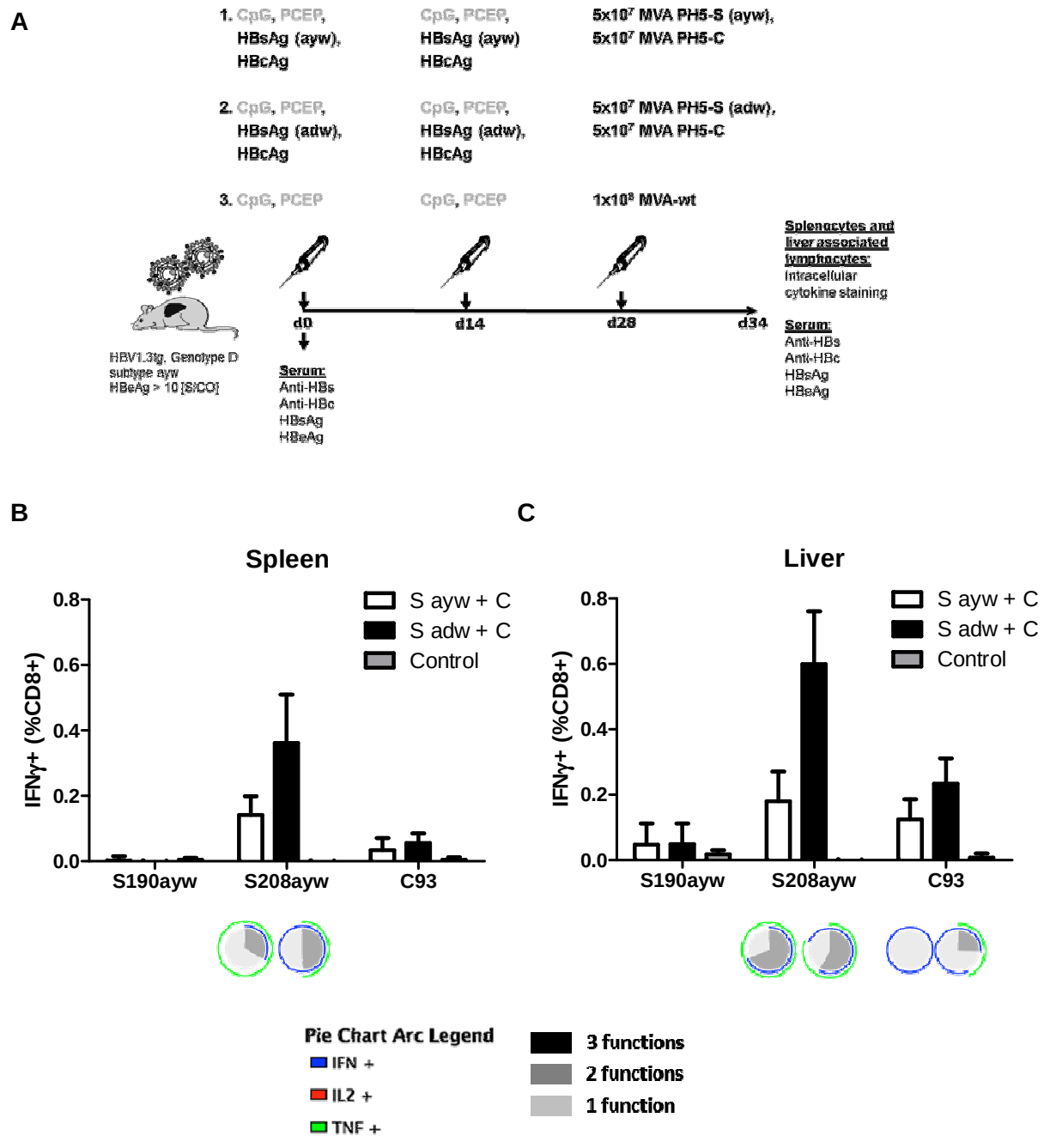

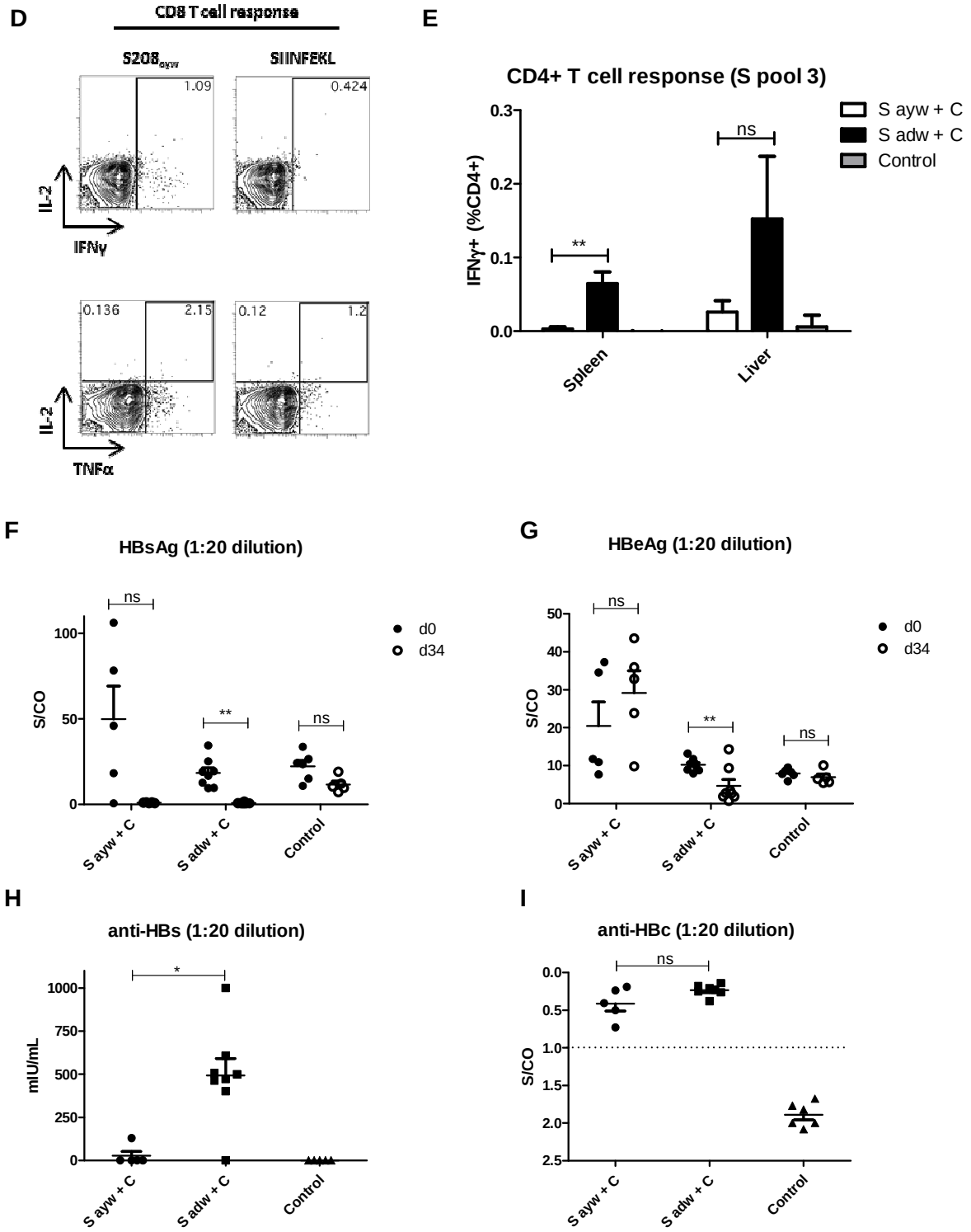

Fig. 2.4.3.1: Comparison of HBsAg subtype effects on eliciting HBV-specific immune responses upon immunization. Vaccinations were performed as depicted in (A). On day 34, splenocytes (B) and LALs (C) were stimulated with HBV-derived peptides S190, S208 or C93 of subtype ayw and CD8 T cells were analyzed for IFNγ, TNFα and IL-2 expression by ICS. Pie charts are shown for strong T cell responses found in group 1 and 2. A typical CD8 T cell response of LALs against S208ayw and the negative ovalbumin-derived control peptide SIINFEKL is shown in (D). CD4 T cells of spleens and livers were stimulated with HBV_{ayw}-derived S pool 3 and analyzed for IFNγ (E). Titers of HBsAg (F), HBeAg (G) were measured in sera on day 0 and 34. Anti-HBs (H) and anti-HBc (I) were measured in sera on day 34. dashed line = detection limit (I); S/CO = signal to cutoff; frequencies of IFNγ+ CD8+ and CD4+ T cells are background subtracted.

As shown in 2.4.3.1 B and C, group 2 (S adw + C) developed a stronger CD8 T cell response in spleen and liver against S208 and C93 upon immunization than group 1 (S ayw + C). The CD8 T cell responses in group 2 showed greater polyfunctionality in spleens and more IFNγ-only producing cells in livers upon stimulation with $S208_{ayw}$ compared to group 1 indicated by the pie charts (2.4.3.1 B and C). The arcs showed that responding T cells lost the ability to express IL-2 in both groups which is also depicted in Fig. 2.4.3.1 D. Group 3 did not develop an HBV-specific immune response which indicated that non-specific immune activation by adjuvants and MVA-wt failed to induces a cellular response against circulating HBV antigens that are constantly expressed. While the CD8 T cell response was not significantly stronger in spleens and livers of group 2 compared to group 1, the CD4 T cell response detected upon stimulation with HBV_{ayw}-derived S Pool 3 peptides was significantly stronger in spleens of group 2 (Fig. 2.4.3.1 E). HBsAg levels decreased in all groups but stronger in group 1 compared to group 3 and significantly in group 2 (Fig. 2.4.3.1 F). HBeAg levels were not significantly changed in group 1 and 3, whereas in group 2 significantly lower HBeAg levels were found (Fig. 2.4.3.1 G). Anti-HBs and anti-HBc antibodies were detected in groups 1 and 2, but not group 3 (Fig. 2.4.3.1 H and I). Moreover, mice group 2 had significantly higher titers of anti-HBs antibodies compared to group 1.
Taken together, these results showed that a MVA with a strong early/late promoter controlling the expression of the gene of interest enables to overcome tolerance in the HBVtg mouse-model. Using the subtype adw of HBsAg that was heterologous to the subtype ayw expressed in the transgenic mouse enhanced the effect of the vaccination.

Immunohistological analyses were performed for mice of group 2 (S adw + C) and 3 (Control) to investigate effects of the vaccination in the livers regarding influx of neutrophils, B and T cells as well as proliferation and apoptosis of hepatocytes. Liver sections of vaccinated mice were compared to liver sections of untreated HBVtg mice. As shown in Fig. 2.4.3.2 A, vaccination led to an influx of B cells indicated by staining of the B cell-specific surface marker B220. This influx was significantly higher in group “S adw + C” compared to untreated mice, but not compared to group receiving only adjuvants and MVA-wt without an HBV-specific trigger (Control). Furthermore, in livers of both groups an influx of T cells was observed, as demonstrated by staining of CD3 (Fig. 2.4.3.2 B). Staining of the proliferation marker Ki67 revealed comparable numbers of proliferating hepatocytes between the two groups (Fig. 2.4.3.2 C). However, a tendency towards higher numbers of infiltrating B and T cells in livers derived from mice of group “S adw + C” (HBV-specific trigger) compared to group “Control” (unspecific trigger) was observed. Interestingly, infiltrates of leukocytes were found in both vaccinated groups (Fig. 2.4.3.2 A and B), but no difference regarding the number of neutrophils was seen by staining of the surface marker Ly6G which is specific for

granulocytes and neutrophils (data not shown). Despite an increased hepatocyte proliferation in treated animals when compared to untreated mice, no increase in apoptotic hepatocytes was seen by staining cleaved caspase 3 (data nor shown).

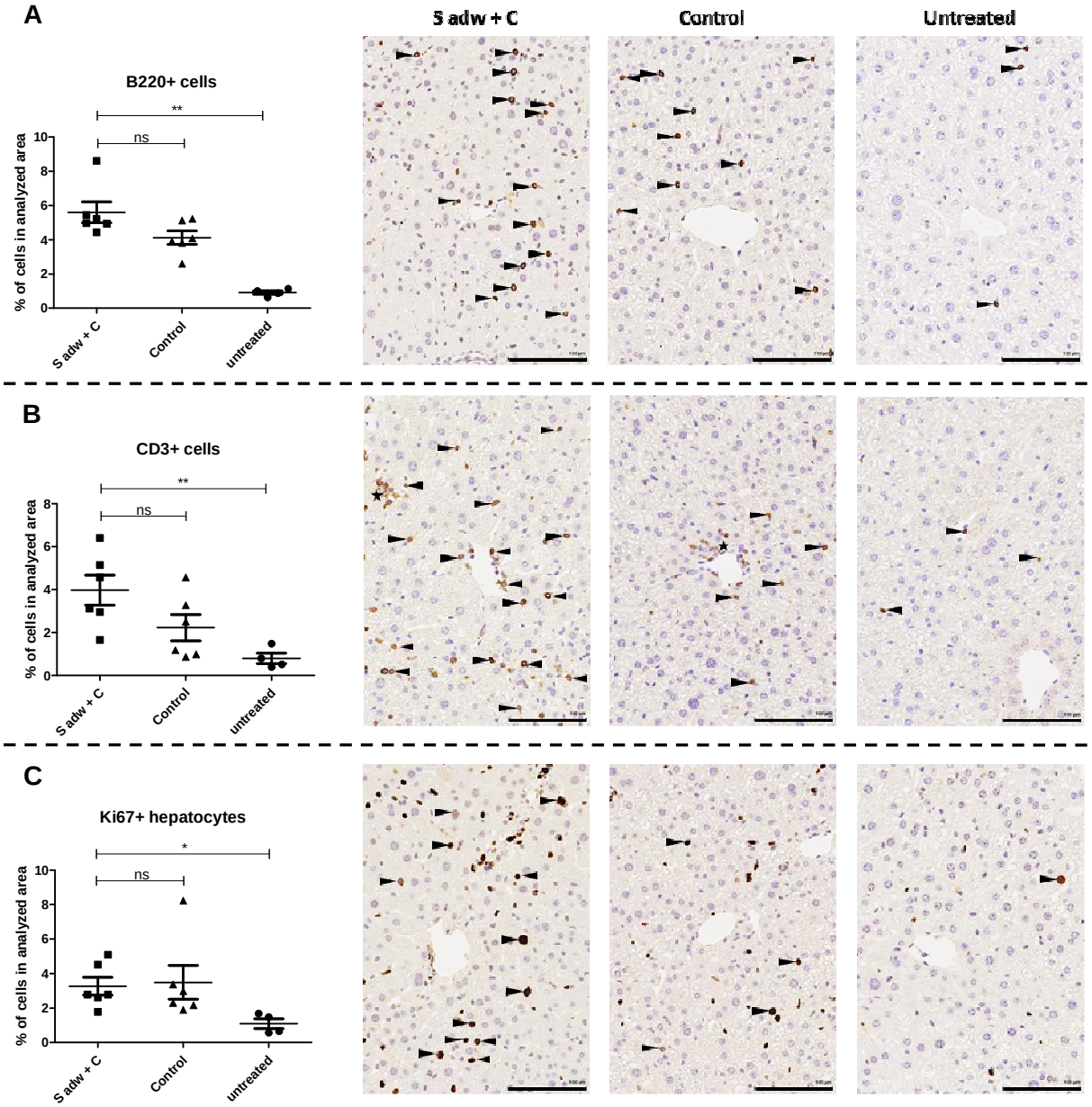

Fig. 2.4.3.2: Immunohistological analysis of livers from HBVtg mice vaccinated with PCEP+CpG+ $HBsAg_{adw}$+HBcAg/MVA-S_{adw}+MVA-C or with PCEP+CpG/MVA-wt (Control) or untreated. Quantifications and representative stainings of B220+ cells (A), CD3+ cells (B) and Ki67+ hepatocytes (C) are shown. Quantifications were performed using SlidePath Tissue Image Analysis 2.0 software. Arrow-heads depict positive cells. Stars indicate inflitrates of lymphocytes. Scale bars: 100 µm.

Taken together, the stainings demonstrated that vaccination led to recruitment of lymphocytes to the liver and enhances proliferation of hepatocytes.

2.4.4 Analysis of immune responses upon vaccination at later time points

Since the immune response was analyzed at day 6 post boost in previous experiments, vaccination studies were performed with analysis 14 days post boost vaccination, to investigate whether the adaptive immune response elicited in HBVtg animals might be lost or suppressed/decreased over time.

A group of three mice was vaccinated on day 0 and 14 with 31.91 µg CpG, 25 µg PCEP, 16 µg $HBsAg_{adw}$ and 16 µg HBcAg, followed by an immunization on day 28 with $5x10^7$ MVA PH5-S_{adw} and $5x10^7$ MVA PH5-C (Fig. 2.4.4.1 A). Mice were sacrificed on day 42 and splenocytes as well as LALs were isolated and analyzed for T cell responses by ICS after stimulation with HBV-derived and MVA-derived peptides. Sera taken on day 0 and 42 were analyzed for HBe- and HBsAg levels as well as HBV-specific antibody titers. Furthermore, levels of alanine-transaminase (ALT) were measured on day 42.

As shown in Fig. 2.4.4.1 B and C, CD8 T cell responses were detected 14 days post boost in spleens and livers against $S208_{ayw}$, peptides of S pool 3, $S208_{adw}$ and the MVA-derived peptide $B8R_{20}$. T cell polyfunctionality in spleen and liver correlated with frequencies of IFNγ producing CD8 T cells upon stimulation with respective peptides/peptide pools indicated by depicted pie charts. Furthermore, the arcs indicate that responding CD8 T cells lost the ability to express IL-2 except upon stimulation with peptides $S208_{adw}$ and $B8R_{20}$ which are not expressed endogenously by HBVtg mice.

HBsAg levels were decreased at day 34 (Fig. 2.4.4.1 D), but HBeAg levels were found to be unaffected by the vaccination (Fig. 2.4.4.1 E). Moreover, high titers of anti-HBs and anti-HBc antibodies were detected (Fig. 2.4.4.1 G and F), but the vaccination did not cause elevated ALT levels (Fig. 2.4.4.1 H) indicating no liver damage.

Taken together, the results show that although HBVtg mice constantly produce HBV particles and antigens, vaccination-induced T cells activated remained functional until at least 14 days post boost. Furthermore, vaccinated HBVtg animals maintained detectable levels of anti-HBV antibodies.

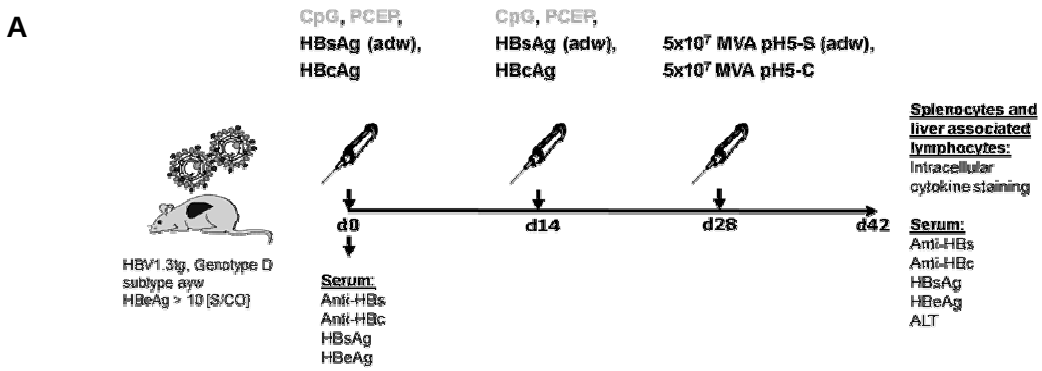
A
CpG, PCEP,
HBsAg (adw),
HBcAg
CpG, PCEP,
HBsAg (adw),
HBcAg
5x10⁷ MVA pH5-S (adw),
5x10⁷ MVA pH5-C
HBV1.3tg, Genotype D
subtype ayw
HBeAg > 10 [S/CO]
d0
d14
d28
d42
Serum:
Anti-HBs
Anti-HBc
HBsAg
HBeAg
Splenocytes and liver associated lymphocytes:
Intracellular cytokine staining
Serum:
Anti-HBs
Anti-HBc
HBsAg
HBeAg
ALT

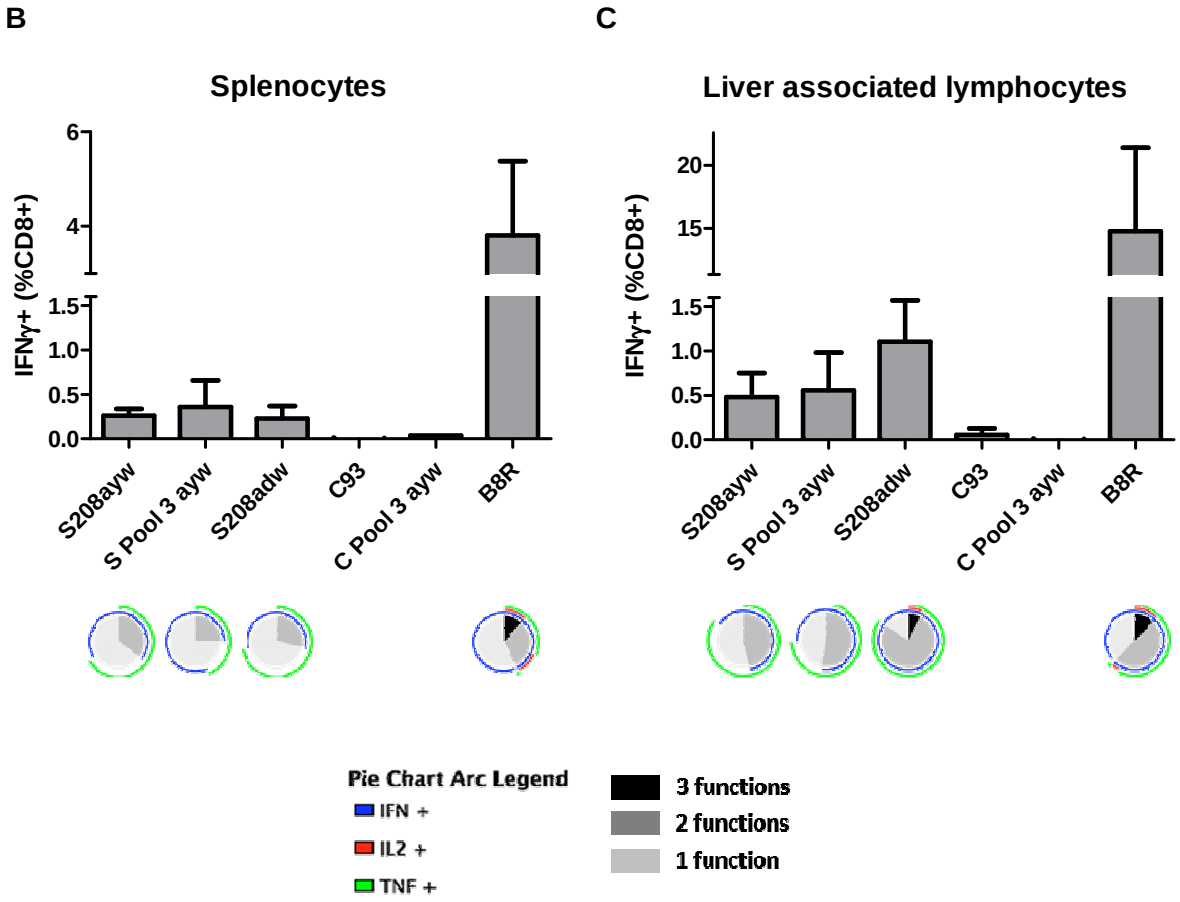
B
Splenocytes
IFNγ+ (%CD8+)
S208ayw
S Pool 3 ayw
S208adw
C93
C Pool 3 ayw
B8R
C
Liver associated lymphocytes
IFNγ+ (%CD8+)
S208ayw
S Pool 3 ayw
S208adw
C93
C Pool 3 ayw
B8R
Pie Chart Arc Legend
IFN +
IL2 +
TNF +
3 functions
2 functions
1 function

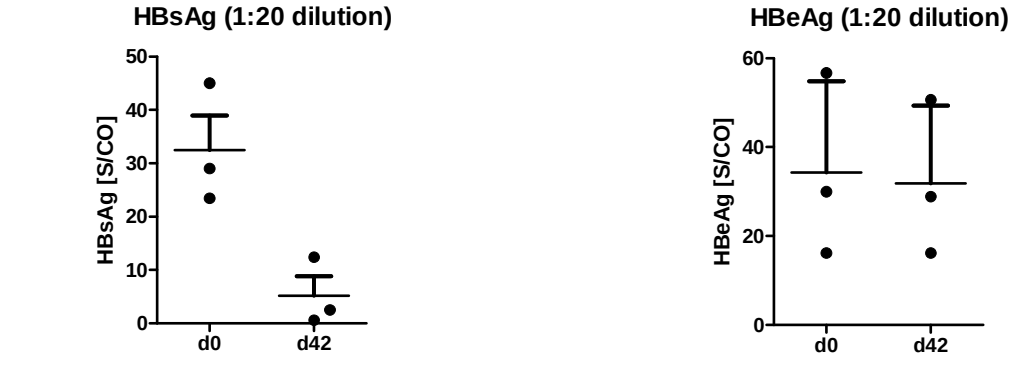
D
HBsAg (1:20 dilution)
HBsAg [S/CO]
d0
d42
E
HBeAg (1:20 dilution)
HBeAg [S/CO]
d0
d42

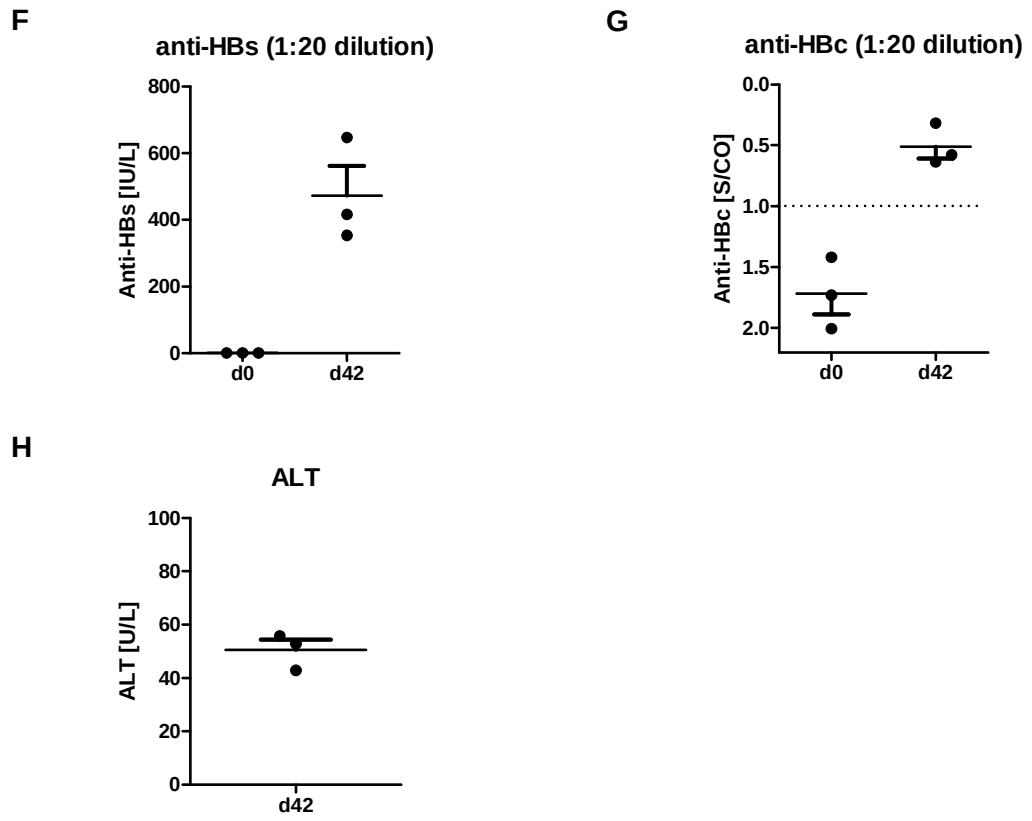

Fig. 2.4.4.1: Analysis of HBV-specific immune responses 14 days post boost. The experimental setup is depicted in (A). On day 42, splenocytes (B) and LALs (C) were stimulated with indicated HBV-derived peptides and peptide pools and analyzed for IFNγ, TNFα and IL-2 expression by ICS. Pies are shown for T cell responses upon stimulation with $S208_{ayw}$, S Pool 3, $S208_{adw}$ and $B8R_{20}$. Titers of HBsAg (D), HBeAg (E), anti-HBs antibodies (F) and anti-HBc antibodies (G) were measured in sera on day 0 and 42. ALT levels were determined in sera at day 42 (H). dashed line = detection limit (G); S/CO = signal to cutoff; frequencies of IFNγ+ CD8+ T cells are background subtracted.

To investigate the persistence of the HBV-specific humoral and cellular response as well as the impact of the vaccination on expression of HBV proteins, HBVtg mice were analyzed 8 weeks after booster immunization. As depicted in Fig. 2.4.4.2 A, a group of mice was vaccinated on day 0 and 14 with 31.91 µg CpG, 25 µg PCEP, 16 µg $HBsAg_{adw}$ and 16 µg HBcAg, followed by an immunization on day 28 with $5x10^7$ MVA PH5-S_{adw} and $5x10^7$ MVA PH5-C. Mice were sacrificed on day 84 and splenocytes as well as LALs were isolated and analyzed for T cell responses by ICS after stimulation with HBV- and MVA-derived peptides. HBe- and HBsAg levels as well as HBV-specific antibody titers in sera were determined on day 0, 42 84.

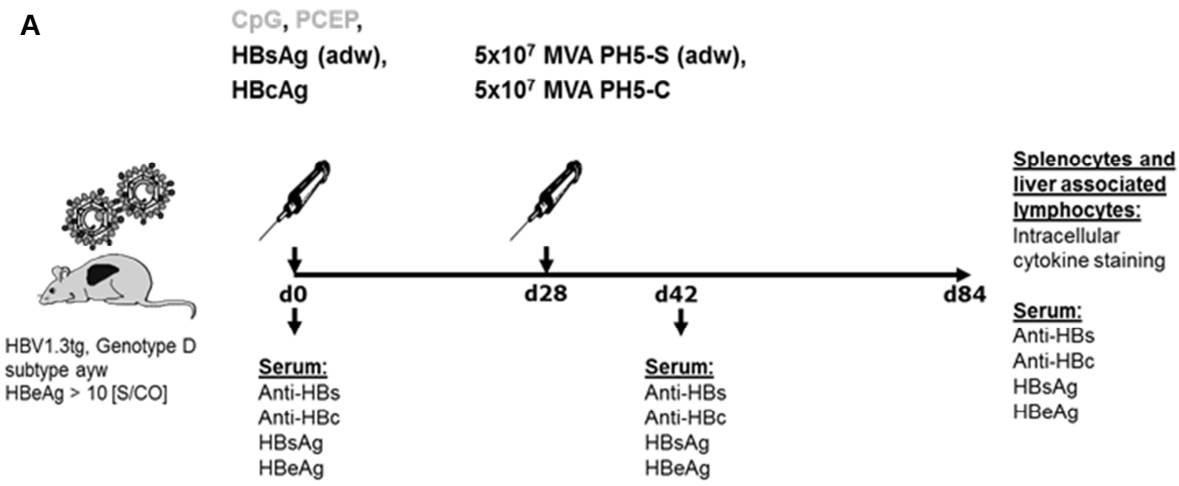
A
CpG, PCEP,
HBsAg (adw),
HBcAg
5x10⁷ MVA PH5-S (adw),
5x10⁷ MVA PH5-C
HBV1.3tg, Genotype D
subtype ayw
HBeAg > 10 [S/CO]
d0
d28
d42
d84
Serum:
Anti-HBs
Anti-HBc
HBsAg
HBeAg
Serum:
Anti-HBs
Anti-HBc
HBsAg
HBeAg
Splenocytes and liver associated lymphocytes:
Intracellular cytokine staining
Serum:
Anti-HBs
Anti-HBc
HBsAg
HBeAg

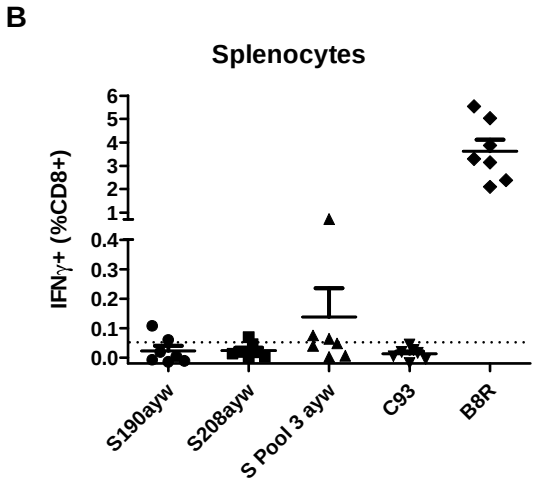
B
Splenocytes
IFNγ+ (%CD8+)
S190ayw
S208ayw
S Pool 3 ayw
C93
B8R

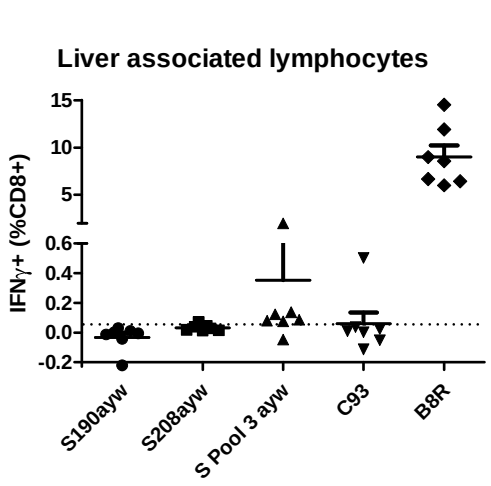
C
Liver associated lymphocytes
IFNγ+ (%CD8+)
S190ayw
S208ayw
S Pool 3 ayw
C93
B8R

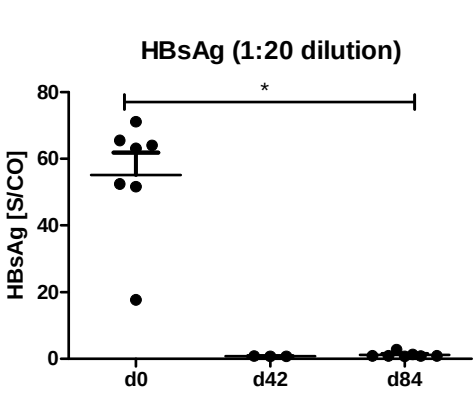
D
HBsAg (1:20 dilution)
HBsAg [S/CO]
*
d0
d42
d84

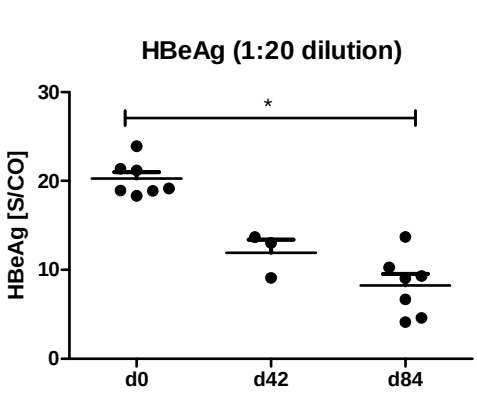
E
HBeAg (1:20 dilution)
HBeAg [S/CO]
*
d0
d42
d84

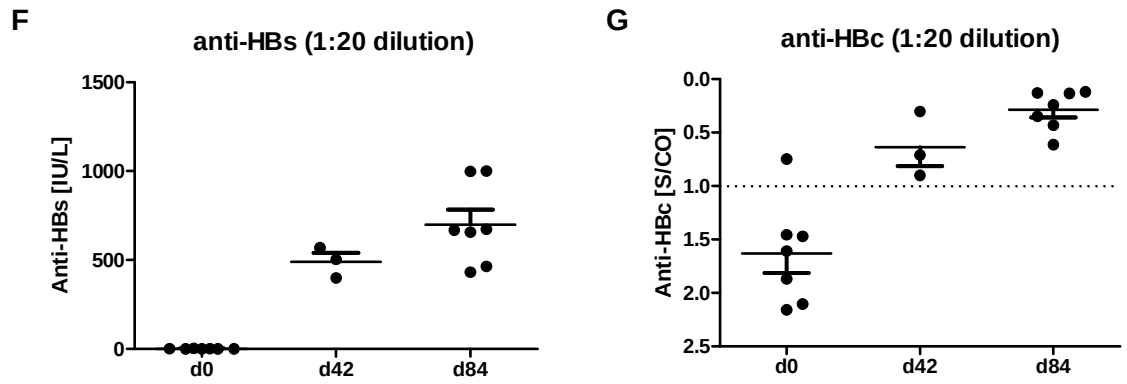

Fig. 2.4.4.2: Analysis of HBV-specific immune responses 56 days post boost. The experimental setup is depicted in (A). On day 84, splenocytes (B) and LALs (C) were stimulated with indicated HBV-derived peptides or peptide pools and CD8 T cells were analyzed for IFNγ expression by ICS. Titers of HBsAg (D), HBeAg (E), anti-HBs anibodies (F) and anti-HBc antibodies (G) were measured in sera taken on day 0, 42 and 84. dashed line = threshold of T cell responses (B) and (C) or detection limit (G); S/CO = signal to cutoff; frequencies of IFNγ+ CD8+ T cells are background subtracted.

As shown in Fig. 2.4.4.2 B and C, a weak CD8 T cell response was detected 56 days post boost upon stimulation with the S pool 3. Strong CD8 T cell responses were directed against the MVA-derived peptide $B8R_{20}$. However, HBsAg and HBeAg levels were significantly reduced when compared to the levels at the start of vaccination (Fig. 2.4.4.2 D and E). High anti-HBs and anti-HBc antibody titers were detected in all mice (Fig. 2.4.4.2 F and G).

Taken together, HBV-specific T cell responses seemed to be almost completely lost two months after vaccination. However, the effect on serological markers was sustained post boost with significantly decreased HBsAg and HBeAg levels and sustained high antibody titers.

2.5 Killing capacity of vaccination-induced CD8 T cells

The experiments performed in C57BL/6 and HBVtg mice showed that the established heterologous prime-boost vaccination strategy induced polyfunctional HBV-specific CD8 T cells. To investigate whether these CD8 T cells are able to specifically lyse target cells in their natural environment, *in vivo* killing assays were performed.

2.5.1 *In vivo* killing assay in C57BL/6 mice

To investigate, if HBV-specific CD8 T cells with full effector functions are induced by the vaccination strategy, an *in vivo* killing assay was performed in wt mice. In this model, there is

no endogenous tolerance with respect to HBV-antigens which might limit functionality of activated, HBV-specific CD8 T cells.

4 mice were vaccinated on day 0 with 31.91 µg CpG, 16 µg $HBsAg_{ayw}$ and 16 µg HBcAg followed by a boost immunization on day 28 with $5x10^7$ MVA PH5-S_{ayw} and $5x10^7$ MVA PH5-C. The protein vaccine formulation contained only CpG because the vaccination study performed earlier (Fig. 2.3.1.1) showed that the CD8 T cell response was stronger without PCEP and induced antibodies played an underpart in this study. In the control group 4 mice were immunized with 31.91 µg CpG on day 0 and $1x10^8$ MVA-wt on day 28. On day 34, $CFSE^{low}$-labeled unloaded control cells and $CFSE^{high}$-labeled C93-loaded target cells were co-transferred at a ratio of 1:1 intravenously into the vaccinated mice. To distinguish the transferred cells from the endogenous cells, the donor mice carried the congenic marker CD45.1 whereas cells from the recipient mice carried the congenic marker CD45.2. Mice were sacrificed on day 35, splenocytes were isolated and analyzed for HBV-specific T cell responses by ICS after stimulation with HBV- and MVA-derived peptides. Additionally, the number of $CFSE_{low}$- and $CFSE_{high}$-cells were detected by FACS (Fig. 2.5.1 A).

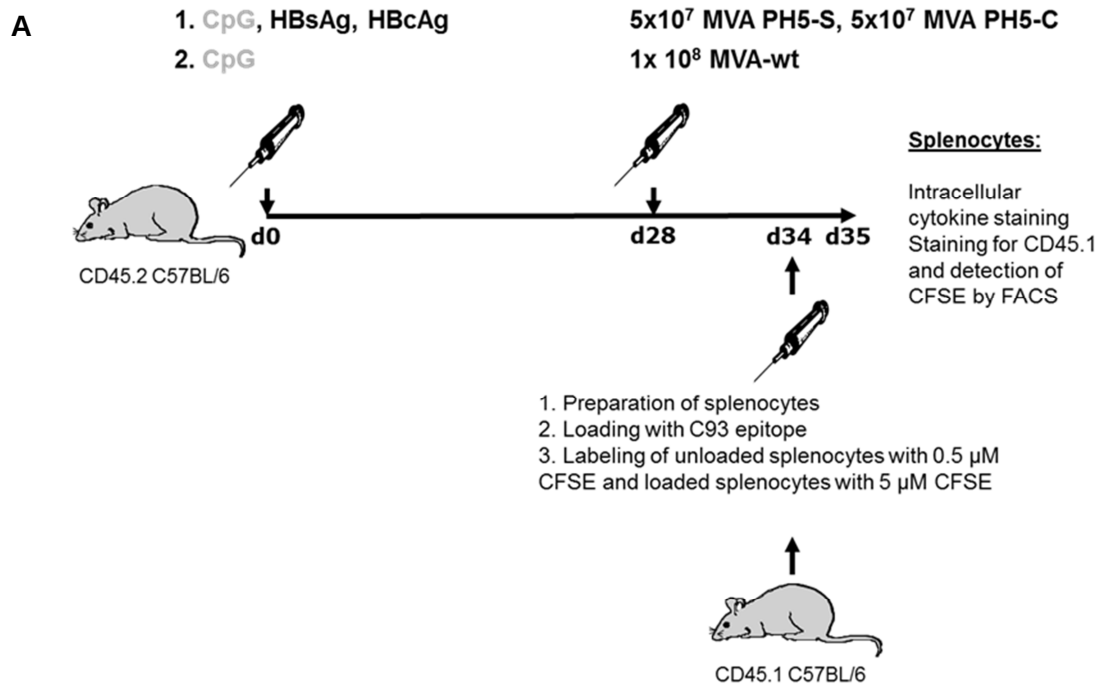

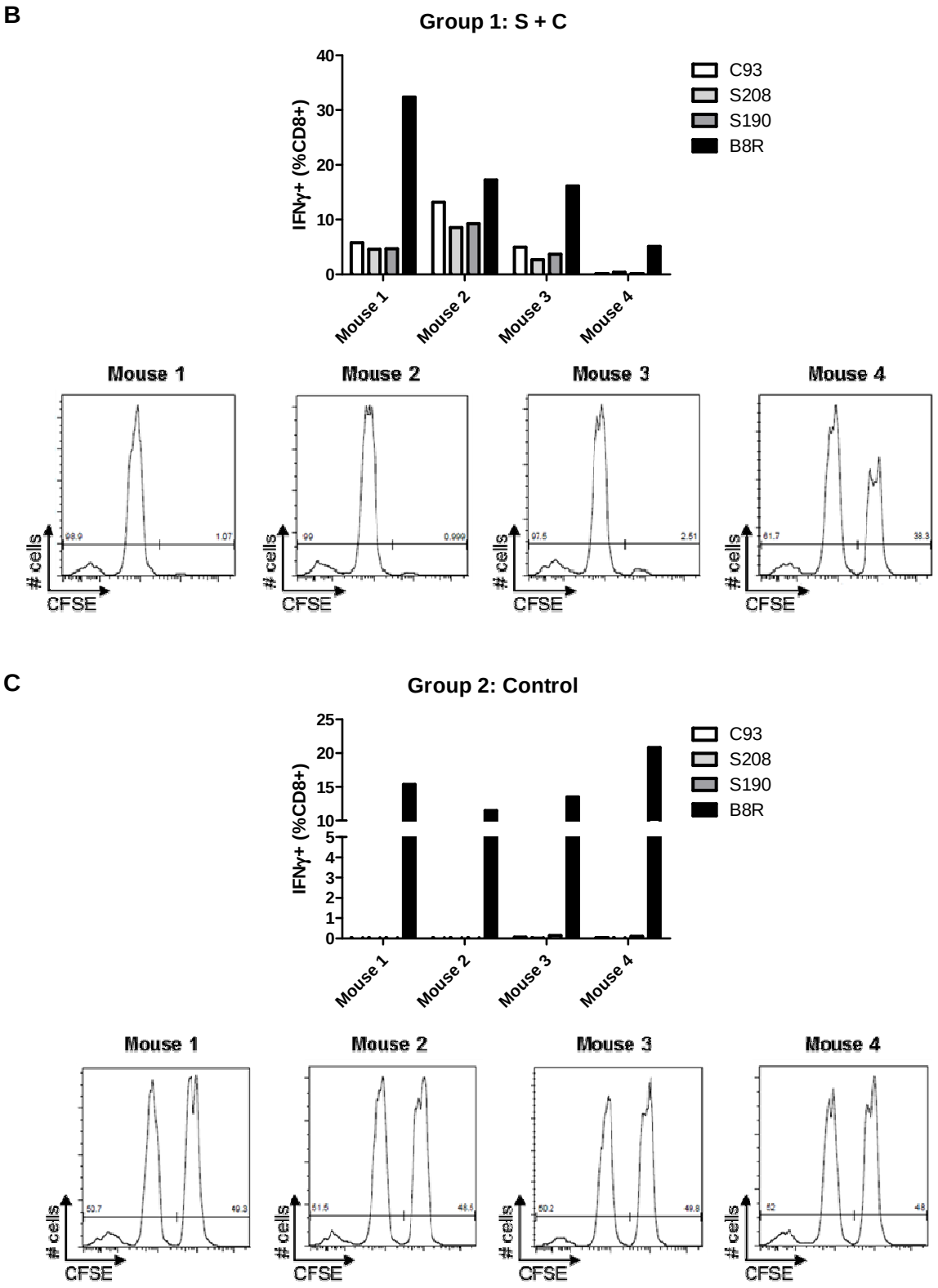

Fig. 2.5.1: Analysis of CD8 T cell responses and cell lysis capacity. The experimental setup is depicted in (A). On day 35, splenocytes were stimulated with indicated HBV- or MVA-derived peptides and CD8 T cells were analyzed for IFNγ expression by ICS (B) and (C). Ratios of transferred CD45.1 positive $CFSE^{low}$ control and $CFSE^{high}$ target cells in spleens after 16 to 18 hours were detected by FACS analysis shown in the lower panels of (B) and (C). Frequencies of IFNγ+ CD8+ T cells are background subtracted.

As shown in Fig. 2.5.1 B, strong HBV-specific immune responses were detected by ICS in mouse 1, 2 and 3 whereas a weak T cell response was observed in mouse 4. However, for all mice the strongest immune response was detected after stimulation with the C93-peptide. The result of the ICS was confirmed by detection of CFSE-labeled cells (Fig. 2.5.1 B lower panel). In mouse 1, 2 and 3 the C93-loaded and $CFSE_{high}$-labeled cells were reduced to 2 to 5 % of the transferred cells indicating a (effective) specific killing of approximately 90% of C93-pulsed targets after 16 to 18 hours. Correlating with the weaker HBV-specific CTL response in mouse 4, there was only 25% specific killing of C93-labeled cells. As expected, the control group mounted an MVA-specific but no HBV-specific CD8 T cell response and therefore no specific killing of C93-loaded cells target cells (Fig 2.5.1 C).
Taken together, the established vaccination strategy was able to induce HBV-specific CD8 T cells that did not only produce cytokines, but were also capable of rapidly killing target cells upon recognition *in vivo*.

2.5.2 *In vivo* killing in a chronic model for HBV infection using AdHBVx-

To test killing abilities of vaccination-induced CD8 T cells in a chronic model for HBV infection, an *in vivo* killing assay was performed in wt mice that were infected with an adenovirus that expresses HBV lacking the X protein. As depicted in Fig. 2.5.2.1, on day 0 wt mice received $2x10^8$ infectious units of the recombinant adenovirus containing an HBV 1.3 overlength genome (genotype D, subtype ayw) with a stop codon at amino acid position 8 within the X-encoding sequence. This dose was shown to mediate low HBV replication rates within the transduced hepatocytes preventing a strong induction of the immune response directed against HBV proteins. Thus, HBV antigens are expressed over a long period of time mimicking a chronic state of HBV infection (Huang 2012). Due to the lack of X protein expression the adenoviral vector was classified as biosafety level 2. The mice transduced with AdHBVx- were vaccinated on day 14 and 28 with 31.91 µg CpG, 25 µg PCEP, 16 µg $HBsAg_{adw}$ and 16 µg HBcAg (group "S+C"; 4 mice) or 31.91 µg CpG and 25 µg PCEP (group "control"; 4 mice) followed by an immunization on day 28 with $5x10^7$ MVA PH5-S_{ayw} and $5x10^7$ MVA PH5-C (S+C) or $1x10^8$ MVA-wt (control). On day 48, equal numbers of $CFSE^{low}$-labeled unloaded control cells and $CFSE^{high}$-labeled $S208_{ayw}$-loaded target cells were transferred intravenously into the vaccinated mice. For loading MHC class I molecules, the $S208_{ayw}$-peptide was chosen because it was recognized predominantly by vaccination-induced HBV-specific CD8 T cells in HBVtg mice as shown before (Fig. 2.5.1). To distinguish the transferred cells from the endogenous cells, the donor mice carried the congenic marker CD45.2 whereas cells from the recipient mice carried the congenic marker CD45.1. Mice were sacrificed on day 49, splenocytes and LALs were isolated and analyzed for T cell

responses by ICS after stimulation with HBV- and MVA-derived peptides. Additionally, numbers of $CFSE^{low}$- and $CFSE^{high}$-cells were determined by FACS. To detect CD4-T_H2 and anti-inflammatory responses, ELISpot analysis for secretion of T_H2-specific cytokines IL-4, IL-5 as well as anti-inflammatory cytokine IL-10 were performed. To visualize the expression of HBV proteins, immunohistological stainings of HBcAg in liver sections were performed. Sera were analyzed on day 6, 14, 28 and 49 for HBsAg-, HBeAg- and ALT-levels and furthermore on day 49, anti-HBs and anti-HBc were determined.

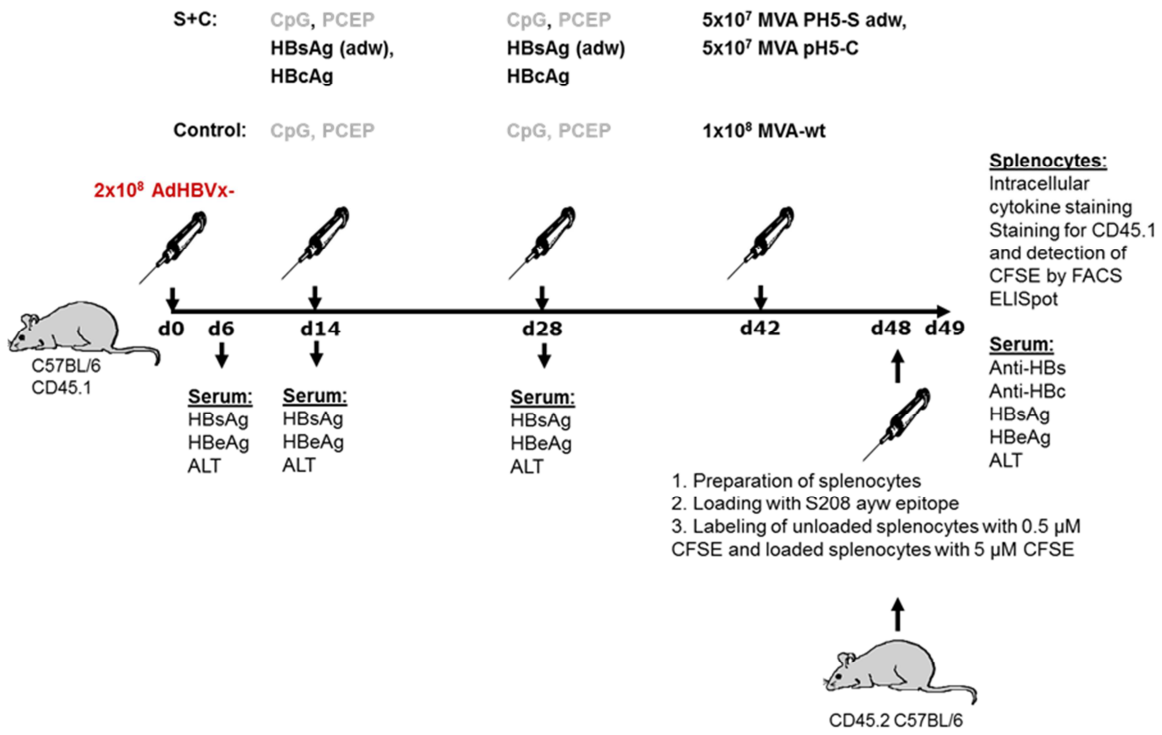

Fig. 2.5.2.1: Experimental setup for analysis of CD8 T cell responses and cell lysis capacity in a mouse model for chronic HBV infection based on adenoviral transfer of a 1.3 fold overlength HBV genome with genotype D and subtype ayw.

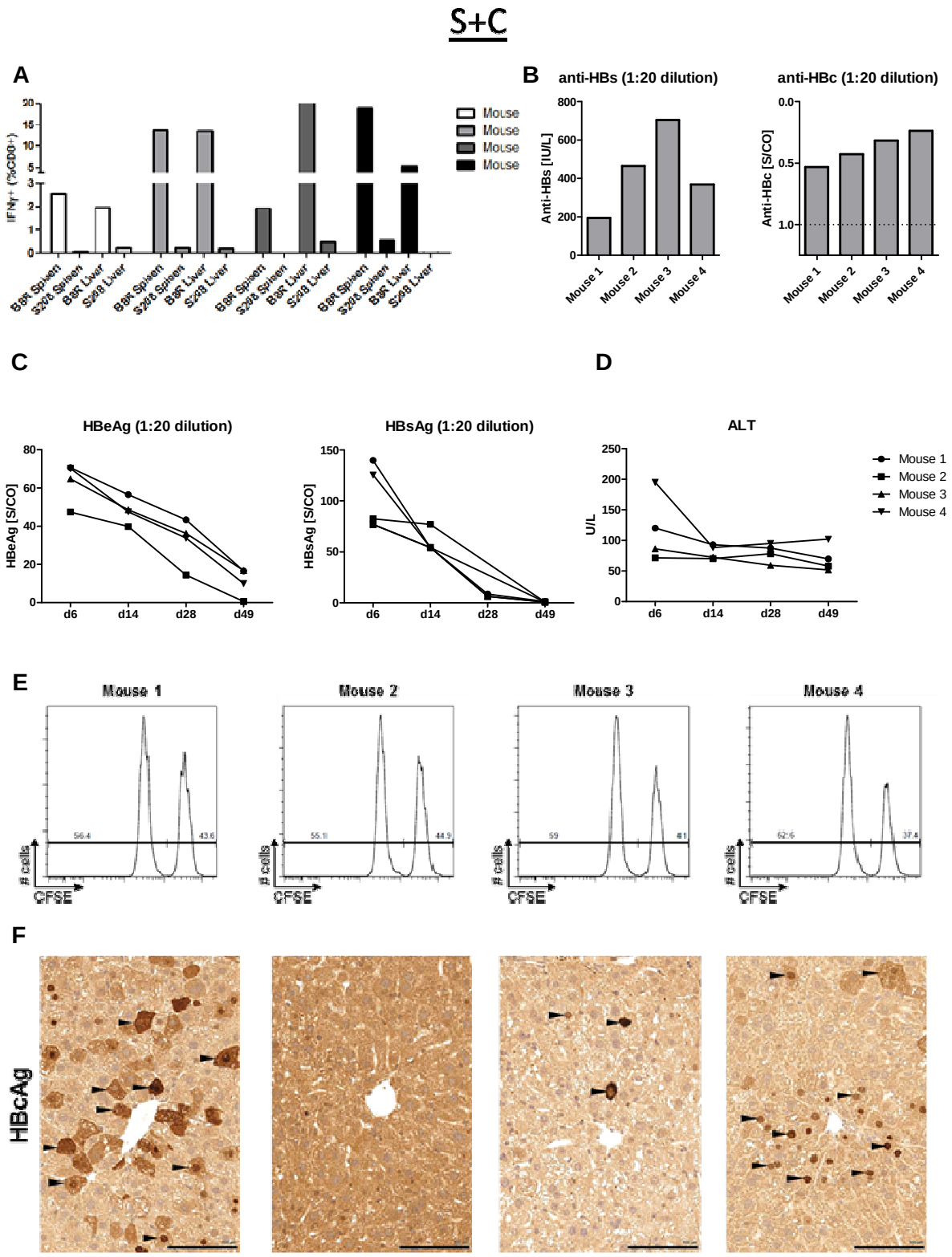

Fig. 2.5.2.2: Analysis of CD8 T cell responses and their cell lysis capacity in mice vaccinated against $HBsAg_{adw}$ and HBcAg (S+C). (A) On day 49, splenocytes and LALs were stimulated with indicated HBV- or MVA-derived peptides and CD8 T cells were analyzed for IFNγ expression by ICS. Anti-HBs and anti-HBc were measured in sera on day 49 (B). HBeAg-, HBsAg-levels (C) and ALT levels (D) were determined on day 6, 14, 28 and 49. (E) Ratios of transferred CD45.2 positive $CFSE^{low}$ control and $CFSE^{high}$ target cells in spleens after 16 to 18 hours were determined by FACS analysis. (F) Immunhistological stainings for HBcAg in liver sections of respective mice were performed. S/CO = signal to cutoff; Arrow-heads depict HBcAg positive cells; Scale bars: 100 µm; Frequencies of IFNγ+ CD8+ T cells are background subtracted.

As shown in Fig. 2.5.2.2 A, the vaccination unable to induce a high number of T cells specific for peptide S208 in spleen or in liver. The highest frequency of specific T cells was found in the liver of mouse 3 and in the spleen mouse 4. Antibodies against HBs- and HBcAg were detected in all mice with the lowest anti-HBs antibody titer in mouse 1 (Fig. 2.5.2.2 B) that correlated with a weak T cell response against the MVA-derived peptide $B8R_{20}$ indicating an inefficient vaccination in this mouse. HBeAg levels decreased in all mice over time, but only in mouse 2 to undetectable levels and HBsAg levels decreased post vaccination to low levels (Fig. 2.5.2.2 C). ALT-levels were slightly elevated in mouse 1, 2 and 3 at day 6, 14 and 28, whereas on day 6 post AdHBVx- infection mouse 4 exhibited considerably elevated ALT levels when compared to the rest of the group (Fig. 2.5.2.2 D). As depicted in Fig. 2.5.2.2 E, a decrease in $CFSE^{high}$ target cell numbers was noted in all mice, but was most evident in mouse 3 and 4. This indicated that the induced T cells were able to kill target cells labeled with HBV-specific peptide S208 in the setting of chronic HBV infection. However, killing efficiency was rather low as suggested by the finding that 78.7 to 94.5 % of transferred target cells were still detected 18 post transfer. Immunohistochemical stainings of HBcAg in liver sections showed that HBcAg was expressed in mouse 1, 3 and 4 on day 49 post AdHBVx-mediated HBV-transmission (Fig. 2.5.2.2 F). These findings correlated with HBeAg levels detected on day 49 post boost (Fig. 2.5.2.2 C).

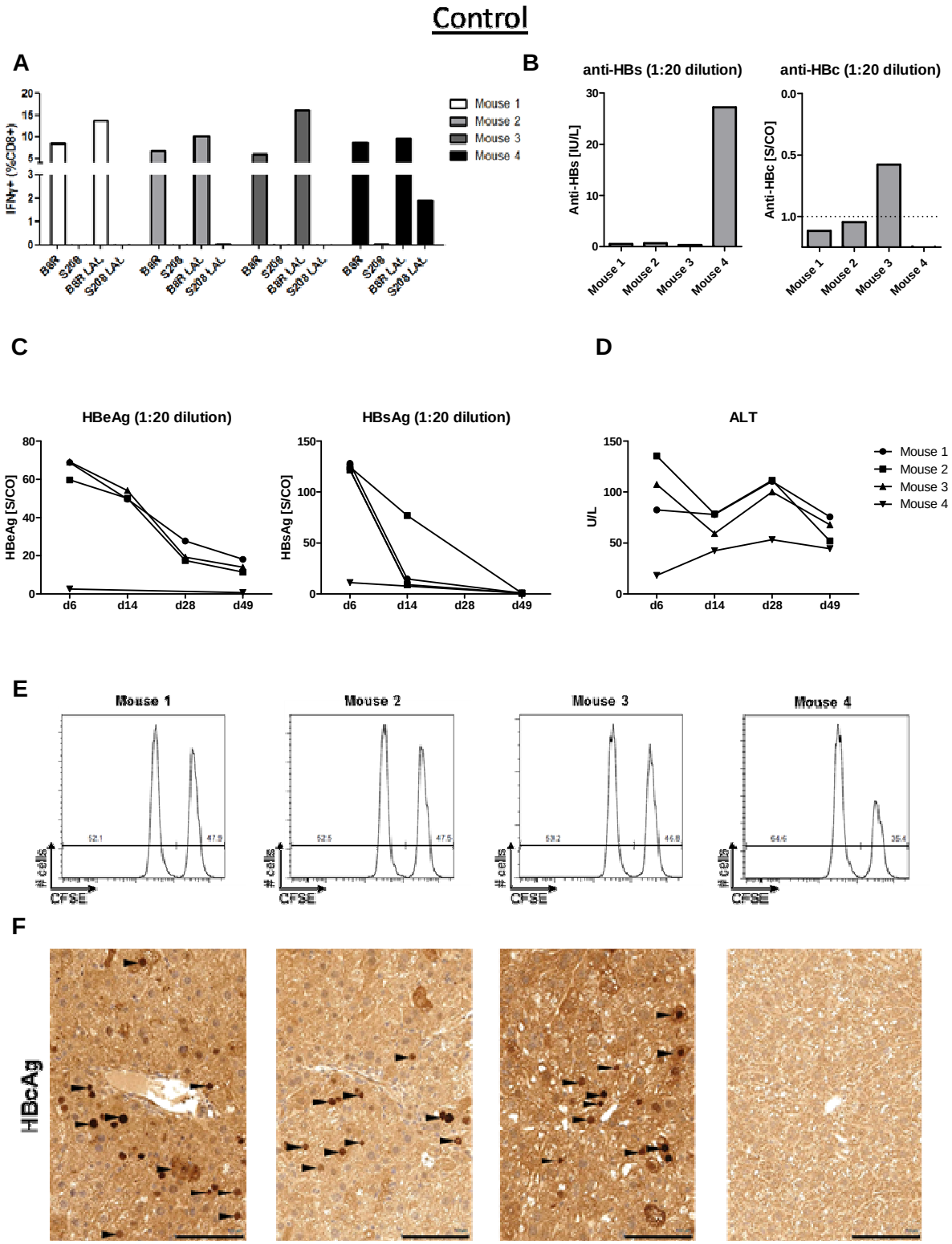

Fig. 2.5.2.3: Analysis of CD8 T cell responses and their cell lysis capacity in mice mock-vaccinated with adjuvants and MVA-wt (control). (A) On day 49, splenocytes and LALs were stimulated with indicated HBV- or MVA-derived peptides and CD8 T cells were analyzed for IFNγ expression by ICS. Anti-HBs and anti-HBc levels were measured in sera on day 49 (B). HBeAg-, HBsAg-levels (C) and ALT levels (D) were determined on day 6, 14, 28 and 49. (E) Ratios of transferred CD45.2 positive $CFSE^{low}$ control or $CFSE^{high}$ target cells isolated from spleens after 16 to 18 hours were detected by FACS analysis. (F) Immunhistological stainings for HBcAg in liver sections of respective mice were performed. S/CO = signal to cutoff; Arrow-heads depict positive cells; Scale bars: 100 µm; Frequencies of IFNγ+ CD8+ T cells are background subtracted.

In the control group, HBV-specific CD8 T cell responses were undetectable upon stimulation with the $S208_{ayw}$ peptide except for mouse 4 (Fig. 2.5.2.3 A). This finding correlated with anti-HBs antibody titers depicted in Fig. 2.5.2.3 B. Interestingly, anti-HBc antibodies were detected in mouse 3, but not mouse 4 indicating an HBsAg-specific immune response in mouse 4. As shown in Fig. 2.5.2.3 C, HBeAg levels decreased over time in all mice, but were low in mouse 4 already on day 6. HBsAg levels decreased to undetectable levels in all mice (Fig. 2.5.2.3 D). The initial low levels of HBe- and HBsAg in mouse 4 indicated that a chronic state of HBV infection was not achieved in this mouse (Fig. 2.5.2.3 D). Supporting this hypothesis ALT-levels measured for mouse 4 were low in comparison to ALT-levels obtained for the other mice within this group which were slightly increased (Fig. 2.5.2.3 D). Specific killing of target cells was only detected in mouse 4 (Fig. 2.5.2.3 E), whereas the ratio of $CFSE^{high}$ target cells to control cells was unchanged in mouse 1, 2 or 3. In line with these results HBcAg was detected after vaccination in mice 1-3, but not in mouse 4 (Fig. 2.5.2.3 F).

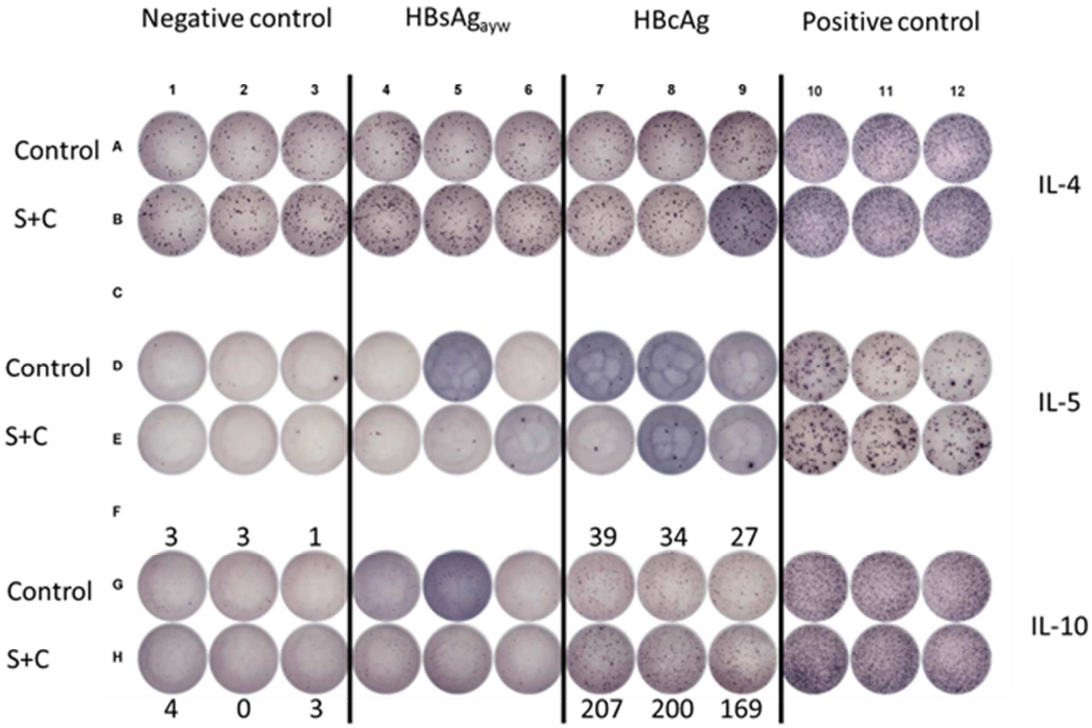

Fig. 2.5.2.4: ELISpot analysis of pooled splenocytes from mice vaccinated with CpG, PCEP and MVA-wt (control group) or against $HBsAg_{adw}$ and HBcAg (S+C group) for expression of cytokines IL-4, IL-5 and IL-10. Numbers are only shown for clear results and indicate the quantity of spot forming cells upon stimulation for 48 h.

ELISpot analysis revealed no detectable IL-4, IL-5 or IL-10 secreting cells upon stimulation with $HBsAg_{ayw}$ after 48 h (Fig. 2.5.2.4). However, after stimulation with HBcAg, IL-10, but not IL-4 or IL-5 secreting cells were detected. Splenocytes of mice vaccinated against $HBsAg_{adw}$

and HBcAg (S+C) produced about 6 times more IL-10 than splenocytes from the control group.

Taken together, these results indicated that the prime-boost vaccination strategy using $HBsAg_{adw}$ and HBcAg induced an HBV-specific immune response. However, efficiency of T cell-mediated killing seems to be impaired in the chronic HBV mouse model based on AdHBVx-. Interestingly, HBcAg stimulated splenocytes of vaccinated AdHBVx- mice also showed a 6-fold increase in IL-10 secretion compared to the unvaccinated controls, which suggests an induction of a HBV core-mediated inhibitory response.

2.6 Studies on effects by components of the protein vaccine

2.6.1 Effect of HBcAg on the overall T cell response

Since the vaccination strategy that included immunizations with 16 µg $HBsAg_{adw}$ and 16 µg HBcAg in prime and the combination of $5x10^7$ MVA PH5-S_{adw} and $5x10^7$ PH5-C in boost resulted in a stronger immune response directed against HBsAg-derived peptides compared to the vaccination strategy including 16 µg $HBsAg_{adw}$ in prime and $1x10^8$ MVA PH5-S_{adw} in boost without HBcAg (Fig. 2.4.1), it was tested if HBcAg has similar effects on the immune system like adjuvants. Comparing the immune responses of those groups gained information about effects of HBcAg on immune responses to the co-administered antigen. Therefore, three groups of wt mice were vaccinated as depicted in Fig. 2.6.1 A. Group 1 was immunized on day 0 with 31.91 µg CpG, 50 µg PCEP, 16 µg $HBsAg_{ayw}$ and 16 µg HBcAg, followed by a boost vaccination on day 28 with $5x10^7$ MVA PH5-S_{ayw} and $5x10^7$ MVA PH5-C. Group 2 was vaccinated on day 0 with 31.91 µg CpG, 50 µg PCEP, 16 µg HBcAg and 16 µg ovalbumin, followed by a boost vaccination on day 28 with $5x10^7$ MVA PH5-C and $5x10^7$ MVA PH5-OVA whereas group 3 which served as a control for HBcAg ,was vaccinated on day 0 with 31.91 µg CpG, 50 µg PCEP 16 µg, $HBsAg_{ayw}$ and 16 µg ovalbumin, followed by a boost vaccination on day 28 with $5x10^7$ MVA PH5-S_{ayw} and $5x10^7$ MVA PH5-OVA with HBsAg and ovalbumin. Mice were sacrificed on day 34 and isolated splenocytes were analyzed for IFNγ expression after stimulation with peptides derived from HBsAg (S190, S208), HBcAg (C93), ovalbumin (SIINFEKL) or MVA (B8R) by ICS.

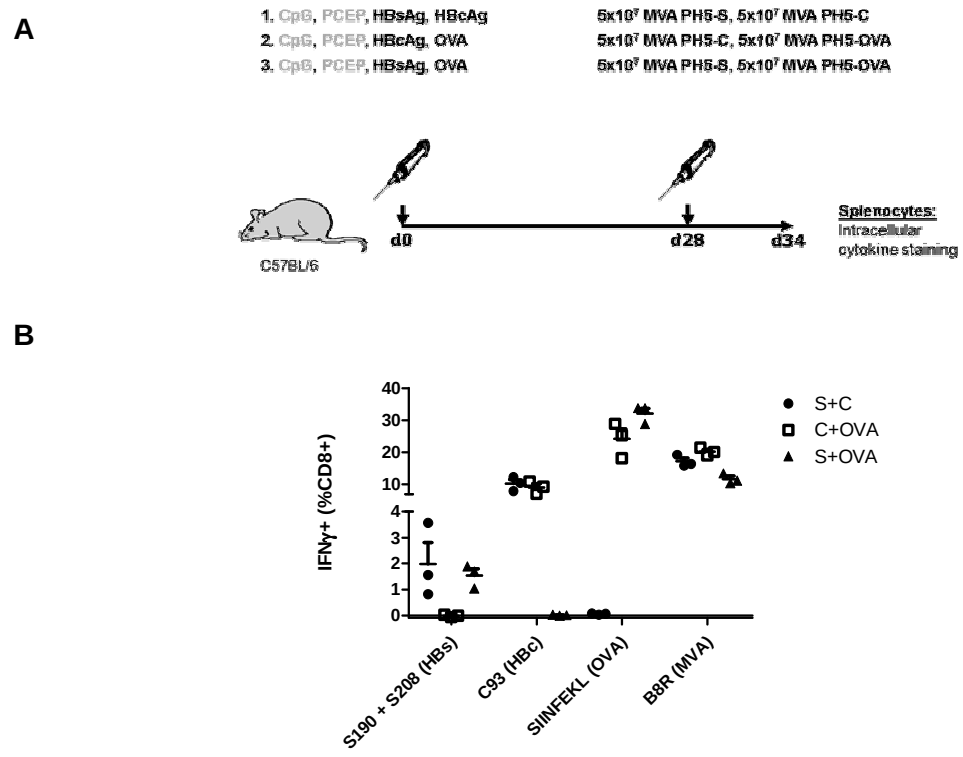

Fig. 2.6.1: Analysis of a potential adjuvant-like effect of HBcAg triggering T cell immune responses against co-administered antigens. The experimental setup is depicted in (A). On day 34, splenocytes (B) were stimulated with indicated HBV-, OVA- or MVA-derived and CD8 T cells were analyzed for IFNγ expression by ICS.

CD8 T cell immune responses detected upon stimulation with HBcAg- and ovalbumin-derived peptides were comparable in groups 1 and 2. Analog immune responses against HBsAg were similar for groups 1 and 3 (Fig. 2.6.1 B).

Thus, no adjuvant-like effect was observed for HBcAg in this experiment.

2.6.2 Effect of the adjuvant PCEP on TLR signaling

To investigate which signaling cascades are important for the different adjuvants and adjuvants combinations, MyD88 or TLR2 knockout mice were vaccinated with (1) 16 µg HBsAg and 16 µg HBcAg; (2) 31.91 µg CpG, 16 µg HBsAg and 16 µg HBcAg; (3) 50 µg PCEP 16 µg HBsAg and 16 µg HBcAg or (4) 50 µg PCEP, 31.91 µg CpG, 16 µg HBsAg and 16 µg HBcAg. Mice were sacrificed on day 8 and splenocytes were analyzed for IFNγ expression after stimulation with HBV-derived peptides by ICS. Additionally, titers of anti-HBs and anti-HBc antibodies were measured in sera on day 8 (Fig. 2.6.2 A). With exception of TLR3 and TLR4, all TLR family members signal of via the adaptor protein MyD88. Therefore MyD88 knockout mice were suitable to investigate whether TLR3/4 or other TLRs might be involved in activation of the immune system by PCEP. To rule out one additional specific

TLR, the effect of adjuvants in TLR2 knockout mice was investigated. TLR2 was additionally interesting because it was published that it recognizes HBcAg (Vanlandschoot 2005).

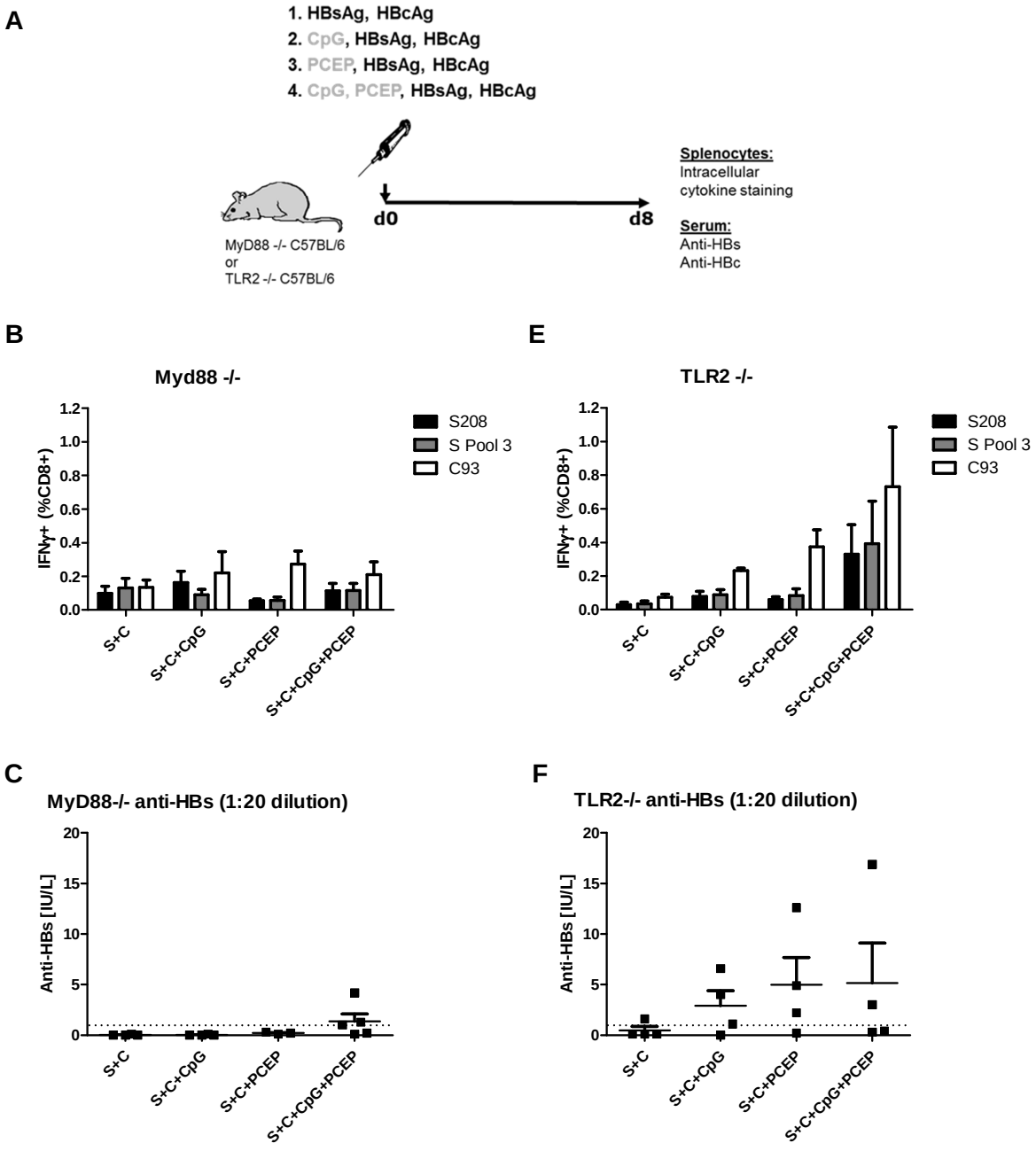

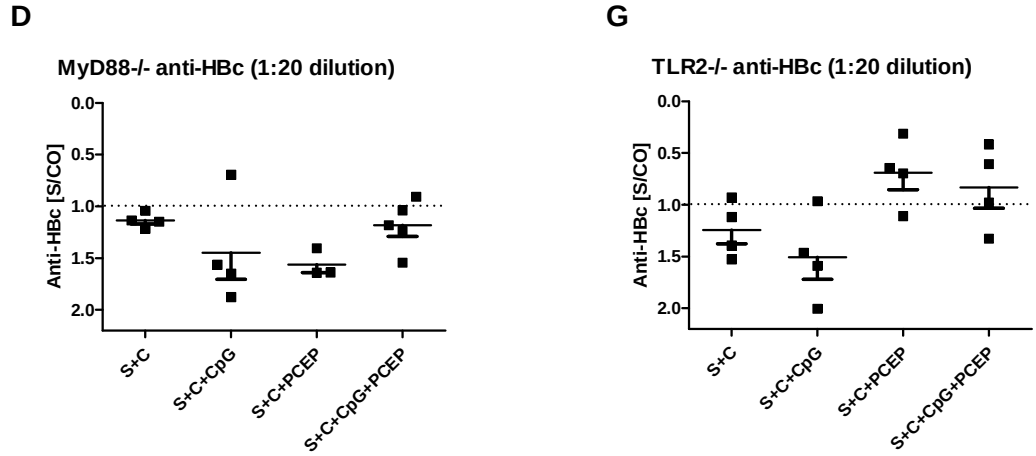

Fig. 2.6.2: Analysis of HBV-specific immune responses in MyD88 or TLR2 knockout mice upon immunization with different protein vaccine formulations. The experimental setup is depicted in (A). On day 8, splenocytes (B and E) were stimulated with indicated HBV-derived peptides and peptide pools and CD8 T cells were analyzed for IFNγ expression by ICS. Titers of anti-HBs (C and F) and anti-HBc (D and G) were measured in sera on day 8. dashed line = detection limit (G); S/CO = signal to cutoff

In MyD88 -/- mice, addition of adjuvants individually or in combination did not enhance T cell responses (Fig. 2.6.2 B) when compared to wt-mice (Fig. 2.3.1.1). Since CpG is known to be recognized by TLR9 and its signaling is MyD88-dependent (Takeda 2007), an enhancement of immune responses was not expected. The same was observed on antibody-titers (Fig. 2.6.2 C and D). However, the observation that addition of PCEP did not enhance immune responses indicated that the effect of PCEP is also MyD88-dependent, but not TLR3 or TLR4. As shown in Fig. 2.6.2 E, T cell responses were enhanced with addition of CpG or PCEP, but stronger with addition of CpG and PCEP in TLR2-/- mice which showed the synergistic effect observed in wt-mice (Fig. 2.3.1.1). Additionally, the synergistic effect of both adjuvants was observed in levels of anti-HBs- and anti-HBc (Fig. 2.6.2 F and G). Therefore it was concluded that TLR2 did not play a role in detection of PCEP.

Taken together PCEP is not recognized by TLR2, 3 or 4 but requires MyD88 for its immune stimulatory function.

2.6.3 Effects of adjuvants on B cells and dendritic cells *in vitro*

To investigate the effect of the single components used in the protein vaccine formulation on B cells and primary bone marrow-derived dendritic cells (BMDCs), studies on activation and antigen uptake were performed in cell culture experiments. To study uptake of HBsAg, B cells were either MACS-purified from spleen or BMDCs were generated from wt mice and incubated with APC-labeled HBsAg (S-APC), HBcAg (C), PCEP and CpG; C, PCEP and

CpG; S-APC, PCEP and CpG; S-APC and CpG; S-APC and PCEP; S-APC alone or S-APC and C. The proportion of the single compounds in the different mixtures was chosen to be the same as in the previous mouse experiments. As negative control, cells were incubated with the protein vaccine formulation containing S-APC, C, PCEP and CpG at 4°C. B cells were incubated for 18 hours and samples were taken at 1, 2, 3, 4, 5, 6, 7, 14, 16 and 18 hours. BMDCs were incubated for 180 minutes and samples were taken at 15, 30, 45, 60, 90, 120 and 180 minutes and HBsAg uptake was analyzed via APC fluorescence. Each time point was measured in duplicates and the mean fluorescence intensity (MFI) of the control group was subtracted of all samples (Fig. 2.6.3.1 and Fig. 2.6.3.2). To investigate B cell or DC activation, the same samples were also assessed for expression of the costimulatory molecule CD80.

A

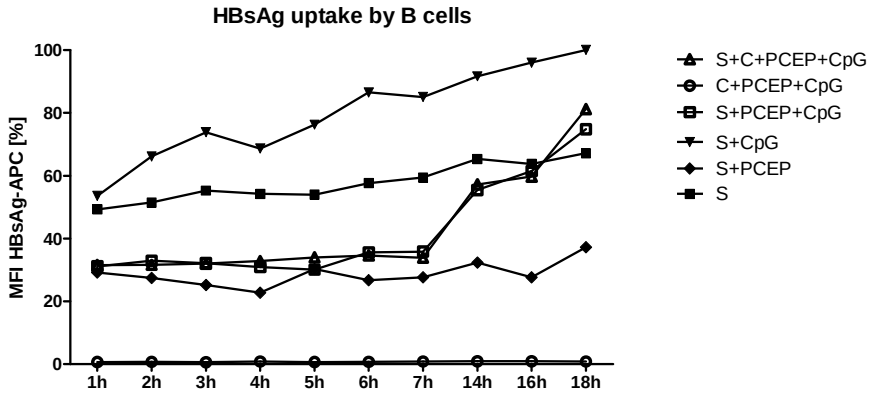

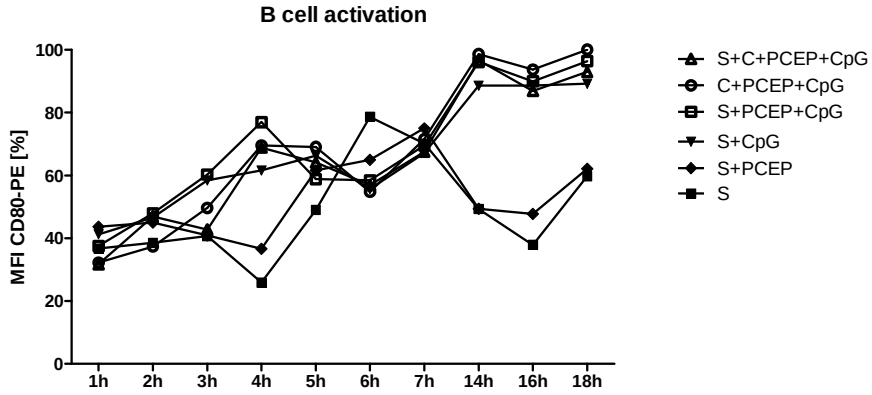

B

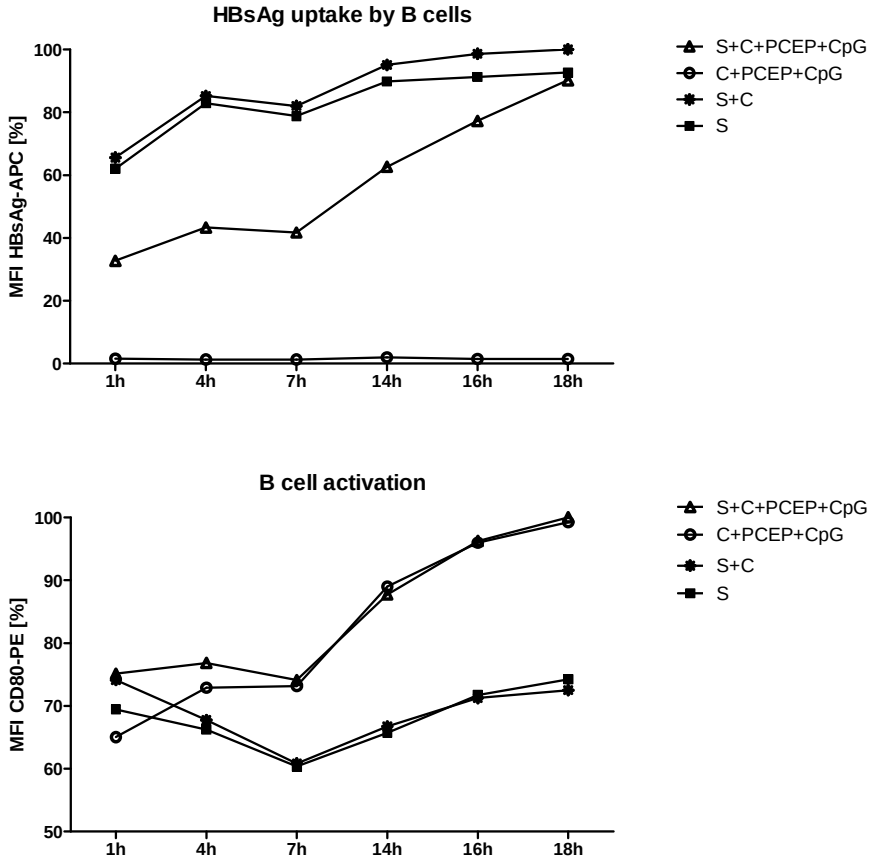

Fig. 2.6.3.1: *In vitro* study of HBsAg uptake by B cells and their activation (A) and (B). B cells were incubated for up to 18 h with indicated mixtures of proteins and adjuvants. HBsAg uptake was measured by MFI of HBsAg labeled with Alexa Fluor 647 (APC)dye detected by FACS. Activation of B cells was measured by mean fluorescence intensity (MFI) of bound surface marker CD80-PE detected by FACS. Control values were subtracted and the mean percentage of maximum activation or uptake is shown.

As shown in Fig. 2.6.3.1 A and B, B cells were activated more strongly and incorporated more HBsAg when CpG was present in the vaccine formulation, whereas PCEP alone did not enhance activation or antigen uptake. However, a marginal synergistic effect of PCEP+CpG on B-cell activation was observed in comparison to the formulation containing only CpG and antigen. The addition of PCEP delayed antigen uptake and using only PCEP as adjuvant led to less activation and antigen uptake. The addition of HBcAg without adjuvants to the labeled HBsAg did not lead to more activation or antigen uptake in B cells over time compared to incubation with HBsAg alone (Fig. 2.6.3.1 B). The effect of CpG or PCEP+CpG was found to be stronger after 14 h of incubation.

Taken together, a direct effect of PCEP or HBcAg on B cells was not observed, but the results showed an enhanced activation and antigen uptake of B cells upon stimulation with CpG or PCEP+CpG. This indicated that the adjuvants used in the protein vaccine formulation

lead to an enhanced overall B cell activation which contributed to overcoming the immune tolerance in HBVtg mice shown above.

Similar results were obtained from experiments in BMDCs shown in Fig. 2.6.3.2. The activation of BMDCs was enhanced by CpG and PCEP+CpG containing formulations, but compared to B cells, BMDCs were activated faster and it was observed that PCEP alone was able to activate BMDCs. HBsAg uptake was delayed but at the same level at 90 min incubation with the formulation containing S+PCEP compared to formulations containing both adjuvants. In both B cells and BMDCs, CpG led to the fastest uptake of antigen. A synergistic effect of PCEP and CpG was not observed in BMDCs.

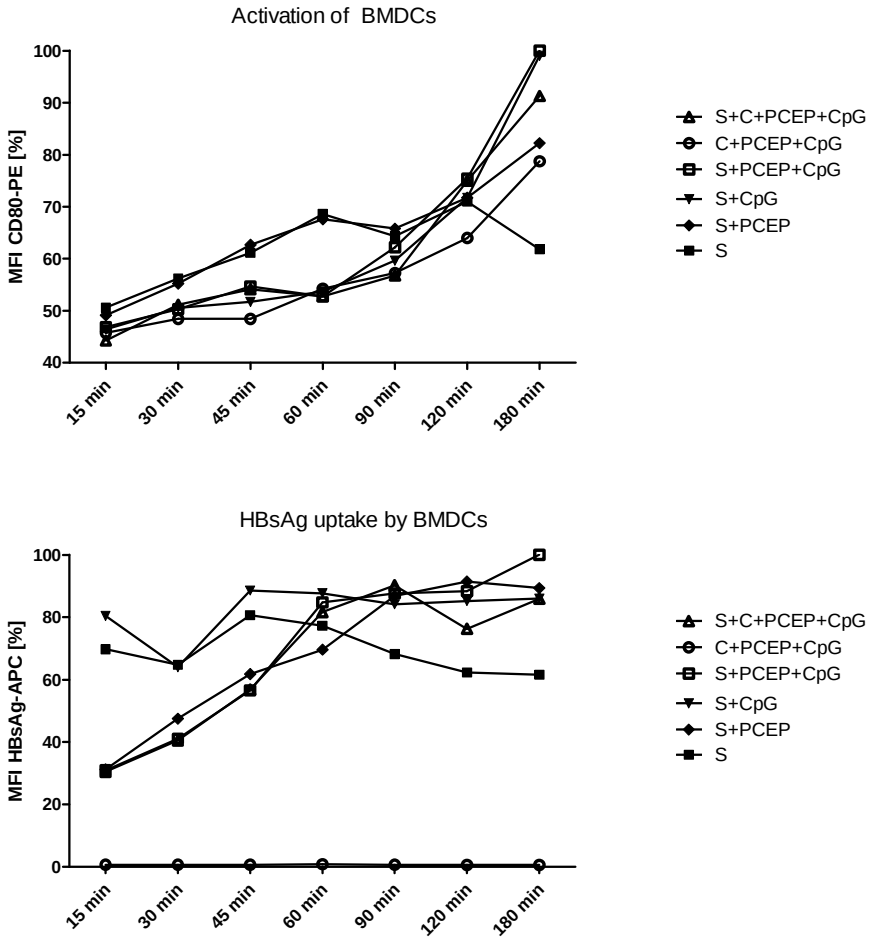

Fig. 2.6.3.2: *In vitro* study of activation and HBsAg uptake by bone marrow derived dendritic cells (BMDCs). BMDCs were incubated for up to 180 min with indicated mixtures of proteins and adjuvants. Activation of BMDCs was measured by MFI of bound surface marker CD80-PE detected by FACS. HBsAg uptake was measured by MFI of HBsAg labeled with Alexa Fluor 647 dye detected by FACS. Control values were subtracted and the mean percentage of maximum activation or uptake is shown.

Taken together, using both adjuvants did not enhance overall activation of BMDCs compared to CpG individually.

2.6.4 Efficiency of prime immunization

Next it was tested, if an increase of adjuvant concentrations could improve activation or HBsAg uptake of B cells. Therefore, purified B cells were incubated with HBsAg-APC and HBcAg in the presence of increasing concentrations of both PCEP and CpG. The first control contained HBcAg and 10-fold increased concentrations of adjuvants, but no HBsAg and was incubated at 37°C. The second control contained HBsAg, HBcAg, PCEP and CpG with the proportion of the components used in animal experiments and was incubated at 4°C.

A

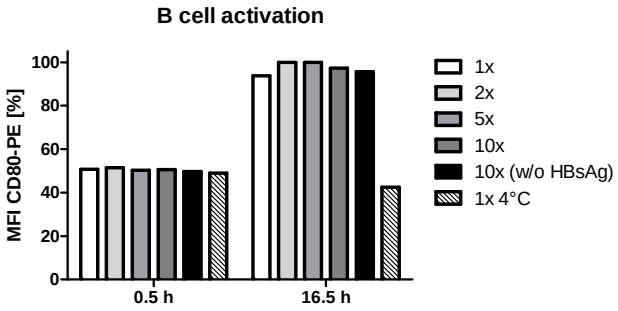

B

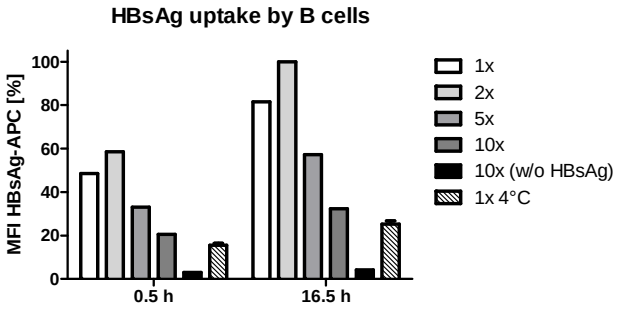

Fig. 2.6.4.1: *In vitro* study of activation and HBsAg uptake by B cells. B cells were incubated for up to 16.5 h with HBsAg + HBcAg + PCEP + CpG with indicated concentrations of adjuvants. Activation of B cells was measured by MFI of bound surface marker CD80-PE detected by FACS (A). HBsAg uptake was measured by MFI of HBsAg labeled with Alexa Fluor 647 (APC) dye detected by FACS (B). Mean percentage of maximum activation/uptake is shown.

As shown in Fig. 2.6.4.1 A, increased concentrations of PCEP and CpG did not lead to stronger B cell activation. HBsAg uptake was enhanced after incubation with double the amount of adjuvants, but was lower using 5 times or 10 times higher concentration of adjuvants (Fig. 2.4.3.3).

Taken together, the proportion of adjuvants to antigens is critical for optimal activation and antigen uptake of B cells.

Additionally, the efficiency of the protein vaccine formulation was tested *in vivo* and compared to an immunization with AdHBVL-. By using AdHBVL- no infectious HBV particles are being produced which classifies the model BSL-2. Wt-mice were vaccinated with either

(1) 5x107 AdHBVL-; (2) 31.91 µg CpG, 50 µg PCEP, 5 µg HBsAg and 5 µg HBcAg or (3) 31.91 µg CpG, 50 µg PCEP, 16 µg HBsAg and 16 µg HBcAg. Mice were sacrificed on day 8; splenocytes were purified and CD8 T cells were analyzed for IFNγ production upon stimulation with HBV-derived peptides by ICS and FACS detection (Fig. 2.6.4.2 A).

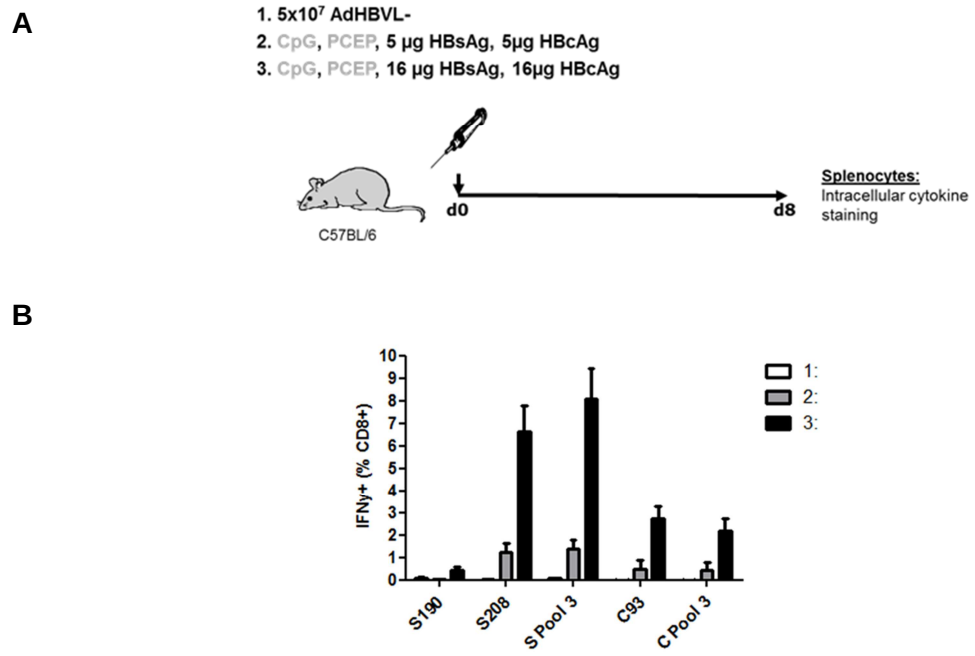

Fig. 2.6.4.2: Comparison of T cell responses upon immunization with AdHBVL- or HBsAg and HBcAg with 10 or 32 µg in total adjuvanted with PCEP and CpG in C57BL/6 mice. (A) Vaccination scheme. On day 8, splenocytes were stimulated with HBsAg-derived peptides S190, S208, S Pool 3 containing 15 mers, HBcAg-derived peptides C93 or C Pool 3 containing 15mers and analyzed for IFNγ expression by ICS (B). Frequencies of IFNγ+ CD8+ T cells are background subtracted.

Immunization with adenovirus expressing all HBV proteins except the L-protein and therefore lacks virus particle formation was not able to induce an HBV-specific CD8 T cell response. Increasing the ratio of adjuvants to antigen did not enhance CD8 T cell responses compared to the standard ratio (2.6.4.2 B).

From this experiment we concluded that the adjuvants to antigen ratio used in the vaccinations described above was in an optimal range to have a maximum effect in priming CD8 T cell responses.

3. Discussion

Therapeutic vaccination is a promising strategy to treat infectious diseases like Hepatitis B. Aiming to activate the immune system of the host against the pathogen which then can be eradicated is considered to be an elegant way of treatment. A major task of a vaccination strategy is to elicit CD8 T cell responses. CD8 T cells play a crucial role in clearing HBV. It was shown that depletion of CD8 T cells during acute HBV infection led to persistence of the virus in chimpanzees (Thimme 2003).

Up to date the success of therapeutic vaccination is very limited. The main reason is the peripheral tolerance towards the viral antigens that is established in chronic hepatitis B patients. Moreover it was shown that persistent infection is associated with exhausted virus-specific CD8 T cells (Jung 1991, Penna 1991, Rehermann 2005, Yang 2010). Therefore, a vaccination strategy is needed that is able to overcome the status of tolerance and induces a strong multispecific and polyfunctional immune response on cellular as well as on humoral level.

Several clinical trials have been performed with vaccines that were designed based on the conventional HBsAg vaccine. In some of these trials HBeAg seroconversion, HBV-specific immune responses and decrease of viral load was observed, however these effects were transient and did not lead to viral clearance (Couillin 1999, Dikici 2003, Jung 2002, Yalcin 2003). Another clinical trial was performed with immunogenic complexes consisting of HBsAg and anti-HBs antibodies. A phase III clinical trial, in which patients received 12 injections of immunogenic complexes or alum as control failed to show therapeutic efficacy (Xu 2013). In previous studies performed in our group by Simone Backes, it was found that a heterologous prime-boost vaccination with adjuvanted protein and recombinant MVA is able to induce a strong CD8 T cell response against HBV in wt mice and HBVtg mice with low antigenemia, but not high antigenemia (HBeAg > 7 S/CO) (Backes, Jäger submitted). It is worth to mention that heterologous vaccination with DNA prime and recombinant MVA boost was also tested in wt mice with a similar outcome (unpublished data) which is generally in line with findings by other groups (McConckey 2003, Hanke 1999). Furthermore, it was found that the vaccination-induced immune response inversely correlated with antigenload in sera of HBVtg mice (Backes, Jäger submitted). This observation is in line with an *in vitro* study with myeloid DCs that differentiated to a more tolerogenic phenotype in presence of HBsAg, indicates its inhibitory effects on the development of an HBV-specific immune response (Op den Brouw 2009).

In this study new findings were gained that might contribute to the development of a therapeutic vaccination to successfully treat chronic hepatitis B patients.

3.1 Adjuvants are key factors for protein-based vaccine formulations

Usually proteins taken up by antigen presenting cells (APCs) are presented on MHC class II and therefore are recognized by CD4 T cells. However, the main targets of a therapeutic vaccination against viral infections are CD8 T cells. Nevertheless it is possible to prime CD8 T cells with a protein-vaccine because APCs are able to present extracellular antigens on MHC class I via cross presentation (Burgdorf 2007). Choosing a beneficial combination of adjuvants for a protein-based vaccine is fundamental to elicit immune responses in a prime-boost vaccination scheme.

In a recent study HBsAg was adjuvanted with monophosphoryl lipid A (MPL) and QS21 in an oil and water emulsion. Although it was able to induce HBsAg specific cellular immune responses and antibodies in patients co-treated with lamivudine, it had no additional clinical effect compared to patients treated with lamivudine alone (Vandepapeliere 2007). The importance of potent adjuvants included in protein-vaccine formulations was also shown in a study with a saponin-based adjuvant called ISCOMATRIX^{TM} performed by Pascale Buchmann in cooperation with our group (Buchmann 2013). ISCOMATRIX^{TM} has essentially the same structure as iscom (immune-stimulating complex) which was first described by Morein and colleagues (Morein 1984). However, there is no incorporation of an antigen. Thus, it can be formulated with a broad variety of antigens with the same immunomodulatory properties as the iscom (Pearse 2005). HBsAg, HBcAg or the combination of both were supplemented with ISOMATRIX^{TM} and used for vaccination studies in wt mice or HBVtg mice that showed HBeAg levels below 10 S/CO prior to treatment. In wt mice, a balanced T_H1/T_H2 type HBV-specific immune response was induced. In HBVtg mice seroconversion was observed and HBV-specific CD8 T cell responses were detected in spleens and livers. However, in high antigenemic HBVtg mice, this vaccination strategy failed to induce an immune response (unpublished data).

As demonstrated in this study, it is possible to enhance immune responses by using the adjuvants PCEP and CpG which have been shown to have synergistic effects (Mutwiri 2008) and thus are more potent for eliciting immune responses in wild type mice (2.3.1). In agreement with the data from Klinman and colleagues, it was demonstrated that addition of CpG alone could enhance the induction CD8 T cell responses (Klinman 2004, Klinman 2006). However, PCEP primarily enhanced humoral responses. The combination of both adjuvants led to strong cellular and humoral immune responses (2.3.1). The addition of aluminum hydroxide in the protein vaccine (using commercial Engerix B vaccine) formulation did not lead to an enhanced CD8 T cell response when comparing the responses against C93 shown in 2.3.1.1 and 2.3.1.2. The difference of the immune responses against HBsAg can be attributed to the amount of HBsAg in Engerix B. Since 1 ml of Engerix B contains 20

µg, it was not possible to use the same amount of HBsAg from Engerix B compared to the recombinant HBsAg. Therefore the amount of HBsAg was 80 times lower when Engerix B was used. However, this dose of HBsAg was found to induce high levels of anti-HBs suggesting that aluminum hydroxide is a powerful adjuvant for induction of humoral responses (2.3.1.2). Moreover, observations made in a study with chronic HBV carriers that received the prophylactic HBsAg vaccine (Francis 1982) showed no benefit for the patients (Dienstag 1982). An alternative attempt to replace the protein-vaccine with an adenoviral vector vaccine expressing HBV antigens lacking the L-protein failed to induce an HBV-specific humoral and cellular immune responses post MVA boost (data not shown) although it was shown that the combination of both viral vectors can be beneficial in studies dealing with vaccinations against malaria (Gilbert 2002, Reyes-Sandoval 2010).

A powerful formulation of a protein-based vaccine is essential for establishing a strong immune response, however as shown in 2.3.2 multiple applications of the protein-based vaccine were not able to boost the CD8 T cell response as efficiently as a single boost with recombinant MVA in wt mice (2.3.1.1). This might be due to a massive induction of neutralizing antibodies against the HBV antigens upon the first (or second) vaccination. Interestingly, an epitope switch with the specificity of responding HBV-specific CD8+ T cells was observed after recombinant MVA boost in mice primed with the protein vaccine. While on day 8 post prime immunization S208-specific CD8 T cells dominated over those recognizing the S190 epitope, the picture was reversed on day 6 post boost immunizations (2.3.1.1). This can be explained by the nature of the epitopes. S208 is an exogenous peptide that is processed when HBsAg is taken up by the APC, whereas S190 is an endogenous peptide that is predominantly presented when HBsAg is produced inside the cytoplasm of APC e.g. upon infection with MVA-S (Schirmbeck 2003).

The polyphosphazene PCEP activates adjuvant core response genes that lead to production of cytokines, chemokines, innate immune receptors, interferon-induced genes and adhesion molecules by cells recruited to the site of injection. It further upregulates expression of TLR9 and TLR4 genes among others (Awate 2012). The data in this study indicate that the TLR-adaptor protein MyD88 plays an important role in eliciting immune responses to antigens adjuvanted with PCEP. Furthermore it could be shown that PCEP's mechanism of action does not involve TLR3 or TLR4 as shown in 2.6.2.

For synthetic polyelectrolytes (SPE) like polyphosphazenes it was shown that they induce formation of nanopores in the cellular membranes of target cells which leads to diffusion of ions. These nanopores distort the natural state of the cell, since the resulting potassium ion drain and influx of calcium ions trigger a compensatory switching of molecular pumps. This serves as a signal for launching other intracellular systems and the cell is in an activated state. The target cell is defined by the antigen that is conjugated with the SPE. Since APCs

take up free antigens they will be activated by the attached SPE. For isolated B cells it was shown *in vitro* that they begin to divide, differentiate and start synthesizing receptors for the recognition of antigens and produce complementary antibodies (Kabanov 2004). This effect is not cell-type specific because it depends on the cell that recognizes the antigen. On the one hand, PCEP had no effect on CD80 expression or antigen uptake by B cells when used individually with HBsAg in the setting of the performed *in vitro* studies (2.6.3). On the other hand, it could be observed in this study that PCEP had a positive effect on CD80 expression and antigen uptake of BMDCs. As shown by Andrianov and colleagues (Andrianov 2005), the polyphosphazene to antigen ratio has an impact on the immunogenicity of the protein vaccine formulation. This aspect was also studied *in vitro* and showed that the ratio of adjuvants to antigens used in the vaccinations was in an optimal range as activation and antigen uptake by B cells were only slightly increased. This finding is supported by the *in vivo* study in wt mice (2.6.4.2) where the ratio of adjuvants to antigen was 3.2 to 1 compared to the normal amount of adjuvants and antigens that were used in vaccination studies in HBVtg mice. However, since the ratio was changed by lowering the amount of antigen and not increasing the amount of adjuvants because of strong reactions at the injection side of the mice caused by the adjuvants, it is also likely that the total amount of antigen accounted for the difference in the induced CD8 T cell responses.

Further observations made in the *in vitro* studies showed that CpG more readily activated both B cells and BMDCs and further enhanced antigen uptake. CpG is known to be recognized by TLR9 which leads to a T_H1 type immune response and enhanced secretion of pro-inflammatory cytokines. CpG 1668 used in this study is similar to clinical grade CpG used in clinical trials (Nierkens 2009). The activation of B cells by CpG could be observed *in vitro* (2.6.3) and was indicated by stronger expression of CD80 which is in line with previous findings (Krieg 1995, Lipford 1997, Krieg 2002). The activation of BMDCs by CpG that was also shown in other studies (Sparwasser 1998) could be confirmed *in vitro* as well which shows that the design of the *in vitro* experiments was suitable to answer questions about activation and antigen uptake by the respective cell types. The synergistic effects of CpG and PCEP were not observed *in vitro* but *in vivo* (2.3.1) which supports findings by Mutwiri and colleagues (Mutwiri 2008, Awate 2012).

The possibility to combine adjuvants leaves a lot of opportunities for improvement of therapeutic vaccination strategies that include protein-based vaccine formulations.

3.2 Strong early/late MVA promoters are necessary for sufficient expression of recombinant proteins

Regarding heterologous prime-boost vaccinations, MVA is a very promising candidate as a boost vector because it is highly immunogenic, has a large packaging capacity and targets efficiently APCs (1.5.2). It has an excellent safety profile and is successfully used in humans. In 2013 a smallpox vaccine called IMVANEX® which contains a further attenuated MVA (MVA-BN) was approved by the "European Medicines Agency" (Vollmar 2006, von Krempelhuber 2010).

To design a MVA vector that allows for an efficient expression of the recombinant antigen, it is important to choose a suitable promoter. In this study, promoters were used that lead to expression in both the early and late phase of the MVA infectious cycle. Thereby recombinant antigens are expressed efficiently over an extended period of time. However, not only the time point of expression is crucial but also the intensity. The promoter P7.5 leads to lower expression of recombinant antigens than PH5 (Wyatt 1996). Since HBsAg has immune suppressive properties (Op den Brouw 2009) and is always present in the serum of the HBVtg animals used in this study, it was investigated if a weak or strong additional expression of HBsAg might be more beneficial for the induction of HBsAg-specific immune responses. While in wt mice HBsAg expression controlled by the P7.5 promoter was sufficient to induce strong HBsAg-specific immune responses (2.3.1), this was not the case in HBVtg mice (2.4.1). However, when expression of HBsAg was controlled by the stronger promoter PH5, an HBsAg-specific immune response was detected in HBVtg mice (2.4.1). The reason might be that MVA infected APCs express and therefore present HBsAg-derived epitopes more efficiently, but do not secrete high levels of HBsAg that would lead to more tolerance against the HBsAg. In case of MVA that expresses HBcAg possible tolerizing effects could be excluded since HBcAg does not play a role in preventing immune responses, but rather is known to be very immunogenic. Therefore the weaker promoter P7.5 was not tested in combination with HBcAg expression.

This is an important finding suggesting that a high-level recombinant antigen expression might be beneficial for the induction of immune responses in this model.

3.3 Heterologous subtype of HBsAg overcomes immune tolerance more efficiently

As shown in a study by McAleer and colleagues, vaccination of chimpanzees with HBsAg subtype adw expressed in yeast and adjuvanted with alum was able to induce anti-HBs antibodies that were protective against the related HBV subtypes adr and ayw (McAller

1984). Small differences in the amino acid sequence of the HBsAg occur at several positions in the polypeptide chain which are responsible for subtype specificities (Ono 1983). However, the region containing epitopes for induction of protective humoral immune responses called the antigen determinant “a” (Ruiz-Tachiquin 2007) is dominant and therefore antibodies specific for one subtype can also neutralize other subtypes (McAleer 1984). In line with this, it was found in the present study that anti-HBs antibodies induced via prime-boost vaccination using the heterologous subtype adw of HBsAg inhibited infection of differentiated HepaRG cells by HBV_{ayw} (2.4.1.1) and were able to decrease HBsAg significantly in HBVtg mice (2.4.3). However there might be a difference in affinity to anit-HBsAg antibodies induced by vaccination with homologous $HBsAg_{ayw}$ that could lead to more efficient complexation of antibodies generated upon vaccination. It could explain the observation that HBsAg levels also dropped in mice vaccinated with $HBsAg_{ayw}$ but only a single mouse had a detectable anti-HBs antibody titers whereas all mice vaccinated using $HBsAg_{adw}$ had high titers of anti-HBs. Moreover, the assay used to determine HBsAg-specific antibody titers detects antibodies derived from both subtypes ayw and adw. Another explanation that high titers of anti-HBs antibodies were detected after vaccination using $HBsAg_{adw}$ is that the immunization was more successful in total and therefore the titers of anti-HBs might be higher in mice vaccinated with the heterologous subtype. Importantly, not all antibodies directed against HBsAg are able to neutralize all different subtypes of HBV as observed in chronic HBV carriers that had heterologous anti-HBs antibodies that were not to be able to neutralize HBsAg in the patients (Zhang 2006).

Cross-reactivity was not only detected on antibody level, but also on T cell level, consistent with findings by Riedl and colleagues (Riedl 2006). Cross-reactivity is an essential feature of T cells given that the amount of possible immunogenic nonamer-peptides is 20^9 and to mount a rapid immune response more than one specific T cell is needed to be present at a time (Mason 1998, Regner 2001). Upon vaccination of HBVtg mice using $HBsAg_{adw}$ higher frequencies of CD8 and CD4 T cells were detected that responded to stimulation with peptides derived from $HBsAg_{ayw}$ than following vaccination using $HBsAg_{ayw}$ (2.4.3). Given that a peripheral tolerance against HBV_{ayw} is established in the used model of chronic HBV infection especially because high titers of HBsAg are present in sera of those mice prior to treatment, it was expected that high affinity T cells would be inhibited or rendered anergic by regulatory mechanisms to react against epitopes derived from HBV_{ayw}. This might be an explanation that vaccination with $HBsAg_{ayw}$ was not as effective as vaccination with heterologous $HBsAg_{adw}$. Interestingly, a CD8 T cell response directed against the S208 peptide of $HBsAg_{adw}$ was detected in HBVtg mice vaccinated with $HBsAg_{ayw,}$ although the frequency was lower compared with the response to S208 derived from $HBsAg_{ayw}$ (Backes, Jäger submitted). This shows that the CD8 T cell cross-reactivity is in both directions.

Notably, CD8 T cell responses towards either S190 subtypes was not observed in vaccinated HBVtg mice. This can be explained by the difference in the amino acid sequence of the epitope. While the S208-epitope sequence of subtypes ayw and adw differ in two amino acids, there is only one amino acid difference in the S190-epitope between the two subtypes (table 4.1.11). Therefore, CD8 T cells recognizing one of those S190-peptides are likely to have a rather similar affinity to the S190 derived from the other subtype and are might therefore be more affected by tolerizing mechanisms Additionally, the induction of S190-specific CD8 T cell responses was found to be rather weak post prime immunization even in wt mice. Therefore it can be speculated that the priming of S190-specific T cells was not sufficient in HBVtg mice and thus a boost immunization could not lead to a solid amount of T cells reacting to the S190-peptide.

Overall, these data suggest that exploiting cross-reactivity of both cellular and humoral components of the immune system might represent a promising strategy to overcome peripheral tolerance in chronic infectious diseases.

3.4 T cells induced by vaccination are polyfunctional, but strongly regulated

The quality of the CD8 T cell responses is essential for the outcome of an infection with HBV. Typically, a weak and monoclonal immune response is associated with a state of chronic infection. In most cases, T cells from those chronically infected patients are unable to proliferate or produce cytokines and lack cytotoxicity. This state of non-responsiveness has been attributed to high levels of persisting viral antigens (Rehermann 2007) and can also be found in the HBVtg mouse model used in the present study. In previous studies it was shown that the ability to produce the pro-inflammatory cytokine IL-2, which is known to induce proliferation of T cells, is one of the first to be lost if a T cell is developing towards an exhausted state. Further functions that are lost are cytotoxicity and the production of TNFα. IFNγ is the last cytokine that is produced before the cell becomes exhausted (Wherry 2004). In contrast, T cells of patients that have recovered from a hepatitis B infection maintain functional and are detectable in high numbers (Rehermann 2007).

In the present study, HBVtg mice that were treated with the most efficient prime-boost vaccination strategy (including two immunizations with the protein vaccine consisting of HBsAg, HBcAg, PCEP and CpG followed by a final boost immunization with recombinant MVAs that express either HBsAg or HBcAg under the control of the strong early/late promoter PH5), showed to some extent the induction of polyfunctional (IFNγ+, TNFα+ IL-2+) peptide $S208_{ayw}$-specific CD8 T cells (2.4.1; 2.4.2 and 2.4.3). However, those cells were present at very low percentages. A rather modest amount of T cells produced two cytokines

namely IFNγ and TNFα. Those cells were either inhibited or lost the ability to express IL-2 which indicates a negative regulation of those cells by other cells like regulatory T cells. Furthermore, most T cells were found to have a monofunctional phenotype only expressing IFNγ or TNFα. The presence of cells that only express TNFα can be explained with unspecific activation due to the purification procedure. Therefore, instead of the total cytokine response, IFNγ production was the main criterion to determine whether an immune response was induced in these mice. In HBVtg mice, T cells are constantly exposed to an inhibitory environment because the hepatocytes that express HBV are protected by all kinds of regulatory mechanisms and eliminated hepatocytes will be substituted by a new hepatocyte that is transgenic for HBV. This might explain the observation that 56 days post boost immunization, there were hardly any HBV-specific CD8 T cell responses detectable (2.4.4). Compared to the cytokine-expression profile of CD8 T cells specific for the foreign antigen B8R which are not impacted by regulatory mechanism regulated, the main difference in the polyfunctionality of HBV-specific T cells is that less cells produce IL-2. In terms of bi-or monofunctionality the percentage of cells is similar. After all, the T cell immune responses induced by the vaccination were found to be stable for at least 14 days in this model. Interestingly, HBsAg were significantly decreased 56 days post immunization with MVA and antibodies-titers were found to be even higher against HBsAg compared to day 42 which shows a sustained effect of the vaccination strategy on humoral level. Interestingly, HBeAg levels were significantly decreased 56 days post immunization as well. However, it is not clear if the HBeAg-levels were affected by the vaccination since HBe-specific antibodies were not determined.

Monitoring the expression of cytokines is a convenient way to investigate T cell responses and it was shown that there are non-cytolytic mechanisms that enable the innate and adaptive immune system to control viral infection (Guidotti 2000). Especially IFNγ and TNFα are known for their antiviral effects and have been shown to play important roles in viral clearance (Kohonen-Corish 1990) (Sambhi 1991). However, cytolytic activity of T cells is still considered to be essential for clearing pathogens from the host. In the present study it was observed that vaccination-induced CD8 T cells effectively killed S208-bearing target cells that were transferred into wt mice (2.5.1). ICS showed that about 5% of target-specific CD8 T cells were sufficient to eliminate 95% of the 5 million transferred target cells in 16 hours. This indicates that the vaccination leads to fully functional HBV-specific CD8 T cells showing the great potential of the developed vaccination strategy.

However, in wt mice there is no tolerance against HBV and its antigens. In high antigenemic HBVtg mice the same experiment was not successful since no killing of transferred target cells could be detected (data not shown). Assuming that killing by HBV-specific CD8 T cells might be inhibited and the frequency of vaccination-induced CD8 T cells was too low, the

experiment was tested in a model of chronic hepatitis B using low dose immunization with an adenoviral vector that expresses the HBV genome lacking the X-protein (2.5.2). This model was not established in our laboratory, but has been shown to represent a useful model to study immune responses against HBV with the advantage that HBV can actually be cleared from the host (Huang 2012). However, this model has its difficulties. Although all mice were treated the same and received the exact same amount of AdHBVx-, one of the control mice developed an immune response against the HBsAg and one mouse developed antibodies against the HBcAg (Fig. 2.5.2.3). Only, a slight killing of target cells was observed in the group of mice that were vaccinated against HBV. This might be due to the weak induction of HBV-specific T cells and the high number of potential target cells since there are also endogenous target cells represented by the hepatocytes that present the S208-epitope. Since ALT levels did not increase post vaccination, it can be concluded that the treatment did not lead to a massive killing of HBV-expressing hepatocytes. Considering the high levels of HBeAg and HBsAg in the sera at the time when the first immunization was performed (day 14), the weak induction of an anti-HBV immune response might be linked to the tolerogenic effects of those antigens. Another hint is provided by the ELISpot analysis (Fig. 2.5.2.4) which showed a much higher amount of splenocytes that produced IL-10 which is a negative regulator for immune responses (Fiorentino 1991, Taga 1992, Steinbrink 1997). Interestingly, the expression of IL-10 was only detected upon stimulation with HBcAg, but not with HBsAg. This might be explained by the higher immunogenicity of the HBcAg, or alternatively by a cross-reactivity of the CD8 T cells with the DNA binding domain of the HBcAg which is very similar to the DNA binding domain of the adenoviral vector and highly immunogenic (personal communication with Stefanie Graf).

In general, the established vaccination strategy leads to expression of antiviral cytokines and enables killing of cells presenting HBV-antigens to CD8 T cells, but is strongly dependent on the level of peripheral tolerance that is present in the host.

3.5 Vaccination leads to influx of immune cells into the liver in HBVtg mice

The main focus of the present study was on the induction of immune responses against HBV. Therefore the events happening upon vaccination in the liver where HBV is mostly present in the HBVtg mice were also a point of interest. As shown in 2.4.2, 2.4.3, 2.4.4 and 2.5.2, the immune response was studied also in the liver by purification of liver associated lymphocytes and ICS analysis. Another possibility to get a picture of the events ongoing in the liver is immunohistological staining of liver sections (Fig. 2.5.2.2). B cells were detected using an antibody against B220 which is a specific membrane protein of the B cells (Coffman

1981), whereas T cells were detected using an antibody against CD3 a member of the TCR complex (Allison 1985, 1987) and proliferating hepatocytes were detected using an antibody specific for the protein Ki67 which is present in all proliferating cells (Scholzen 2000). By adjusting carefully the quantification protocol of the software used for analysis, it was possible to count only proliferating Ki67+ hepatocytes.

Upon vaccination with or without HBV-antigens an influx of B and T cells was observed, indicating recruitment of adaptive immune cells to the liver. The presence of more immune cells in mice that were vaccinated only with adjuvants and MVA-wt can be explained by the route of immunization. Since the MVA-boost was injected intraperitoneally, the liver was affected and a lot of cells mainly APCs were infected directly in the liver. However, a tendency to more influx of immune cells after vaccination containing HBV-antigens was detected which indicates a recruitment of HBV-specific immune cells. This finding is consistent with the data obtained by ICS of liver associated lymphocytes. A major concern against therapeutic vaccination is that the induction of an immune response against HBV in chronic carriers could lead to an exacerbation of chronic hepatitis B and/or liver decompensation (Hilleman 2003). In the present study, no significant ALT elevation was observed indicating no severe liver damage. This observation is supported by the liver histology which did not show any abnormality. This is in line with observations made by Buchman and colleagues in the same mouse model (Buchmann 2013) and Lau and colleagues who performed bone marrow transplantation from donors with naturally acquired immunity into chronically infected patients (Lau 2002). However in the present study, a significant increase of proliferating hepatocytes was observed in vaccinated mice compared to untreated mice. This effect was not specific for mice that were treated with the vaccination including HBV-antigens indicating that the proliferation occurred upon vaccination with MVA.

Taken together, it was observed that immune cells infiltrate the liver slightly more after vaccination including HBV-antigens which does not lead to severe liver damage and can therefore be considered to be safe.

3.6 Final Conclusion

In the present study new insights were gained into aspects that are important in the development of a successful therapeutic vaccination strategy against chronic hepatitis B virus infection. It was demonstrated that combination of adjuvants that benefit from each other can modulate immune responses from T cell- or antibody-focused to cellular and humoral immune responses. Moreover, antigens can be combined to elicit immune responses to a broader spectrum of viral epitopes. In an environment of tolerance, antigens

that induce cross-reactive immunity might be key to a successful treatment. Furthermore, a strong expression of antigens by recombinant MVA is crucial for an effective boost immunization. Although in the HBVtg mouse-model the immune response was limited and responsive T cells were not detected 56 days post MVA immunization, there were still antibodies detectable and HBs- as well as HBeAg-levels were decreased to low levels which means there was a sustained effect of the vaccination. Considering that antigenemia plays an important role in the success of a therapeutic vaccination (Backes, Jäger submitted), a later time point of the final immunization or further immunizations at later time points might enhance the T cell response. Another option to enhance immune responses in chronic carriers might be to interfere with regulatory mechanisms that lead to T cell exhaustion (Barber 2006, Maier 2007, Velu 2009, Liu 2014). As proposed by Kutscher and colleagues (Kutscher 2012) treatment of chronic hepatitis B patients with nucleoside or nucleotide analogs prior to therapeutic vaccination presents a promising strategy to eradicate the virus and cure the patient.

4. Materials and Methods

4.1 Materials

4.1.1 Laboratory equipment

Name	Type	Manufacturer
Centrifuges	Avanti J-25	Beckman (Munich)
	Megafuge 1.0R	Heraeus (Hanau)
	Biofuge fresco	Heraeus (Hanau)
	Biofuge pico	Heraeus (Hanau)
	5417C	Eppendorf (Hamburg)
	5417R	Eppendorf (Hamburg)
CO_2 Incubator	Function Line Hera Cell 150	Heraeus (Hanau)
	Cellstar	Nunc (Wiesbaden)
Cup sonicator	Sonopuls HD200/UW200	Bandelin (Berlin)
Electrotransformator	E. coli Pulser	Bio-Rad (Munich)
ELISpot reader	ImmunoSpot S5 UV Analyser	CTL (Shaker Heights, USA)
Flow cytometer	FACS Canto	Becton Dickinson (Heidelberg)
	FACS Canto II	Becton Dickinson (Heidelberg)
Freezer (-20°C)	Excellence	Bauknecht (Stuttgart)
Freezer (-80°C)	Hera freeze	Heraeus (Hanau)
	Ult 2090	Revco (Asheville, USA)
Freezing Container	Mr. Frosty	Thermo Fisher Scientific (Waltham, USA)
Fridge (4°C)	UT6-K	Bauknecht (Stuttgart)
Hemocytometer	counting chamber	Brand (Wertheim)
Horizontal Electrophoresis System	A1 Gator	Owl Scientific
	A2 Gator	(Portsmouth, USA)
Ice machine	AF200	Scotsman (Milan, Italy)
Immunoassay system	AxSYM	Abbott Laboratories (North Chicago, USA)
Incubation shaker	Innova 4430	New Brunswick Scientific (Nürtingen)
Laminar flow	HERAsafe HS 12	Heraeus (Hanau)

Magnetic stirrer	Ikamag Reo	IKA Werke (Staufen)
Micropipette	Pipetman P2-1000 Eppendorf Research 10-5000	Gilson (Middleton, USA) Eppendorf (Hamburg)
Microscope	Axiovert 25 Kolleg SHB 45 Fluoview FV101	Carl Zeiss (Oberkochen) Eschenbach (Nürnberg) Olympus (Tokio, Japan)
Microwave	900W	Siemens (Munich)
Multichannel pipette	Discovery 20-200	Kinesis (Langenfeld)
Nitrogen container	Cryo 200	Forma Scientific (Waltham, USA)
PCR Cycler	GeneAmpR PCR System 2700	Applied Biosystems (Foster City, USA)
pH-Meter	InoLab pH Level 1	WTW GmbH (Weilheim)
Pipettor	Easy jet Pipetman Accu-jet	Eppendorf (Hamburg) Gilson (Middleton, USA) Brand (Wertheim)
Power supply unit	Model 200 / 2.0 Power Pac	Bio-Rad (Munich) Biometra (Goettingen)
Rotor	Typ 19, SW28, SW41	Beckamnn (Munich)
Semi-dry blotting system	Trans-Blot SD Semi-Dry Transfer Cell	Bio-Rad (Munich)
Slidescanner microscope	SCN 400	Leica (Wetzlar)
Steam Sterilizer	Varioklav 500E	H+P (Oberschleißheim)
Thermomixer/-block	Thermomixer 5436 Comfort	Eppendorf (Hamburg) Eppendorf (Hamburg)
Ultracentrifuge	Optima LE-8K	Beckmann (Munich)
Ultrasound needle	UW 200	Bandelin electronic (Berlin)
UV Lamp	UVT 2035	Hero Lab (Wiesloch)
Vortexer	VF2 Vortex Genie 2	IKA Werke (Staufen Scientific Industries (Bohemia, USA)
Waterbath	Assistant VTE Var 3185	Hecht (Sondheim)

4.1.2 Software

Product	Manufacturer
FacsDIVA	Becton Dickinson (Heidelberg)
FlowJo 6.4.2	Treestar (Ashland, USA)
GraphPadPrism 4	Graph Pad Software (San Diego, USA)
Light Cycler 480 Software	Roche (Basel, Switzerland)
Microsoft Office 2010	Microsoft (Redmond, USA)
Pestle v5.0.1	Provided by Mario Roederer, NIH (USA)
SlidePath Digital Image Hub 4.0	Leica Microsystems (Wetzlar)
SlidePath Tissue Image Analysis 2.0	Leica Microsystems (Wetzlar)
Spice v4.1.5	Provided by Mario Roederer, NIH (USA)

4.1.3 Kits

Product	Manufacturer
AxSYM AUSAB Reagent Pack	Abbott Laboratories (North-Chicago, USA)
AxSYM Core Reagent Pack	Abbott Laboratories (North-Chicago, USA)
AxSYM HBe 2.0 Reagent Pack	Abbott Laboratories (North-Chicago, USA)
AxSYM HBsAg (V2) Reagent Pack	Abbott Laboratories (North-Chicago, USA)
B Cell Isolation Kit, mouse	Miltenyi Biotec (Bergisch Gladbach)
BD Cytofix/Cytoperm Kit	BD Biosciences (Heidelberg)
ELISpot plus Kit, mouse	Mabtech (Nacka Strand, Sweden)
Gene Jet Plasmid Miniprep Kit	Fermentas (St. Leon-Rot)
High Pure Viral Nucleic Acid Kit	Roche (Basel, Switzerland)
LightCycler 480 SYBR Green I Master	Roche (Basel, Switzerland)
Toxinsensor Chromogenic LAL Endotoxin Assay Kit	GeneScript (Piscataway, USA)
QIAGEN Plasmid Maxi Kit	QIAGEN (Hilden)
QIAquick Gel Extraction Kit	QIAGEN (Hilden)
QIAquick PCR Purification Kit	QIAGEN (Hilden)

4.1.4 Chemicals, Reagents, Medium supplements

Product	Manufacturer
1 kb DNA ladder	Invitrogen (Karlsruhe)
2-β-Mercaptoethanol	Sigma (Munich)

Acrylamid/Bisacrylamid (30 %)	National Diagnostics (Atlanta, USA)
Agarose	Gibco/BRL (Eggenstein)
Aminocaproic acid	Sigma (Munich)
Ammonium chloride	Roth (Karlsruhe)
Ammonium persulfate (APS)	Merck (Darmstadt)
Ampicilin (Amp)	Serva (Heidelberg)
Carboxyfluorescein succinimidyl ester (CFSE)	Molecular Probes (Eugene, USA)
Casein extract	Roth (Karlsruhe)
Concavanalin A	Sigma (Munich)
Bacto Agar	Difco Laboratories (Detroit, USA)
Bovine serum albumin (BSA)	Sigma (Munich)
Brompehnol blue	Serva (Heidelberg)
Desoxyribonucleotides	Roche (Basel, Switzerland)
Dimethyl sulfoxide (DMSO)	Merck (Darmstadt)
Ethylenediaminetetraacetic acid (EDTA)	Sigma (Munich)
Ethanol	Merck (Darmstadt)
Ethidium bromide	Serva (Heidelberg)
Ethidium monoacid bromide (EMA)	Invitrogen (Carlsbad, USA)
Fetal bovine serum (FBS) fetalclone II	Thermo Fisher Scientific (Waltham, USA)
Fetal calf serum (FCS)	Gibco/BRL (Eggenstein)
Ficoll LSM 1077	PAA (Pasching, Austria)
FuGene 6	Roche (Basel, Switzerland)
Gentamicin	Ratiopharm (Ulm)
Glucose	Sigma (Munich)
GlutaMAX	Life Technologies (Carlsbad, USA)
Glycerol	Roth (Karlsruhe)
Granulocyte macrophage colony-stimulating factor (GM-CSF)	In-house production kindly provided from the group of Ingo Drexler
HCl	Merck (Darmstadt)
Heparin-Natrium 25000	Ratiopharm (Ulm)
Human insulin	Sanofi-Aventis (Paris, France)
Hydrocortisone	Pfizer (New York, USA)
Ionomycin	Sigma (Munich)
Lipopolysaccharide (LPS)	Sigma (Munich)
Methanol	Merck (Darmstadt)

Monopotassium phosphate	Roth (Karlsruhe)
Monosodium phosphate	Roth (Karslruhe)
NP-40	Serva (Heidelberg)
PAGERuler Prestained ladder	Thermo Scientific (Waltham, USA)
Paraform aldehyde (PFA)	Sigma (Munich)
Penicilin-Streptamycin (Pen-Strep)	Lonza (Basel, Switzerland)
Percoll	GE Healthcare (Little Chalfont, UK)
Phenol	Roth (Karlsruhe)
Phorbol 12-myrstate 13-acetate (PMA)	Sigma (Munich)
Phosphate buffered saline (PBS)	Lonza (Basel, Switzerland)
Phytohemagglutinin (PHA)	Sigma (Munich)
Pierce ECL Western Blotting Substrate	Thermo Scientific (Waltham, USA)
Pokeweed mitogen (PWM)	Sigma (Munich)
Potassium chloride	Roth (Karlsruhe)
PVDF-membrane	Zefa (Harthausen)
Reti-Phenol/Chloroform/Isoamyl alcohol	Roth (Karlsruhe)
RPMI 1640	Gibco/BRL (Eggenstein) Lonza (Basel, Switzerland)
Skim Milk Powder	Fluka (Buchs, Switzerland)
Sodium bicarbonate	Roth (Karlsruhe)
Sodium acetate	Sigma (Steinheim)
Sodium azide	Roth (Karlsruhe)
Sodium chloride	Roth (Karlsruhe)
Sodium dodecyl sulfate (SDS)	Serva (Heidelberg)
Sucrose	Calbiochem (Billerica, USA)
Tertamethylethylenediamine (TEMED)	Bio-Rad (Munich)
Tris	Roth (Karlsruhe)
Trypan blue	Biochrom KG (Berlin)
Tween 20	Sigma (Munich)
William's Medium	Life technologies (Carlsbad, USA)
Yeast extract	Roth (Karlsruhe)

4.1.5 Consumables

Product	**Manufacturer**
3MM-Filter papier	Whatman (Maidstone, UK)

ART Pipette tips	Molecular Bioproducts (San Diego, USA)
Beakers	Brand (Wertheim)
Bottles	Brand (Wertheim) Schott (Mainz)
Cell culture flasks (T75, T185, T225)	Greiner (Nürtingen) Nunc (Wiesbaden) TPP (Trasadingen, Switzerland)
Cell culture plates 6-, 12-, 96-well	Corning (New York, USA)
Cell scraper	TPP (Trasadingen, Switzerland)
Cell strainer 100 µm	BD Pharmingen (Hamburg)
Erlenmeyer flasks	Brand (Wertheim)
FACS tubes	Bio-Rad (Munich)
Falcon tubes (15 ml, 50 ml)	BD Pharmingen (Hamburg)
Gene pulser cuvettes	Bio-Rad (Munich)
Gloves	Kimberly-Clark (Mainz) Meditrade (Kiefersfelden)
Graduated cylinders	Brand (Wertheim)
Microtiter plates (96-well)	Roche (Basel, Switzerland)
PCR reaction tubes	Eppendorf (Hamburg)
Petri dishes	Nunc (Wiesbaden)
Pipette 'Cellstar' (2-25 ml)	Corning (New York, USA) Sarstedt (Nürmbrecht)
Reaction tubes (0.5 ml, 1.5 ml, 2 ml)	Eppendorf (Hamburg)
Reflovet Plus reader	Roche (Basel)
Sterile filters (Minisart 0.2-0.45 µm)	Sartorius AG (Göttingen)
Syringes (5 ml, 10 ml, 50 ml) **Omnifix-F 1ml**	BD Pharmingen Braun (Melsungen)
Ultracentrifuge tubes (UltraClear)	Beckmann (Munich)
Whatman Papier "thick"	Bio-Rad (Munich)

4.1.6 Buffers and solutions

Buffer	Composition
1,2 CsCl buffer	26,8 % CsCl (v/w) 10 mM Tris-HCl pH 8.0

1,4 CsCl buffer	53 % CsCl (v/w) 10 mM Tris-HCl pH 8.0
A1 buffer	300 mM Tris 20 % Methanol (v/v) Fill up to 1 liter with ddH_2O
A2 buffer	25 mM Tris 20 % Methanol (v/v) Fill up to 1 liter with ddH_2O
Cathode buffer	25 mM Tris 40 mM aminocaproic acid 20 % Methanol (v/v) Fill up to 1 liter with ddH_2O
Crude extraction buffer 10x (pH 8.8)	750 mM Tris 200 mM Ammonium sulfate 12 mM Magnesium chloride
Dialysis buffer	10 mM Tris-HCl pH 8.0 4 % Sucrose (w/v) 2 mM $MgCl_2$
DNA loading buffer (5x)	99.95 % Glycerol (v/v) 0.04 % Bromphenol blue (w/v) 0.01 % Na_2PO_4 (v/v)
FACS buffer	1 % BSA (w/v) 0.02 % NaN_3, from 20 % stock (w/v) in 1x PBS
LB agar	1.5 % Agar In LB medium
LB-medium pH 7.0	1 % Casein extract (w/v) 0.5 % Yeast extract (w/v) 0.5 % NaCl (w/v) 0.1 % Glucose (w/v)
Paraformaldehyde (PFA)	2 % Paraformaldehyde (w/v), in PBS buffer
PBS buffer pH 7.4	0.14 M NaCl 2.7 mM KCl 3.2 mM Na_2HPO_4 1.5 mM KH_2PO_4

Proteinase K	1 mg/ml Proteinase K 1.5 mM $CaCl_2$
Protein loading buffer pH 6.8 (2x)	50 mM Tris 20 % Glycerol (v/v) 2 % SDS (w/v) 0.04 % Bromphenol blue (w/v) 84 mM 2-Mercaptoethanol
SDS-PAGE running buffer pH 8.3 (10x)	2 M Glycine 250 mM Tris 1 % SDS (w/v) Fill up to 1 liter with ddH_2O
Sucrose 36 % pH9.0	36 % sucrose (w/v) in 10 mM Tris
TAC buffer	90 % NH_4Cl from 0.16 M stock 10 % Tris pH7.65 from 0.17 M stock
TAE buffer pH 8.0	40 mM Tris/HCl 1 mM EDTA
TBS-T buffer pH7.4 (10x)	200 mM Tris/HCl 1.4 M NaCl 1 % Tween 20 (v/v) Fill up to 1 liter with ddH_2O
TEN buffer pH 7.4 (10x)	1 M NaCl 100 mM Tris 10 mM EDTA
Tris buffer pH 9.0	1 mM
Tris buffer pH 9.0	10 mM
Tris buffer pH 8.0	10 mM

Unless indicated otherwise, buffers were prepared in ultrapure H_2O miliQ. The pH was adjusted with NaOH or HCl.

4.1.7 Media

Cell culture media	Composition
Freezing medium	90 % FCS (heat inactivated at 56°C) 10 % DMSO

Collagenase digestion medium	RPMI 1640 5 % FCS (heat inactivated at 56°C) 0.4 % Collagenase type IV (w/v)
Differentiation medium	William's medium supplemented with: 10 % FBS Fetalclone II (no heat inactivation) 1 % Penicillin-Streptomycin (v/v) 1% glutaMax 0.023 IU/ml human insulin 4,7 µg/ml Hydrocortisone 80 µg/ml Gentamicin 1.8 % DMSO (v/v)
DMEM for HEK293H cells	10 % FCS (heat inactivated at 56°C) 1 % Pen-Strep 1 % L-Glutamin 1 % Sodium pyruvate 1 % minimum essential medium (MEM)
LB agar	1.5 % Agar In LB medium
LB medium pH 7.0	1 % Casein extract (w/v) 0.5 % Yeast extract (w/v) 0.5 % NaCl (w/v) 0.1 % Glucose (w/v)
RPMI 10 %; 5 %; 2 %	RPMI 1640 supplemented with: 2-10 % FCS (heat inactivated at 56°C) 1 % Pen-Strep

4.1.8 Enzymes

Product	**Manufacturer**
Alcaline Phosphatase - Calf Intestine (CIAP)	Roche (Basel, Switzerland)
Collagenase type 4, CLS4	Worthington (Lakewood, USA)
Phosphatase	Roche (Basel, Switzerland)
Proteinase K	Roth (Karslruhe)
PmeI (NEB4 buffer, BSA)	New England Biolabs (Ipswich, UK)
RNase A	Machery-Nagel (Düren)

T4 DNA Ligase	Roche (Basel, Switzerland)
Trypsin	Life technologies (Carlsbad, USA)

4.1.9 Plasmids

Plasmid	Source
pIIIΔHR-PH5 (transfer plasmid)	Institute of Virology, Helmholtz-Zentrum
pSVB45M (template for L adw)	Institute of Virology, Helmholtz-Zentrum
pSVHBV1LE (template for Core adw)	Institute of Virology, Helmholtz-Zentrum

4.1.10 Synthetic Oligonucleotides

Name	Sequence
Primer qPCR:	
HBV 3053 fw	5' TAC TAG GAG GCT GTA GGC ATA 3'
HBV 134 rev	5' GGA GAC TCT AAG GCT TCC C 3'
C forw adw	5' GGC CGT TTA AAC ATG GAG GAC ATT GAC CCT TAT AAA 3'
C-PmeI rev	5' GGC CGT TTA AAC CTA ACA TTG AGA TTC CCG A 3'
L forw adw	5' GGC CGT TTA AAC ATG GGG ACG AAT CTT TCT G 3'
S rev adw	5' GGC CGT TTA AAC TTA AAT GTA TAC CCA GAG ACA 3'
S-stop1	5' CTC GTG TTA GAG GCG GGG TTC TTC TTG TTG ACA AGA ATC CT 3'
S-stop2	5' AAC CCC GCC TGT AAC ACG AG 3'
Del III 3' (GS83)	5' GAA TGC ACA TAC ATA AGT ACC GGC ATC TCT AGC AGT 3'
Del III 5' (FIII1b)	5' CAC CAG CGT CTA CAT GAC GAG CTT CCG AGT TCC 3'
K1Lint-1	5'- TGA TGA CAA GGG AAA CAC CGC -3
K1Lint-2	5'- GTC GAC GTC ATA TAG TCG AGC -3'

4.1.11 Synthetic peptides

Peptide	MHC Restriction	Amino acid sequence	Origin	Source
β-Gal$_{96}$	H2-K^b	DAPIYTNV	ß-Galactosidase	Kindly provided by Ingo Drexler
B8R$_{20}$	H2-K^b	TSYKFESV	MVA	Kindly provided by Ingo Drexler
C18	HLA-A2	FLPSDFFPSV	HBV	JPT (Berlin)

C93	H2-K^b	MGLKFRQL	HBV	JPT (Berlin)
C107	HLA-A2	CLTFGRETV	HBV	JPT (Berlin)
C120	HLA-A2	VSFGVWIRTPPA	HBV	JPT (Berlin)
C128	H2-K^b	TPPAYRPPNAPIL	HBV	JPT (Berlin)
C Pool 3	H2-K^b	Peptides 31-43	HBV	Thinkpeptides (Oxford, UK)
OVA$_{257}$	H2-K^b	SIINFEKL	Chicken	JPT (Berlin)
S183	HLA-A2	FLLTRILTI	HBV	JPT (Berlin)
S190 adw	H2-K^b	VWLSAIWM	HBV	JPT (Berlin)
S190 ayw	H2-K^b	VWLSVIWM	HBV	JPT (Berlin)
S208 adw	H2-K^b	IVSPFIPL	HBV	JPT (Berlin)
S208 ayw	H2-K^b	ILSPFLPL	HBV	JPT (Berlin)
S335	HLA-A2	WLSLLVPFV	HBV	JPT (Berlin)
S Pool 3	H2-K^b	Peptides 37-54	HBV	Thinkpeptides (Oxford, UK)

4.1.12 Antibodies

Specificity	Manufacturer	Used dilutions
anti-B220 FITC	eBioscience (San Diego, USA)	1:250
anti-mCD4 PE	eBioscience (San Diego, USA)	1:100
anti-mCD8a Pacific Blue	eBioscience (San Diego, USA)	1:100
anti-mCD11c PE-Cy7	eBioscience (San Diego, USA)	1:200
anti-mCD45.1 APC	eBioscience (San Diego, USA)	1:100
anti-mCD80 PE	eBioscience (San Diego, USA)	1:200
anti-mIFNγ FITC	eBioscience (San Diego, USA)	1:300
anti-mIL-2 APC	eBioscience (San Diego, USA)	1:200
anti-TNFα PE-Cy7	eBioscience (San Diego, USA)	1:200
F$_C$-block anti-mCD16	BD Bioscience (San Jose, USA)	1:100
Hepatect CP 100 IU/mL antibody	Biotest Pharma (Dreieich)	1:62.5

4.1.13 Cell lines

Cell line	Description
BHK-21	Baby hamster kidney fibroblasts
CEF	Primary chicken embryo fibroblasts
HEK-293H	Human embryonic kidney cells
HuH-7	Human hepatocellular carcinoma cells
RK-13	Rabbit kidney cells

4.1.14 Antigens

Antigen	Manufacturer
HBcAg	RheinBiotech (Düsseldorf) APP Latvijas Biomedicīnas (Riga, Latvia)
$HBsAg_{ayw}$	RheinBiotech (Düsseldorf)
$HBsAg_{adw}$	RheinBiotech (Düsseldorf)
Ovalbumin	Kindly provided by Dr. Ingo Drexler

4.1.15 Viruses

Virus	Description
AdHBVL-	Adenovirus expressing HBV lacking the L-protein
AdHBVX-	Adenovirus expressing HBV lacking the x-protein
MVA-C	MVA-PH5Core, MVA expressing HBcAg regulated by early/late promoter PH5
MVA-OVA	MVA-OVA P7.5, obtained from I. Drexler (Kastenmulller, Gasteiger et al, 2007)
MVA-P7.5S	MVA-P7.5S_{ayw}, MVA expressing HBsAg subtype ayw regulated by early/late promoter P7.5 (weaker than PH5)
MVA-S_{adw}	MVA-PH5S_{adw}, MVA expressing HBsAg subtype adw regulated by early/late promoter PH5
MVA-S_{ayw}	MVA-PH5S_{ayw}, MVA expressing HBsAg subtype ayw regulated by early/late promoter PH5
MVA-wt	MVA IInew, a wildtype strain

4.2 Bacteriological techniques

4.2.1. Culture of *Escherichia coli*

E. coli were generally cultured in liquid LB media with shaking or on agar plates at 37°C.
After transformation bacteria were cultured at 37°C for 1 h in 1 ml LB medium with shaking before transferring them onto LB agar plates containing 100 µg/ml ampicillin and incubation at 37°C overnight.

4.2.2 Preparation of electrocompetent *E. coli* DH10B

E.coli DH10B were cultured in 500 ml LB medium at 37°C under shaking until an optic density (OD) of 0.8 to 0.9 at wavelength 600 nm was reached. The bacteria culture was then cooled down on ice for 20 min and then centrifuged at 5000 rpm and 4°C for 15 min. Afterwards the pellet was washed three times with 500 ml ice cold sterile H_2O miliQ with subsequent centrifugation at 5000 rpm and 4°C for 15 min. The pellet was resuspended in 20 ml ice cold 10 % glycerol and centrifuged at 5000 rpm and 4°C for 15 min. At last, the pellet was resuspended in 1.5 ml ice cold 10% glycerol, aliquoted in cold 0.5 reaction tubes and stored at -80°C.

4.2.3 Transformation of *E. coli* DH10B via electroporation

In pre-cooled gene-pulser cuvettes, 25 µl of electrocompetent *E. coli* DH10B were mixed with 5 µl plasmid DNA and pulsed at 1.8 kV, 200 Ω and 25 µF with an *E. coli* pulser. The cuvette was washed with 1 ml LB medium and the mixture was transferred into a 1.5 ml reaction tube. After incubation for 60 min at 37°C with shaking, the mixture was transferred onto a LB agar plate containing 100 µg/ml ampicillin for selection of transformed bacteria.

4.2.4 Isolation of plasmid DNA

Bacteria colonies were picked, transferred into 3 ml of LB medium containing 100 µg/ml ampicillin and cultured overnight at 37°C with shaking. The following day, bacteria were pelleted by centrifugation at 13000 rpm for 5 min and plasmids were isolated with the Gene Jet Plasmid Miniprep Kit according to manufacturer's instructions. DNA was eluted in 50 µl sterile H_2O miliQ.
For high yield isolation of Plasmid DNA, 300 ml of LB medium containing 100 µg/ml ampicillin were inoculated with 1 ml of a bacteria overnight culture and incubated at 37°C with shaking. The following day, bacteria were pelleted by centrifugation at 5000 rpm and 4°C for 15 min and plasmid isolation was performed with the QIAGEN Plasmid Maxi Kit after manufacturer's

instructions. DNA was eluted in 300 µl sterile H_2O miliQ and the concentration was measured.

4.3 Cell culture techniques

4.3.1 Cell culture passaging

Cells were cultured in RPMI 10% in T175 cell culture flasks if not indicated otherwise. For passaging, cells were washed two times with 10 ml PBS and mobilized by 3 ml Trypsin and pipetting up and down. RK-13 and BHK-21 cells were split twice a week in a 1:10 dilution.

4.3.2 Cryopreservation of cells

Cells were resuspended in 500 µl freezing medium, transferred into cryo tubes and cooled down in Mr. Frosty freezing containers in -80°C freezers. Cells were stored at -80°C.

4.3.3 Thawing of cells

Cells were thawed in a water bath and immediately transferred with a pipette into a 50 ml Falcon tube containing 40 ml RPMI. After centrifugation at 1500 rpm for 5 min, cells were washed with 40 ml RPMI followed by centrifugation with the same conditions. The cell pellet was then resuspended in 3 ml RPMI 10% and transferred into a T175 cell culture flask containing 22 ml RPMI 10% and cultured at 37°C in a CO_2 incubator. One vial of cells was used for one cell culture flask.

4.4 Molecular biology

4.4.1 PCR for preparation of recombinant MVAs

To generate new recombinant MVAs expressing $HBcAg_{adw}$ or the $L\text{-protein}_{adw}$, polymerase chain reactions (PCR) were performed. PCR allows amplifying specific genes or gene fragments. The gene encoding $HBcAg_{adw}$ was amplified with PCR conditions shown in table 4.4.1.1 and temperature settings shown in table 4.4.1.2.

Table 4.4.1.1: PCR mix for amplifying the DNA sequence of $HBcAg_{adw}$

Component	Volume
pSVHBV1LE	1 µl
C forw adw [5 pmol/µl]	1 µl
C-PmeI rev [5 pmol/µl]	1 µl
PCR Mix (Roche)	50 µl
PCR H_20	47 µl

Table 4.4.1.2: Temperature settings for amplifying the DNA sequence of $HBcAg_{adw}$

Phase	Temperature	Time
I: Initial Denaturation	94°C	1 min
II (30x):		
Denaturation	94°C	0 min 15 sec
Annealing	55°C	0 min 30 sec
Elongation	72°C	1 min
III: Final Elongation	72°C	7 min
IV: Hold	4°C	∞

To generate a MVA that expresses the L-$protein_{adw}$ it was necessary to perform two PCRs in a first step that are shown in table 4.4.1.3 and 4.4.1.4 with the temperature settings shown in table 4.4.1.5, and one additional PCR in a second step to receive the sequence encoding the complete L-$protein_{adw}$ shown in table 4.4.1.6 with the same temperature settings.

Table 4.4.1.3: Mixture for PCR A

Component	Volume
pSVB45M	1 µl
L forw adw [5 pmol/µl]	1 µl
S-stop 2 [5 pmol/µl]	1 µl
PCR Mix (Roche)	50 µl
PCR H_20	47 µl

Table 4.4.1.4: Mixture for PCR B

Component	Volume
pSVB45M	1 µl
S rev adw [5 pmol/µl]	1 µl
S-stop 1 [5 pmol/µl]	1 µl
PCR Mix (Roche)	50 µl
PCR H_20	47 µl

Table 4.4.1.5: Temperature settings of PCRs used for construction of the L-protein$_{adw}$ DNA sequence

Phase	Temperature	Time
I: Initial Denaturation	94°C	2 min
II (30x):		
Denaturation	94°C	0 min 15 sec
Annealing	54°C	0 min 30 sec
Elongation	72°C	1 min
III: Final Elongation	72°C	7 min
IV: Hold	4°C	∞

Table 4.4.1.6: Final PCR to create the DNA sequence for the L-protein$_{adw}$

Component	Volume
DNA of PCR A	3 µl
DNA of PCR B	3 µl
L forw adw [5 pmol/µl]	1 µl
S rev adw [5 pmol/µl]	1 µl
PCR Mix (Roche)	50 µl
PCR H_20	47 µl

4.4.2 Analytical gel electrophoresis

The size of the PCR products were analyzed by electrophoresis in 1% agarose gels that were prepared using 1x TAE and DNA-intercalating dye ethidium bromide (5 µg/100 ml gel). The PCR products were mixed with DNA-loading buffer and electrophoresis was performed at 75-85 V for 30 to 50 min. To determine the size and concentration of the DNA, 10 µl of 1

kb DNA ladder was used as standard. After electrophoresis the gel was analyzed using UV light with a wavelength of 312 nm and photographed.

4.4.3 Purification of DNA from agarose gels

To purify PCR products from template DNA, primers and other reaction components, agarose gel electrophoresis was performed and the parts of the gel that contain the DNA fragments of interest were excised with a scalpel. The DNA was extracted using the QIAquick Gel Extraction Kit according to manufacturer's instructions and eluted in 30-50 µl sterile H_2O miliQ.

4.4.4 Restriction enzyme digestion

The DNA fragments encoding for $HBcAg_{adw}$ and $L\text{-protein}_{adw}$ produced by the PCRs described above and the target vector pIIIΔHR-PH5 that allows homologous recombination with the MVA genome in deletion III, contain the specific sequence detectable by the restriction enzyme PmeI. To be able to ligate the genes of interest into the target vector, restriction digestion was performed at 37°C for 2 h with the reaction mixture showed in table 4.4.4.1 and 4.4.4.2. 1 unit PmeI was used to digest 1 µg of DNA.

Table 4.4.4.1: Reaction mixture for restriction digestion of pIIIΔHR-PH5

Component	Volume
pIIIΔHR-PH5	3 µl
PmeI	3 µl
NEB4 buffer	4 µl
BSA	0.4 µl
H_20	29.6 µl

Table 4.4.4.2: Reaction mixture for restriction digestion of DNA encoding for $HBcAg_{adw}$ or $L\text{-protein}_{adw}$

Component	Volume
DNA encoding for HBcAg or L-protein	30 µl
PmeI	5 µl
NEB4 buffer	6 µl
BSA	0.6 µl
H_20	18.4 µl

After digestion, the plasmid DNA was purified by agarose gel electrophoresis with the QIAquick Gel extraction kit and the DNA fragments encoding $HBcAg_{adw}$ or $L\text{-protein}_{adw}$ were purified with the QIAquick PCR purification kit according to manufacturer's instructions.

4.4.5 Dephosphorylation of the target vector plasmid

To prevent self-ligation of the linearized plasmid DNA the free phosphate at the 3' end was removed by dephosphorylation using alkaline phosphatase (AP) with conditions shown in table 6.4.5.

Table 4.4.5: Reaction mix for dephosphorylation of the linearized plasmid DNA

Component	Volume
pIIIΔHR-PH5	30 µl
Alkaline Phosphatase	6 µl
10x buffer	8 µl
H_20	36 µl

After incubation for 1 h at 37°C, the reaction was stopped by adding 4 µl of 0.5 M EDTA and incubation at 70°C for 15 min. The DNA was purified with the QIAquick PCR purification kit according to manufacturer's instructions, eluted with 30 µl sterile H_20 miliQ and verified by agarose gel electrophoresis.

4.4.6 Ligation

DNA fragments were mixed at a vector to insert ration of 1:3 with 1 unit ligase/µg DNA in a total volume of 20 µl containing 2 µl 10x ligase buffer. Ligations were carried out at 14°C overnight in a water bath. The reaction was stopped by incubation at 70°C for 10 min. The DNA was then precipitated with addition of 1 ml EtOH and 40 µl 3 M sodium acetate and incubation for at least 30 min at -80°C. After centrifugation at 13500 rpm for 30 min, the pellet was washed with 1 ml 70 % EtOH and centrifuged again at 13500 rpm for 5 min. The DNA pellet was air-dried and then dissolved in 15 µl sterile H_2O miliQ.

4.4.7 Determination of DNA concentration

The dsDNA concentration was photometrically measured at a wavelength of 260 nm against H_2O. An adsorption of 1 equals a concentration of 50 µg/ml dsDNA, therefore the concentration was calculated as follows:

Concentration of dsDNA (µg/ml) =adsorption at 260 nm x 50 µg/ml x dilution factor

4.4.8 Sequencing of constructed plasmids

Each constructed plasmid sequence was analyzed by sequencing to verify the inserted sequence. The DNA sequencing was performed by GATC Biotech (Konstanz).

4.4.9 Transfection and co-infection for homologous recombination

To generate recombinant MVA *in vitro*, CEF cells, kindly provided by Robert Baier, were infected with MVA-wt and subsequently transfected with constructed plasmids pIIIΔHR-PH5 containing $HBcAg_{adw}$ or L_{adw} gene sequences.

CEFs were infected with MOI 0.01 in 1 ml RPMI 10% in a 6 well plate and incubated for 1 h at 37°C in a CO_2 incubator. During incubation mix A containing RPMI and 6 µl FuGene 6 and mix B containing 1.5 µg DNA in a total volume of 3 µl sterile H_2O miliQ were prepared for transfection according to manufacturer's instructions. Mix A was incubated for 5 min at room temperature, followed by mixing A and B and incubation for 15 min at room temperature. The transfection solution was added drop wise to the infected cells followed by incubation at 37°C in a CO_2 incubator for 48 h. Transfected and coinfected cells were harvested with a cell scraper and viruses were released from the cells by three freeze-thaw cycles and ultra-sonication.

4.4.10 Passaging of recombinant MVA on RK-13 cells

MVA that incorporated the recombinant cassette were selected by passaging on RK-13 cells. *K1L* included in the cassette allows MVA to overcome the restriction to avian cells which enables MVA to build colonies on RK-13 cells and therefore is to be handled under BSL2 conditions. The virus solution was diluted in 10^{-1} steps in RPMI 10% from 10^{-1} to 10^{-4}. Colonies were picked preferably from wells with high dilutions with a pipette in 20 µl volume under the microscope and diluted in 500 µl RPMI 10 %. After two freeze-thaw cycles and ultra-sonication 200 µl of the solution was used to infect the next passage. Infection was always performed in three dilutions 10^{-1} to 10^{-3} on 90 to 100% confluent RK-13 cells in 6-well

plates with RPMI 10%. Prior to infection growth medium was removed and 1ml of virus dilutions were added.

4.4.11 Test PCRs for successful recombination into the MVA genome

Colonies build from single virions on RK-13 cells were picked and transferred in 500 µl RPMI 10% in 1.5 ml reaction tubes and stored at -80°C. After thawing MVAs were ultra-sonicated for 30 seconds on ice and 200 µl were used to infect 100 % confluent BHK21 cells in a total volume 1200 µl RPMI 10% in a 12-well plate. After incubation for 24 hours at 37°C in a CO_2 incubator, 800 µl medium were removed and cells were scraped from the plate in the remaining 400 µl medium and transferred into a 1.5 ml reaction tube. Two freeze-thaw cycles were performed followed by digestion with Proteinase K (table 4.4.11.1) at 56°C for 3-4 h up to overnight.

Table 4.4.11.1: Conditions for protein digestion

50 µl	**TEN-buffer (10 %)**
23 µl	**SDS (20 %)**
50 µl	**Proteinase K**
Added to 400 µl cell suspension	

After incubation, 800 µl of Phenol/Chloro/Isoamylalcohol were added followed by vortexing and centrifugation at 13000 rpm and 4°C for 5 min, the upper aqueous phase was transferred into a new reaction tube. After adding 1 ml 100% EtOH and 40 µl 3 M sodium acetate and subsequent vortexing, the mixture was incubated at -80°C for at least 30 min up to overnight. The precipitated DNA was pelleted by centrifugation at 13 000 rpm for 20 min at 4°C, the supernatant was discarded and the pellet was washed with 70 % EtOH followed by centrifugation at 13000 rpm and 4°C for 20 min. The EtOH was removed and the pellet was air-dried for 30 min. The DNA pellet was then dissolved in 25 µl sterile H_2O miliQ and stored at -20°C.

For testing the recombinant MVAs for insertion of the recombinant cassette, two PCRs were performed. The first PCR is specific for the *K1L*-gene. Table 4.4.11.2 shows the PCR reaction mix and table 4.4.11.3 shows the PCR cycler program.

Table 4.4.11.2: PCR mix for *K1L*

Component	Volume
DNA	2 µl
K1Lint-1 [5 pmol/µl]	1 µl
K1Lint-2 [5 pmol/µl]	1 µl
PCR Mix (Roche)	25 µl
PCR H_20	21 µl

Table 4.4.11.3: Temperature settings for *K1L*-PCR

Phase	Temperature	Time
I: Initial Denaturation	94°C	2 min
II (30x):		
Denaturation	94°C	0 min 30 sec
Annealing	55°C	0 min 30 sec
Elongation	72°C	1 min
III: Final Elongation	72°C	7 min
IV: Hold	4°C	∞

The second PCR is a confirmation that the homologous recombination occurred in deletion III (Del III) of the MVA genome. Table 4.4.11.4 shows the PCR reaction mix and table 4.4.11.5 shows the PCR cycler program.

Table 4.4.11.4: PCR mix for deletion III insertion

Substance	Volume
DNA	2 µl
Del III 3' (GS83) [5 pmol/µl]	1 µl
Del III 5' (FIII1b) [5 pmol/µl]	1 µl
PCR Mix (Roche)	25 µl
PCR H_20	21 µl

Table 4.4.11.5: Temperature settings for *K1L*-PCR

Phase	Temperature	Time
I: Initial Denaturation	94°C	2 min
II (30x):		
Denaturation	94°C	0 min 30 sec
Annealing	55°C	0 min 40 sec
Elongation	72°C	3 min
III: Final Elongation	72°C	7 min
IV: Hold	4°C	∞

4.4.12 Selection on CEF cells and limiting dilution

Recombinant MVA selected on RK-13 cells were passaged three times on permissive CEF cells to allow spontaneous loss of the *K1L*-gene by a second homologous recombination. The obtained cell lysates were serially diluted from 10^{-1} to 10^{-8} with the dilutions 10^{-7} and 10^{-8} plated on one 96-well plate containing CEF cells. After 5 days incubation at 37°C in a CO_2 incubator infected cells were identified under the microscope by cytopathic effect analysis. The infected cells were immobilized by scraping and resuspended with a multichannel pipette. From the infected wells 50% of the solution was transferred into a V-bottom 96-well plate for DNA extraction while the remaining 50% were transferred into 1.5 ml reaction tubes containing 400 µl RPMI 10% and stored at -80°C.

Cells for DNA extraction were pelleted at 1400 rpm for 2 min and resuspended in 20 µl crude extraction buffer which was prepared freshly with 100 µl 10x crude extraction buffer, 100 µl Proteinase K, 25 µl 20% Tween 20 and 775 µl sterile H_2O miliQ. After incubation at 56°C for 10 h, the solutions were transferred into 1.5 ml reaction tubes and incubated at 95°C for 10 min. 2 µl of DNA samples were analyzed by PCRs for *K1L* and Del III insertion as described above. The samples that were negative in the *K1L* PCR and positive in the Del III PCR were used for creating a highly purified virus stock.

4.4.13 Amplification and purification of MVA

For amplification of recombinant MVAs 30 to 40 T225 cell culture flasks of 90-100% confluent CEFs, kindly provided by Robert Baier, were infected with $1x10^7$ virions per flask in 5 ml of RPMI 10%. After incubation for 1 h at 37°C, 20 ml of RPMI 10% were added and the flasks were incubated for 2 days at 37°C until a cytopathic effect was visible. The cells containing recombinant MVA were then mobilized with a cell scraper and harvested by centrifugation at 4000 rpm and 4°C for 5 min in 50 ml Falcon tubes. The cell pellets were

pooled and finally resuspended in 30 ml of 10 mM Tris pH 9.0. After three freeze-thaw cycles, cells were treated with an ultrasound needle for 30 sec on ice with subsequent centrifugation at 4000 rpm and 4°C for 5 min. The supernatant was transferred into a new 50 ml Falcon tube and the remaining pellet was resuspended in 22.5 ml of 10 mM Tris pH 9.0. The treatment was repeated which resulted in 75 ml of 10 mM Tris pH 9.0 buffer that contains the virus.

To obtain highly pure MVA stocks remaining cellular debris and proteins were separated from virus particles by ultra-centrifugation of the supernatant through 36 % sucrose cushions. Therefore six ultracentrifugation tubes for Beckman rotor SW28 were filled with 25 ml autoclaved 36 % sucrose and overlayed with 12.5 ml virus solution. After centrifugation at 13500 rpm and 4°C for 1.5 h the supernatant was discarded and the pellets were dried for 10 min and finally resuspended in 12 ml 10 mM Tris pH 9.0. The second purification step was performed in six ultra-centrifugation tubes for Beckman rotor SW41 containing 10 ml of 36 % sucrose that were overlayed with 2 ml virus solution. After centrifugation at 13500 rpm and 4°C for 1.5 h the supernatant was discarded and the pellets were dried for 10 min. Finally the pellets were resuspended in a total volume of 400 µl 1 mM Tris pH 9.0 and the virus was stored at -80°C in a cryo tube.

4.4.14 Titration of MVA stocks

The titer of newly generated MVA stocks was determined by infection of confluent freshly isolated CEFs or BHK-21 cells in flat-bottom 96-well plates with a total volume of 200 µl RPMI 2 %. Dilutions of 10^{-6} to 10^{-11} were added with duplicates for the dilutions 10^{-7} to 10^{-11} on the cells. As control RPMI 2% was added to eight wells. After one week incubation at 37°C in a CO_2 incubator, infected wells were counted and the viral titer in IU/ml was calculated with the following equation:

$$y = (10\text{^}\left(a - 0.5 + \left(\frac{xa}{16}\right) + \left(\frac{xb}{16}\right) + \left(\frac{xc}{16}\right)\right)) * 10$$

a represents the highest dilution with 100 % of infected wells (e.g. 10^{-8}; *a* = 8) and *xa*, *xb* and *xc* representing the numbers of infected wells in further dilutions (Mayr 1974).

4.4.15 Amplification and titration of the recombinant adenovirus AdHBVL-

To amplify the glycerol stock of AdHBVL-, 9x T175 cell culture flasks with HEK 293H cells were prepared. At the time when the cells were 80% confluent they were infected with $5x10^9$/ml of AdHBVL- followed by a medium exchange after 3 h. The infected cells detach after 48-72 hours post infection. Upon detachment, cells and medium had been collected and

centrifuged at 2000 rpm for 5 min. After discarding the supernatant except the last 20 ml the pellets were resuspended and pooled followed by three freeze-thaw cycles. Afterwards the suspension was centrifuged at 4000 rpm for 10 min until the supernatant was clear. The supernatant contained the virus.

For purification two centrifuge tubes for the SW28 rotor were filled with 8 ml of 1.4 CsCl solution which was carefully overlayed with 6 ml of 1.2 CsCl solution. Finally 10 ml of the virus-containing supernatant were loaded on the CsCl gradient and the centrifuge tubes were filled up with 8 ml 10 mM Tris pH 8.0 and 2 ml mineral oil. After centrifugation at 100 000 g for 1.5 h without breaking, the fractions containing the AdHBVL- (Fig. 4.4.15 A) are pooled and diluted 1:2 with 10 mM Tris pH 8.0 and loaded again on new CsCl gradients and centrifuged the same way as described above. The fractions containing the AdHBVL- (Fig. 4.4.15 B) are pooled again but not diluted.

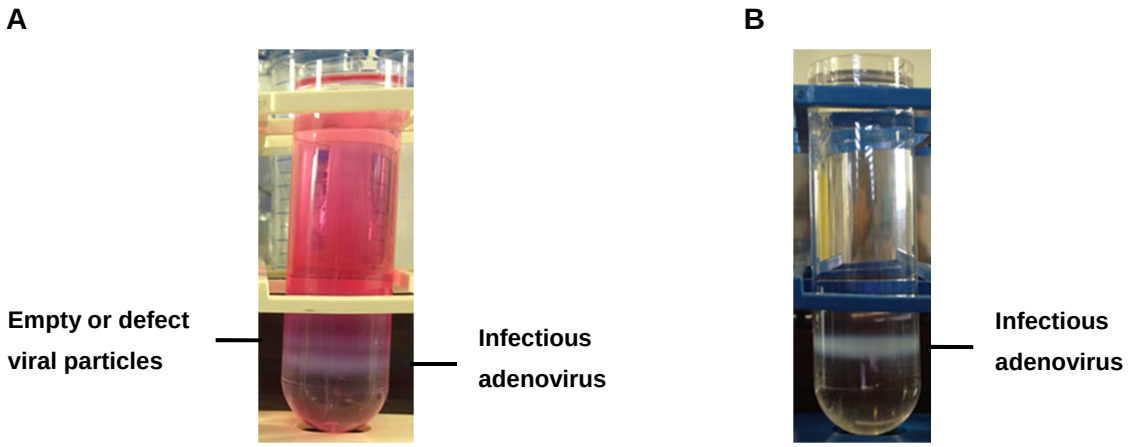

Fig. 4.4.15: CsCl gradients post first (A) and second (B) centrifugation.

The toxic CsCl was removed by dialysis. The dialysis slide was washed for 30 sec in dialysis buffer and then filled with the AdHBVL- containing solution. After incubation for 1 h in 800 ml dialysis buffer with stirring, the dialysis buffer was exchanged for the first time and then a second time after 2 h of incubation. The final incubation lasted for 3 h and then the AdHBVL- was sucked out of the dialysis slide, aliquoted and stored at -80°C.

To determine the amount of infectious units a titration was performed using HEK293H cells in 12 well plates. 10^6 cells were infected by the time they were 80% confluent in a volume of 1 ml medium. Therefore an aliquot of the virus stock was thawed and diluted in the following manner: 100 µl, 30 µl, 10 µl and 3 µl of the virus stock were added to the top row of the plate. 100 µl of each well from the wells of the top row were transferred to the well below in the middle row. This leads to a virus solution volume of 1 µl, 0.3 µl, 0.1µl and 0.03 µl. The last row represents the uninfected controls. A second 12 well plate was prepared in the same manner. After 48 h incubation at 37°C in a CO_2 incubator the result could be analyzed.

Calculation of the virus titer is based on the assumption that an MOI of 3-5 leads to detachment of 10^6 cells in 48 h. Thus the lowest volume of viral stock solution that lead to detachment of the cells contained 3-5 infectious particles per cell. This method of determining the viral titer is not exact and has an error of a factor two to three. Table 4.4.15 shows the titers represented by the volume of virus that leads to total infection in 48 h.

Table 4.4.15: Titers by initial volume of virus for infection

100 µl	$5x10^7$ IU/ml	1 µl	$5x10^9$ IU/ml
30 µl	$1.7x10^8$ IU/ml	0.3 µl	$1.7x10^{10}$ IU/ml
10 µl	$5x10^8$ IU/ml	0.1 µl	$5x10^{10}$ IU/ml
3 µl	$1.7x10^9$ IU/ml	0.03 µl	$1.7x10^{11}$ IU/ml

4.4.16 Determination of endotoxin content in HBcAg preparation

Since there was no information about endotoxin content in the HBcAg that was used for vaccinations, a chromogenic limulus amebocyte lysate (LAL) endotoxin assay kit (ToxinSensor by Genescript) was used after manufacturer's instructions. The protein vaccine containing $HBsAg_{ayw}$, HBcAg, PCEP and CpG was tested undiluted and diluted (1:1000, 1:15000) as well as HBcAg in dilutions 1:1000 and 1:15000 alone and PCEP undiluted and in a 1:1000 dilution. The absorbance of the samples at 545 nm was measured with a photometer.

4.5 Treatment of mice

4.5.1 Mouse strains

In this study female and male C57BL/6 and $CD45.1^+$ C57BL/6 mice were used at the age of eight weeks or older for vaccination experiments or as cell donors for the preparation of bone marrow derived dendritic cells and B cells or target cells for *in vivo* killing assays. CD45.1 is a congenic marker that developed through a polymorphism of the CD45 allele. It is a surface marker of myeloid cells that can be stained with fluorescent antibodies and allows distinguishing transferred cells from host cells.

As model organism for chronic HBV infection tg[HBV 1.3 genome]Chi32 (HBV1.3.32) mice (Guidotti 1995) were used. These mice carry a greater-than-genome length construct of the HBV genome with the 3' terminus at nucleotide 1982 which is downstream of the polyadenylation site in the HBV genome and the 5' terminus upstream of the X promoter and

enhancer I. Those mice replicate HBV in liver and in kidney. They release infectious particles and antigens HBs and HBe into the blood, but show no detectable immunity against HBV antigens. They also show no sign of liver disease (Guidotti 1995). Since in newborn mice no viral RNA is detectable and the expression starts not before the first weeks of development (Guidotti 1995), they can serve as a model for vertically transmitted HBV infection. If not indicated otherwise, high antigenemic mice with an HBeAg titer higher than 10 S/CO were used.

Additionally TLR2 and MyD88 knockout mice were used to study the effect of the protein vaccine used in the immunizations. These mice were bred on C57BL/6 background.

To test the vaccination in a setting of human MHC molecules, HHDII mice were used which are transgenic for human MHC HLA-A2 and have knockouts for β2m and H-2D^{b}.

4.5.2 Anesthesia

Prior to painful treatments like retrobulbar blood sample collection, mice were anesthetized with ketamine (Ketanest 100 mg/kg bodyweight) and barbiturate (Rampun, 5 mg/kg bodyweight). These narcotics were injected in the lower right quadrant of the abdomen in a volume of 10 ml/kg bodyweight in 0.9 % NaCl solution. The success of the anesthesia was tested via a pain stimulus at the tip of the tail before blood was taken. During the procedure the animals were kept under warm conditions using an infrared lamp.

4.5.3 Blood sample collection

Retrobulbar bleeding was performed under anesthesia with a glass capillary. The capillary tube is directed toward the major venous structures of the orbit. Bleeding was induced via rotation of the capillary and the blood was collected in 1.5 ml reaction tubes. Alternatively blood was taken from the facial vein using a lancet.

4.5.4 Subcutaneous injection

The protein vaccine was injected in a volume of 50 µl PBS subcutaneously in the neck or gluteal. Mice were manually immobilized and no anesthesia was used.

4.5.5 Intraperitoneal injection

The viral vaccine vectors were injected in a volume of 250 µl 0.9 % NaCl intraperitoneally. The maximum dose of viral vectors was 1x10^{8} in total. Mice were manually immobilized and no anesthesia was used.

4.5.6 Intravenous injection

The injection of CFSE labeled target cells (maximum $1x10^7$ IU) and AdHBVx- ($2x10^8$ IU) was performed in a volume of 200 µl PBS. The site of injection (tail vein) was disinfected and cleaned with 70 % alcohol. The mice were pre-warmed with an infrared lamp and then fixated. Prior to the injection no anesthesia was used.

4.6 *Ex vivo* immunological analysis

After completion of the experiment mice were sacrificed using CO_2 and blood, spleen and liver were taken for analysis.

4.6.1 Preparation of Splenocytes

Spleens were removed from mice and squished through a cell strainer with a plunger. Remaining cells were washed with a total volume of 15 ml ice cold RPMI medium. After centrifugation at 1500 rpm and 4°C for 5 min erythrocytes were lysed by incubation with TAC medium at 37°C for two minutes. Cells were washed with 40 ml ice cold RPMI, filtered through a cell strainer and centrifuged as described above. The pellet was then resuspended in 3 ml RPMI 10%.

4.6.2 Preparation of liver associated lymphocytes

Livers were perfused with ice cold PBS and transferred into a petri dish containing RPMI medium. The gallbladder was removed and a small part from the liver was transferred into 6 ml 4 % PFA kindly provided by the group of Mathias Heikenwälder (Institute of Virology, Helmholtz Zentrum München). The remaining part of the liver was squished thoroughly through a cell strainer with a plunger and washed with a total volume of 15 ml ice cold RPMI. After pelleting the cells by centrifugation at 1500 rpm and room temperature for 5 min, the pellet was resuspended in 10 ml collagenase digestion medium and incubated for 20-40 min at 37°C in a CO_2 incubator. Digested livers were centrifuged again at 1500 rpm and room temperature for 10 min and afterwards resuspended in 3 ml 40% Percoll containing Heparin and loaded on a 3 ml 80% Percoll cushion in a 15 ml Falcon tube. After centrifugation at 2600 rpm and room temperature for 20 min with the break turned off, the lymphocyte fraction located above the 80% Percoll cushion (Fig 4.6.2) was transferred into a 50 ml Falcon tube and washed with 40 ml ice cold RPMI followed by centrifugation at 1500 rpm and 4°C for 5

min. If necessary an erythrocyte lysis was performed as described above. Finally the cells were resuspended in a minimal amount of RPMI 10% FCS to cover all different stimulations.

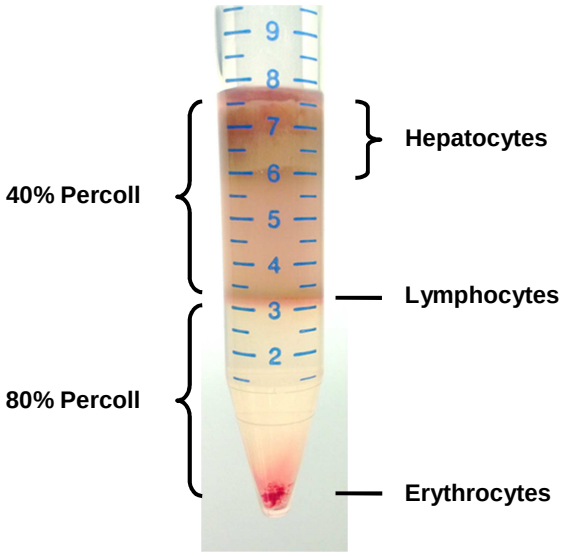

Fig 4.6.2: Percoll gradient post centrifugation.

4.6.3 Preparation of peripheral blood mononuclear cells (PBMC)

For preparation of PBMCs, 100 µl of blood was mixed with 70 µl Heparin (1:5 diluted with PBS). After centrifugation at 400 g for 5 min, the pellet was resuspended in 5 ml TAC buffer and incubated for 20 min at room temperature. After erythrocyte lysis the cells were washed with 40 ml cold RPMI centrifuged at 400 g and 4°C for 5 min and finally resuspended in RPMI 10 %.

4.6.4 Cell counting

Cells were counted in a 1:40 dilution. Therefore 50 µl of cells were diluted 1:10 with 450 µl RPMI mixed thoroughly and 50 µl were diluted further 1:4 with 125 µl RPMI and 25 µl of 0.4 % Trypan blue solution. Cells were counted in a hemocytometer under a microscope. The mean of two counted quadrates were used to calculate the total cell number as follows:

Cells/ml = mean of two counted quadrates x 40 (dilution factor) x 10^4

4.6.5 Stimulation of isolated cells

Cells were counted and adjusted with RPMI 10% to 20 million cells / ml. For each stimulation 4 million cells were plated into a U-bottom 96-well plate and incubated with 0.25 µg of different peptides and 0.25 µg Brefeldin A (BFA) in a total volume of 270 µl. Negative controls were either SIINFEKL or β-gal kindly provided by Ingo Drexler. First the 200 µl of cells were mixed with 50 µl peptide diluted in RPMI 10 %. After one hour of incubation at 37°C in a CO_2 incubator, BFA was added gently with subsequent incubation for 13 hours in the incubator.

4.6.6 Intracellular cytokine staining

After stimulation, cells were transferred into a V-bottom 96-well plate and dead cells were stained with a 1:2000 dilution of ethidium monoazide bromide (EMA) for 20 min on ice with light exposure in 50 µl FACS buffer. After two washing steps with 180 µl FACS buffer and centrifugation at 1400 rpm and 4°C for 2 min surface markers were stained with PB-conjugated anti-CD8α and PE-conjugated anti-CD4 diluted 1:100 in FACS buffer for 30 min on ice followed by two washing steps as described above. Prior to intracellular cytokine staining, cells were permeabilized using the Cytofix/Cytoperm kit. Cells were incubated with 50 µl / well Cytofix/Cytoperm for 15 min on ice in the dark. After a washing step with 150 µl 1x Perm/Wash intracellular cytokines were stained by incubation with FITC anti–IFN-γ diluted 1:300, PECy7-anti-TNFα and APC-anti-IL-2 diluted 1:200 with FACS buffer in a volume of 50 µl for 30 min on ice in the dark. After two washing steps with 180 µl 1x Perm/Wash cells were resuspended in 90 µl and transferred into FACS tubes containing 90 µl FACS buffer and 30 µl 2 % paraformaldehyde (PFA). Stained and fixed cells were stored at 4°C in the dark for up to 6 days. Samples were measured on a FACS Canto II and analyzed with FlowJo software.

4.6.7 Multimer staining

For staining of specific TCRs on splenocytes and LALs, PE-conjugated multimers S190 (VWLSVIWM) or MVA-derived $B8R_{20}$ (TSYKFESV), kindly provided by Dirk Busch, were used. Four million cells were transferred into a V-bottom 96-well plate and incubated in 50 µl with F_C-block (0.5 mg/ml) which was diluted 1:1000 in FACS buffer for 20 minutes on ice in the dark. After two washing steps with 180 µl of cold FACS buffer including centrifugation at 1400 rpm and 4°C for 2 min, cells were incubated with PE-conjugated multimers for 20 min on ice in the dark in a volume of 40 µl. Then cells were stained by 20 min incubation on ice in the dark with APC-conjugated CD8α in a 1:100 dilution in a total volume of 60 µl FACS buffer. After two washing steps with 180 µl FACS buffer and applying propidium iodide (PI)

for staining dead cells, samples were measured on a FACS Canto II and analyzed with FlowJo software.

4.6.8 Flow cytometry

To characterize single cells by surface markers or intracellular stainings flow cytometry was used. Cells are aspirated through a fine needle into a detection channel where they pass several laser beams which can determine cell size and granularity through the forward light scatter (FSC) and the sideward light scatter (SSC). By using antibodies that are labeled with fluorochromes with different emission spectra it is possible to analyze a variety of different markers. The detector system of the FACS cytometer converts the optical readout into digital information that can be analyzed by FACS-Diva or FlowJo. The standard gating strategy after intracellular cytokine staining is shown in Fig. 4.6.8. To analyze the polyfunctionality of T cells Boolean gates were defined in FlowJo.

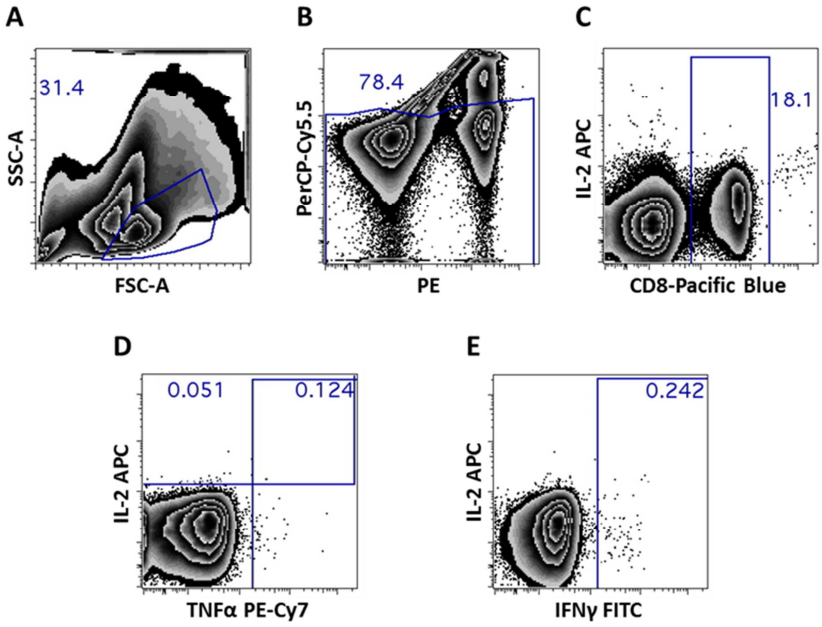

Fig. 4.6.8: Gating strategy for analysis of CD8 T cells from spleen and their expression of cytokines. The first step (A) is to identify the lymphocyte population. (B) Dead cells are excluded and (C) CD8 positive T cells are discrimintaed. CD8 T cells producing IL-2 and/or TNFα are detected by the gates set in D and IFNγ producing cells are gated in E.

4.6.9 Enzyme Linked Immuno Spot

ELISpot assays for IL-4, IL-5 and IL-10 release by mouse splenocytes were performed separately using ELISpot plus for Mouse Kits (MABTECH, Nacka Strand, Sweden). 1.5 x 10^6 splenocytes per well were plated on 96-well plates, which had been pre-coated with an antibody against mouse IL-4, IL-5 or IL-10 in 200 µl culture medium. Cells were left unstimulated or stimulated with 5 µg/ml recombinant $HBsAg_{ayw}$ or recombinant HBcAg for 48

h at 37°C. As positive controls cells were stimulated with 50 ng/ml PMA + 1 µg/ml Ionomycin for IL-4 expression, 2.5 µg/ml PWM + 1 µg/ml Ionomycin for IL-5 expression and 5 µg/ml PHA + 1µg/ml LPS + 2 µg/ml Concanavalin A for IL-10 expression. Washing, counterstaining and visualization of spots were performed according to the manufacturer's instructions. Counting and analysis of spots was performed on ImmunoSpot S5 UV Analyser.

4.6.10 *In vivo* killing assay

A group of C57BL/6 mice were immunized on day 0 with 16 µg of recombinant $HBsAg_{ayw}$, 16 µg of recombinant HBcAg and 31.91 µg CpG and boosted with $5x10^7$ IU MVA-S_{ayw} and $5x10^7$ IU MVA-core on day 28. The control group was immunized with 31.91 µg CpG only and boosted with $1x10^8$ MVA-wt. On day 34, splenocytes of C57BL/6 mice that carry the congenic marker CD45.1 were loaded with the C_{93}-peptide by incubation at 37°C for 45 min, washed two times with 20 ml cold PBS with 10 min centrifugation steps at 4°C with 1500 rpm and labeled with 5 µM carboxyfluorescein succinimidyl ester (CFSE) by incubation at 37°C for 10 min and on ice for 5 min. As control splenocytes of the same mice were not loaded but labeled with 0.5 µM CFSE. After labeling, the cells were washed again two times with 20 ml cold PBS like described above and mixed. 10 million cells were injected per mouse intravenously in a volume of 200 µl PBS into both groups of immunized mice. After 16 to 18 hours the mice were sacrificed and four million splenocytes were stained for CD45.1 and analyzed by FACS. In parallel four million splenocytes per well were stimulated for 5 hours with the peptides $B8R_{20}$, S190, S208, C93 and SIINFEKL. Afterwards an intracellular cytokine staining was performed like described above. Data were acquired by FACS analysis on a FACS Canto II and analyzed with FlowJo.

4.6.11 Serological analysis

Blood of mice was centrifuged twice at 6000 g for 10 min to separate cells from serum. Serum alanine aminotransferase (ALT) activity was measured using a Reflovet Plus reader in freshly prepared serum which was afterwards stored at -20°C. Serum levels of HBsAg, HBeAg, anti-HBs and anti-HBc were quantified if not indicated otherwise in 1:20 dilutions using AxSYM assays after thawing.

4.6.12 Purification of viral DNA from serum and qPCR

Purification of viral DNA from 20 µl serum was performed with the High Pure Viral Nucleic Acid Kit by Roche according to manufacturer's conditions. Viral DNA was eluted with 50 µl of provided elution buffer.

Quantitative real-time PCR (qPCR) was used to determine the amount of viral DNA/ml serum with PCR reaction mix shown in table 4.6.12.1 and cycler program shown in table 4.6.12.2.

Table 4.6.12.1: PCR mix for quantification of HBV DNA

Substance	Volume
DNA	4 µl
HBV 3053 fw [20 µM]	0.5 µl
HBV 134 rev [20 µM]	0.5 µl
SYBR Green I Master	5 µl

Table 4.6.12.2: Cycler program used for qPCR

Phase	Target (°C)	Acquisition Mode	Hold (sec)	Ramp Rate (°C/s)	Acquisition (per °C)	Sec Target (°C)	Step Size (°C)	Step Delay (cycles)
I: Denaturation	95°C	None	300	4.4	-	0	0	0
II: Amplification (45x)								
Denaturation	95°C	None	15	4.4	-	0	0	0
Annealing	60°C	None	15	2.2	-	0	0	0
Elongation	72°C	Single	20	4.4	-	0	0	0
III: Melting Curve								
Segment 1	95°C	None	1	4.4	-	-	-	-
Segment 2	65°C	None	60	2.2	-	-	-	-
Segment 3	95°C	Continuous	-	0.11	5	-	-	-
III: Cooling	40°C	None	30	2.2	-	0	0	0
IV: Hold	4°C		∞					

As standard HBV rcDNA 1.3 isolated from supernatant of HepG2.2.15 cells (kindly provided by Dr. Christian Bach) was used. The standard curve was prepared with 10^1, 10^2, 10^3 and 10^4 DNA molecules. The negative control was H_20. Titers were calculated with the following equation:

Viral DNA/ml serum = concentration (light cycler) x 12.5 (dilution factor of purified viral DNA) x 50 (dilution factor of initial serum)

4.6.13 Neutralization assay

Differentiated HepaRG, kindly provided by Dr. Julie Lucifora, were infected with an MOI of 200 in 12 well plates in duplicates with HBV genotype D subtype ayw in the presence of diluted serum of vaccinated mice containing anti-HBs at 37°C in a CO_2 incubator. The serum was diluted in 500 µl differentiation medium 1:33, 1:100, 1:333, and 1:1000. As positive control 0.8 IU of the hepatect CP 100 IU/mL antibody was used, the negative control contained medium. 24 hours post infection the cells were washed three times with PBS and 1 ml of differentiation medium was added. Supernatants were collected on day 4, 7 and 10 post infection and HBsAg was quantified by AXSYM assays in 1:20 dilutions.

4.7 Histological analysis

Slices of perfused liver were fixed in 6 ml 4% PFA at room temperature for 2 days or longer and embedded in paraffin. All stainings were performed in cooperation by members of the group of Mathias Heikenwälder (Institute of Virology, Helmholtz Zentrum München). Liver sections were stained with hematoxylin and eosin (HE). Hematoxylin stains basophilic structures like DNA in the nucleus in blue while eosin stains eosinophilic structures which are composed of intra- and extracellular proteins and therefore show the cytoplasm in red. Additionally liver sections were stained with antibodies against B220, CD3, cleaved caspase 3, F4/80, HBcAg, Ki67, and Ly6G. All stainings were scanned with a Leica SCN 400 slide scanner and analyzed with SlidePath Tissue Image Analysis 2.0 in cooperation with Dr. Marc Ringelhan.

4.8 *In vitro* studies

To study the effect of the compounds present in the protein vaccine especially the effect of the adjuvants on uptake and activation, B cells and BMDCs were stimulated with various combinations of the used compounds.

4.8.1 Isolation of B cells

B cells were purified from spleens of C57BL/6 mice with a B cell purification kit from Miltenyi Biotec after manufacturer's instructions. Cells were resuspended in 3 ml of RPMI 10%. They were used for studying the induction of antigen uptake and activation upon incubation with adjuvants (CpG, PCEP) and antigens (HBsAg, HBcAg) in different combinations.

4.8.2 Preparation of bone marrow derived dendritic cells

Femora and tibiae from both hind legs were cut out from a C57BL/6 mouse and the muscles were removed. The bones were washed for 30 sec with 70% EtOH and then placed into a petri dish containing RPMI medium. Both ends of the bones were cut off with scissors and the bone marrow was flushed out completely with a syringe. The cells were transferred into a 50 ml tube and resuspended thoroughly. After centrifugation at 1500 rpm and room temperature for 5 min, the pellet was resuspended in 3 ml TAC buffer and incubated for 2 min at 37°C in a water bath. After washing with 40 ml RPMI medium and centrifugation at 1500 rpm and room temperature for 5 min, the pellet was resuspended in 4 ml BMDC differentiation medium containing 10 % GM-CSF. Cells were distributed equally in 4 petri dishes and cultured in BMDC differentiation medium for 7 days. After 4 days 10 ml of BMDC differentiation medium was added. Differentiated BMDCs were used for studying the induction of antigen uptake and activation upon incubation with adjuvants (CpG, PCEP) and antigens (HBsAg, HBcAg) in different combinations.

4.8.3 Labeling of HBsAg

HBsAg was labeled with 10% Alexa Fluor 647 dye in presence of 10% 1M sodium bicarbonate by incubation at 22°C for 1 h with shaking. During incubation the buffer of a Biospin 30 column was exchanged by washing the column three times with 500 µl PBS and centrifugation at 1000 g and 4°C for 1.5 min after the first and the second washing step and centrifugation at 1000 g and 4°C for 2.5 min after the third washing step. The column was then stored at 4°C and used for filtering the excess dye which did not bind to the protein during the incubation. The protein/dye mix was loaded onto the column that was placed into a FACS tube and the excess dye was separated from the protein by centrifugation at 1000 g and 4°C for 4 min. The labeled HBsAg was detected in the APC channel of the FACS Canto II and was used for *in vitro* studies in BMDCs and B cells.

4.8.4 Stimulation of cells

Isolated cells were stimulated in RPMI 10% with different antigen/adjuvants combinations in order to investigate effects on antigen-uptake by the cells and activation of the cells. In general 0.4 µg antigen, 0.624 µg PCEP and 0.384 µg CpG were used per well. This represents the same ratio of antigen/adjuvants that was used in mouse immunizations. To see if HBcAg has an additional effect 0.4 µg were added per well. 200 000 cells were used per well and incubated at 37°C in a CO_2 incubator in a flat bottom 96-well plate. BMDCs were stimulated for 15, 30, 45, 60, 90, 120 and 180 min. B cells were stimulated for 1, 2, 3, 4, 5, 6,

7, 14, 16 and 18 h. As negative control 200 000 cells were incubated with the antigen/adjuvants combination containing all components and incubated at 4°C for 180 min or 18 h respectively. All time points and stimulations were conducted in duplicates.

4.8.5 Staining and readout

Stimulated cells were transferred into a V-bottom 96-well plate and centrifuged immediately at 1400 rpm and 4°C for 2 min. After discarding the supernatant, staining of dead cells was performed in 100 µl FACS buffer with EMA (1:2000) for 20 min on ice with light exposure. Subsequently the cells were washed twice with 180 µl FACS buffer by centrifugation at 1400 rpm and 4°C for 2 minutes. Afterwards, the surface molecules were stained. B cells were incubated with anti-mB220 FITC in a dilution of 1:250 and anti-mCD80 PE in a dilution of 1:200. BMDCs were incubated with anti-mCD11c PE-Cy7 and anti-mCD80 PE in dilutions of 1:200 in 50 µl FACS buffer per well for 30 min on ice in the dark. Again the cells were washed two times with 180 µl FACS buffer by centrifugation at 1400 rpm and 4°C for 2 min. Finally cells were resuspended in 90 µl FACS buffer transferred into FACS tubes containing 15 µl 2 % PFA. Samples were measured on a FACS Canto II and analyzed with FlowJo.

4.9 Statistical analysis

All statistical analyses were performed using GraphPad Prism4 software. Results are expressed as mean ± standard error of the mean. Differences between groups were analyzed for statistical significance using two- tailed Student’s t-tests and Wilcoxon signed rank test.

References

Acres B, Bonnefoy JY. Clinical development of MVA-based therapeutic cancer vaccines. Expert Rev Vaccines 2008;7:889-893.

Afolabi MO, Ndure J, Drammeh A, Darboe F, Mehedi SR, Rowland-Jones SL, Borthwick N, et al. A phase I randomized clinical trial of candidate human immunodeficiency virus type 1 vaccine MVA.HIVA administered to Gambian infants. PLoS One 2013;8:e78289.

Akira S, Uematsu S, Takeuchi O. Pathogen recognition and innate immunity. Cell 2006;124:783-801.

Anderson G, Jenkinson EJ, Moore NC, Owen JJ. MHC class II-positive epithelium and mesenchyme cells are both required for T-cell development in the thymus. Nature 1993;362:70-73.

Ando K, Moriyama T, Guidotti LG, Wirth S, Schreiber RD, Schlicht HJ, Huang SN, et al. Mechanisms of class I restricted immunopathology. A transgenic mouse model of fulminant hepatitis. J Exp Med 1993;178:1541-1554.

Andrianov AK, Marin A, Chen J. Synthesis, properties, and biological activity of poly[di(sodium carboxylatoethylphenoxy)phosphazene]. Biomacromolecules 2006;7:394-399.

Andrianov AK, Marin A, Roberts BE. Polyphosphazene polyelectrolytes: a link between the formation of noncovalent complexes with antigenic proteins and immunostimulating activity. Biomacromolecules 2005;6:1375-1379.

Andrianov AK, Svirkin YY, LeGolvan MP. Synthesis and biologically relevant properties of polyphosphazene polyacids. Biomacromolecules 2004;5:1999-2006.

Anitescu M, Chace JH, Tuetken R, Yi AK, Berg DJ, Krieg AM, Cowdery JS. Interleukin-10 functions in vitro and in vivo to inhibit bacterial DNA-induced secretion of interleukin-12. J Interferon Cytokine Res 1997;17:781-788.

Antoine G, Scheiflinger F, Dorner F, Falkner FG. The complete genomic sequence of the modified vaccinia Ankara strain: comparison with other orthopoxviruses. Virology 1998;244:365-396.

Awate S, Wilson HL, Lai K, Babiuk LA, Mutwiri G. Activation of adjuvant core response genes by the novel adjuvant PCEP. Mol Immunol 2012;51:292-303.

Bartenschlager R, Schaller H. Hepadnaviral assembly is initiated by polymerase binding to the encapsidation signal in the viral RNA genome. EMBO J 1992;11:3413-3420.

Beck J, Nassal M. Hepatitis B virus replication. World J Gastroenterol 2007;13:48-64.

Bertoletti A, Naoumov NV. Translation of immunological knowledge into better treatments of chronic hepatitis B. J Hepatol 2003;39:115-124.

Beutler B, Jiang Z, Georgel P, Crozat K, Croker B, Rutschmann S, Du X, et al. Genetic analysis of host resistance: Toll-like receptor signaling and immunity at large. Annu Rev Immunol 2006;24:353-389.

Billerbeck E, Bottler T, Thimme R. Regulatory T cells in viral hepatitis. World J Gastroenterol 2007;13:4858-4864.

Blackman M, Kappler J, Marrack P. The role of the T cell receptor in positive and negative selection of developing T cells. Science 1990;248:1335-1341.

Blander JM, Medzhitov R. On regulation of phagosome maturation and antigen presentation. Nat Immunol 2006;7:1029-1035.

Block TM, Guo H, Guo JT. Molecular virology of hepatitis B virus for clinicians. Clin Liver Dis 2007;11:685-706, vii.

Bock CT, Schranz P, Schroder CH, Zentgraf H. Hepatitis B virus genome is organized into nucleosomes in the nucleus of the infected cell. Virus Genes 1994;8:215-229.

Bock CT, Schwinn S, Locarnini S, Fyfe J, Manns MP, Trautwein C, Zentgraf H. Structural organization of the hepatitis B virus minichromosome. J Mol Biol 2001;307:183-196.

Bonvin M, Achermann F, Greeve I, Stroka D, Keogh A, Inderbitzin D, Candinas D, et al. Interferon-inducible expression of APOBEC3 editing enzymes in human hepatocytes and inhibition of hepatitis B virus replication. Hepatology 2006;43:1364-1374.

Bonvin M, Greeve J. Hepatitis B: modern concepts in pathogenesis--APOBEC3 cytidine deaminases as effectors in innate immunity against the hepatitis B virus. Curr Opin Infect Dis 2008;21:298-303.

Bruss V. Hepatitis B virus morphogenesis. World J Gastroenterol 2007;13:65-73.

Buchmann P, Dembek C, Kuklick L, Jager C, Tedjokusumo R, von Freyend MJ, Drebber U, et al. A novel therapeutic hepatitis B vaccine induces cellular and humoral immune responses and breaks tolerance in hepatitis B virus (HBV) transgenic mice. Vaccine 2013;31:1197-1203.

Burk RD, Hwang LY, Ho GY, Shafritz DA, Beasley RP. Outcome of perinatal hepatitis B virus exposure is dependent on maternal virus load. J Infect Dis 1994;170:1418-1423.

Cavenaugh JS, Awi D, Mendy M, Hill AV, Whittle H, McConkey SJ. Partially randomized, non-blinded trial of DNA and MVA therapeutic vaccines based on hepatitis B virus surface protein for chronic HBV infection. PLoS One 2011;6:e14626.

Chen M, Sallberg M, Hughes J, Jones J, Guidotti LG, Chisari FV, Billaud JN, et al. Immune tolerance split between hepatitis B virus precore and core proteins. J Virol 2005;79:3016-3027.

Chen M, Sallberg M, Thung SN, Hughes J, Jones J, Milich DR. Nondeletional T-cell receptor transgenic mice: model for the CD4(+) T-cell repertoire in chronic hepatitis B virus infection. J Virol 2000;74:7587-7599.

Chisari FV, Pinkert CA, Milich DR, Filippi P, McLachlan A, Palmiter RD, Brinster RL. A transgenic mouse model of the chronic hepatitis B surface antigen carrier state. Science 1985;230:1157-1160.

Cornberg M, Protzer U, Petersen J, Wedemeyer H, Berg T, Jilg W, Erhardt A, et al. [Prophylaxis, diagnosis and therapy of hepatitis B virus infection - the German guideline]. Z Gastroenterol 2011;49:871-930.

Dandri M, Burda MR, Burkle A, Zuckerman DM, Will H, Rogler CE, Greten H, et al. Increase in de novo HBV DNA integrations in response to oxidative DNA damage or inhibition of poly(ADP-ribosyl)ation. Hepatology 2002;35:217-223.

Dandri M, Burda MR, Torok E, Pollok JM, Iwanska A, Sommer G, Rogiers X, et al. Repopulation of mouse liver with human hepatocytes and in vivo infection with hepatitis B virus. Hepatology 2001;33:981-988.

Dane DS, Cameron CH, Briggs M. Virus-like particles in serum of patients with Australia-antigen-associated hepatitis. Lancet 1970;1:695-698.

Dar A, Lai K, Dent D, Potter A, Gerdts V, Babiuk LA, Mutwiri GK. Administration of poly[di(sodium carboxylatoethylphenoxy)]phosphazene (PCEP) as adjuvant activated mixed Th1/Th2 immune responses in pigs. Vet Immunol Immunopathol 2012;146:289-295.

Daub H, Blencke S, Habenberger P, Kurtenbach A, Dennenmoser J, Wissing J, Ullrich A, et al. Identification of SRPK1 and SRPK2 as the major cellular protein kinases phosphorylating hepatitis B virus core protein. J Virol 2002;76:8124-8137.

Dorrell L, Yang H, Ondondo B, Dong T, di Gleria K, Suttill A, Conlon C, et al. Expansion and diversification of virus-specific T cells following immunization of human immunodeficiency virus type 1 (HIV-1)-infected individuals with a recombinant modified vaccinia virus Ankara/HIV-1 Gag vaccine. J Virol 2006;80:4705-4716.

Drexler I, Staib C, Kastenmuller W, Stevanovic S, Schmidt B, Lemonnier FA, Rammensee HG, et al. Identification of vaccinia virus epitope-specific HLA-A*0201-restricted T cells and comparative analysis of smallpox vaccines. Proc Natl Acad Sci U S A 2003;100:217-222.

Drillien R, Spehner D, Hanau D. Modified vaccinia virus Ankara induces moderate activation of human dendritic cells. J Gen Virol 2004;85:2167-2175.

Dunachie SJ, Walther M, Vuola JM, Webster DP, Keating SM, Berthoud T, Andrews L, et al. A clinical trial of prime-boost immunisation with the candidate malaria vaccines RTS,S/AS02A and MVA-CS. Vaccine 2006;24:2850-2859.

Dusheiko G. Side effects of alpha interferon in chronic hepatitis C. Hepatology 1997;26:112S-121S.

Engelke M, Mills K, Seitz S, Simon P, Gripon P, Schnolzer M, Urban S. Characterization of a hepatitis B and hepatitis delta virus receptor binding site. Hepatology 2006;43:750-760.

Foster GR, Germain C, Jones M, Lechler RI, Lombardi G. Human T cells elicit IFN-alpha secretion from dendritic cells following cell to cell interactions. Eur J Immunol 2000;30:3228-3235.

Foster WK, Miller DS, Marion PL, Colonno RJ, Kotlarski I, Jilbert AR. Entecavir therapy combined with DNA vaccination for persistent duck hepatitis B virus infection. Antimicrob Agents Chemother 2003;47:2624-2635.

Fourel G, Couturier J, Wei Y, Apiou F, Tiollais P, Buendia MA. Evidence for long-range oncogene activation by hepadnavirus insertion. EMBO J 1994;13:2526-2534.

Francis DP, Hadler SC, Thompson SE, Maynard JE, Ostrow DG, Altman N, Braff EH, et al. The prevention of hepatitis B with vaccine. Report of the centers for disease control multi-center efficacy trial among homosexual men. Ann Intern Med 1982;97:362-366.

French DL, Laskov R, Scharff MD. The role of somatic hypermutation in the generation of antibody diversity. Science 1989;244:1152-1157.

Gallegos AM, Bevan MJ. Central tolerance: good but imperfect. Immunol Rev 2006;209:290-296.

Ganem D, Prince AM. Hepatitis B virus infection--natural history and clinical consequences. N Engl J Med 2004;350:1118-1129.

Gerlich WH. Medical virology of hepatitis B: how it began and where we are now. Virol J 2013;10:239.

Glebe D, Urban S. Viral and cellular determinants involved in hepadnaviral entry. World J Gastroenterol 2007;13:22-38.

Glebe D, Urban S, Knoop EV, Cag N, Krass P, Grun S, Bulavaite A, et al. Mapping of the hepatitis B virus attachment site by use of infection-inhibiting preS1 lipopeptides and tupaia hepatocytes. Gastroenterology 2005;129:234-245.

Goonetilleke N, Moore S, Dally L, Winstone N, Cebere I, Mahmoud A, Pinheiro S, et al. Induction of multifunctional human immunodeficiency virus type 1 (HIV-1)-specific T cells capable of proliferation in healthy subjects by using a prime-boost regimen of DNA- and modified vaccinia virus Ankara-vectored vaccines expressing HIV-1 Gag coupled to CD8+ T-cell epitopes. J Virol 2006;80:4717-4728.

Gripon P, Cannie I, Urban S. Efficient inhibition of hepatitis B virus infection by acylated peptides derived from the large viral surface protein. J Virol 2005;79:1613-1622.

Guermonprez P, Valladeau J, Zitvogel L, Thery C, Amigorena S. Antigen presentation and T cell stimulation by dendritic cells. Annu Rev Immunol 2002;20:621-667.

Guidotti LG, Ando K, Hobbs MV, Ishikawa T, Runkel L, Schreiber RD, Chisari FV. Cytotoxic T lymphocytes inhibit hepatitis B virus gene expression by a noncytolytic mechanism in transgenic mice. Proc Natl Acad Sci U S A 1994;91:3764-3768.

Guidotti LG, Ishikawa T, Hobbs MV, Matzke B, Schreiber R, Chisari FV. Intracellular inactivation of the hepatitis B virus by cytotoxic T lymphocytes. Immunity 1996;4:25-36.

Guidotti LG, Matzke B, Schaller H, Chisari FV. High-level hepatitis B virus replication in transgenic mice. J Virol 1995;69:6158-6169.

Guner R, Karahocagil M, Buyukberber M, Kandemir O, Ural O, Usluer G, Inan D, et al. Correlation between intrahepatic hepatitis B virus cccDNA levels and other activity markers in patients with HBeAg-negative chronic hepatitis B infection. Eur J Gastroenterol Hepatol 2011;23:1185-1191.

Hadziyannis SJ, Papatheodoridis GV. Hepatitis B e antigen-negative chronic hepatitis B: natural history and treatment. Semin Liver Dis 2006;26:130-141.

Hamilton-Williams EE, Lang A, Benke D, Davey GM, Wiesmuller KH, Kurts C. Cutting edge: TLR ligands are not sufficient to break cross-tolerance to self-antigens. J Immunol 2005;174:1159-1163.

Harper MS, Barrett BS, Smith DS, Li SX, Gibbert K, Dittmer U, Hasenkrug KJ, et al. IFN-alpha treatment inhibits acute Friend retrovirus replication primarily through the antiviral effector molecule Apobec3. J Immunol 2013;190:1583-1590.

Hernandez J, Aung S, Redmond WL, Sherman LA. Phenotypic and functional analysis of CD8(+) T cells undergoing peripheral deletion in response to cross-presentation of self-antigen. J Exp Med 2001;194:707-717.

Huang LR, Gabel YA, Graf S, Arzberger S, Kurts C, Heikenwalder M, Knolle PA, et al. Transfer of HBV genomes using low doses of adenovirus vectors leads to persistent infection in immune competent mice. Gastroenterology 2012;142:1447-1450 e1443.

Jager A, Dardalhon V, Sobel RA, Bettelli E, Kuchroo VK. Th1, Th17, and Th9 effector cells induce experimental autoimmune encephalomyelitis with different pathological phenotypes. J Immunol 2009;183:7169-7177.

Jakob T, Walker PS, Krieg AM, Udey MC, Vogel JC. Activation of cutaneous dendritic cells by CpG-containing oligodeoxynucleotides: a role for dendritic cells in the augmentation of Th1 responses by immunostimulatory DNA. J Immunol 1998;161:3042-3049.

Kabanov VA. From synthetic polyelectrolytes to polymer-subunit vaccines. Review. Heidelberg, ALLEMAGNE: Springer, 2004: 20.

Kann M, Gerlich WH. Effect of core protein phosphorylation by protein kinase C on encapsidation of RNA within core particles of hepatitis B virus. J Virol 1994;68:7993-8000.

Kann M, Schmitz A, Rabe B. Intracellular transport of hepatitis B virus. World J Gastroenterol 2007;13:39-47.

Kann M, Sodeik B, Vlachou A, Gerlich WH, Helenius A. Phosphorylation-dependent binding of hepatitis B virus core particles to the nuclear pore complex. J Cell Biol 1999;145:45-55.

Kao JH, Wu NH, Chen PJ, Lai MY, Chen DS. Hepatitis B genotypes and the response to interferon therapy. J Hepatol 2000;33:998-1002.

Kastenmuller W, Drexler I, Ludwig H, Erfle V, Peschel C, Bernhard H, Sutter G. Infection of human dendritic cells with recombinant vaccinia virus MVA reveals general persistence of viral early transcription but distinct maturation-dependent cytopathogenicity. Virology 2006;350:276-288.

Katoh M, Tateno C, Yoshizato K, Yokoi T. Chimeric mice with humanized liver. Toxicology 2008;246:9-17.

Klaus GG, Pepys MB, Kitajima K, Askonas BA. Activation of mouse complement by different classes of mouse antibody. Immunology 1979;38:687-695.

Klinman DM. Adjuvant activity of CpG oligodeoxynucleotides. Int Rev Immunol 2006;25:135-154.

Klinman DM, Currie D, Gursel I, Verthelyi D. Use of CpG oligodeoxynucleotides as immune adjuvants. Immunol Rev 2004;199:201-216.

Kosinska AD, Zhang E, Johrden L, Liu J, Seiz PL, Zhang X, Ma Z, et al. Combination of DNA prime--adenovirus boost immunization with entecavir elicits sustained control of chronic hepatitis B in the woodchuck model. PLoS Pathog 2013;9:e1003391.

Kosinska AD, Zhang E, Lu M, Roggendorf M. Therapeutic vaccination in chronic hepatitis B: preclinical studies in the woodchuck. Hepat Res Treat 2010;2010:817580.

Krieg AM. CpG motifs in bacterial DNA and their immune effects. Annu Rev Immunol 2002;20:709-760.

Krug A, Towarowski A, Britsch S, Rothenfusser S, Hornung V, Bals R, Giese T, et al. Toll-like receptor expression reveals CpG DNA as a unique microbial stimulus for plasmacytoid dendritic cells which synergizes with CD40 ligand to induce high amounts of IL-12. Eur J Immunol 2001;31:3026-3037.

Kuhober A, Pudollek HP, Reifenberg K, Chisari FV, Schlicht HJ, Reimann J, Schirmbeck R. DNA immunization induces antibody and cytotoxic T cell responses to hepatitis B core antigen in H-2b mice. J Immunol 1996;156:3687-3695.

Kumar M, Satapathy S, Monga R, Das K, Hissar S, Pande C, Sharma BC, et al. A randomized controlled trial of lamivudine to treat acute hepatitis B. Hepatology 2007;45:97-101.

Kutscher S, Bauer T, Dembek C, Sprinzl M, Protzer U. Design of therapeutic vaccines: hepatitis B as an example. Microb Biotechnol 2012;5:270-282.

Lang T, Lo C, Skinner N, Locarnini S, Visvanathan K, Mansell A. The hepatitis B e antigen (HBeAg) targets and suppresses activation of the toll-like receptor signaling pathway. J Hepatol 2011;55:762-769.

Levrero M, Pollicino T, Petersen J, Belloni L, Raimondo G, Dandri M. Control of cccDNA function in hepatitis B virus infection. J Hepatol 2009;51:581-592.

Li N, Zhang L, Chen L, Feng W, Xu Y, Chen F, Liu X, et al. MxA inhibits hepatitis B virus replication by interaction with hepatitis B core antigen. Hepatology 2012;56:803-811.

Li YX, Gao QW, Zhang YH, Guo Y, Li BW, Wang HX, Wang YL, et al. [An investigation on the transmission routes and early diagnosis of intrauterine infection induced by hepatitis B virus]. Zhonghua Gan Zang Bing Za Zhi 2004;12:18-20.

Liang D, Hagenbuch B, Stieger B, Meier PJ. Parallel decrease of Na(+)-taurocholate cotransport and its encoding mRNA in primary cultures of rat hepatocytes. Hepatology 1993;18:1162-1166.

Liaw YF. Natural history of chronic hepatitis B virus infection and long-term outcome under treatment. Liver Int 2009;29 Suppl 1:100-107.

Lipford GB, Bauer M, Blank C, Reiter R, Wagner H, Heeg K. CpG-containing synthetic oligonucleotides promote B and cytotoxic T cell responses to protein antigen: a new class of vaccine adjuvants. Eur J Immunol 1997;27:2340-2344.

Liu L, Chavan R, Feinberg MB. Dendritic cells are preferentially targeted among hematolymphocytes by Modified Vaccinia Virus Ankara and play a key role in the induction of virus-specific T cell responses in vivo. BMC Immunol 2008;9:15.

Liu MA. DNA vaccines: an historical perspective and view to the future. Immunol Rev 2011;239:62-84.

Lok AS, McMahon BJ. Chronic hepatitis B: update 2009. Hepatology 2009;50:661-662.

Lucifora J, Arzberger S, Durantel D, Belloni L, Strubin M, Levrero M, Zoulim F, et al. Hepatitis B virus X protein is essential to initiate and maintain virus replication after infection. J Hepatol 2011;55:996-1003.

Lucifora J, Xia Y, Reisinger F, Zhang K, Stadler D, Cheng X, Sprinzl MF, et al. Specific and nonhepatotoxic degradation of nuclear hepatitis B virus cccDNA. Science 2014;343:1221-1228.

Lutsiak ME, Robinson DR, Coester C, Kwon GS, Samuel J. Analysis of poly(D,L-lactic-co-glycolic acid) nanosphere uptake by human dendritic cells and macrophages in vitro. Pharm Res 2002;19:1480-1487.

Lutwick LI, Robinson WS. DNA synthesized in the hepatitis B Dane particle DNA polymerase reaction. J Virol 1977;21:96-104.

Mancini-Bourgine M, Fontaine H, Brechot C, Pol S, Michel ML. Immunogenicity of a hepatitis B DNA vaccine administered to chronic HBV carriers. Vaccine 2006;24:4482-4489.

Mason WS, Cullen J, Moraleda G, Saputelli J, Aldrich CE, Miller DS, Tennant B, et al. Lamivudine therapy of WHV-infected woodchucks. Virology 1998;245:18-32.

Mason WS, Halpern MS, England JM, Seal G, Egan J, Coates L, Aldrich C, et al. Experimental transmission of duck hepatitis B virus. Virology 1983;131:375-384.

Mathis D, Benoist C. Levees of immunological tolerance. Nat Immunol 2010;11:3-6.

Mauss S, Berg T, Rockstroh J, Sarrazin C, Wedemeyer H. Hepatology 2013: A Clinical Textbook. 4th ed: Flying Publisher, 2013: 575.

McMahon BJ, Alward WL, Hall DB, Heyward WL, Bender TR, Francis DP, Maynard JE. Acute hepatitis B virus infection: relation of age to the clinical expression of disease and subsequent development of the carrier state. J Infect Dis 1985;151:599-603.

McNeal MM, Rae MN, Ward RL. Effects of different adjuvants on rotavirus antibody responses and protection in mice following intramuscular immunization with inactivated rotavirus. Vaccine 1999;17:1573-1580.

Mercer DF, Schiller DE, Elliott JF, Douglas DN, Hao C, Rinfret A, Addison WR, et al. Hepatitis C virus replication in mice with chimeric human livers. Nat Med 2001;7:927-933.

Meyer H, Sutter G, Mayr A. Mapping of deletions in the genome of the highly attenuated vaccinia virus MVA and their influence on virulence. J Gen Virol 1991;72 (Pt 5):1031-1038.

Michalak TI, Pasquinelli C, Guilhot S, Chisari FV. Hepatitis B virus persistence after recovery from acute viral hepatitis. J Clin Invest 1994;94:907.

Milich DR, Chen M, Schodel F, Peterson DL, Jones JE, Hughes JL. Role of B cells in antigen presentation of the hepatitis B core. Proc Natl Acad Sci U S A 1997;94:14648-14653.

Milich DR, Chen MK, Hughes JL, Jones JE. The secreted hepatitis B precore antigen can modulate the immune response to the nucleocapsid: a mechanism for persistence. J Immunol 1998;160:2013-2021.

Miyara M, Sakaguchi S. Natural regulatory T cells: mechanisms of suppression. Trends Mol Med 2007;13:108-116.

Moraleda G, Saputelli J, Aldrich CE, Averett D, Condreay L, Mason WS. Lack of effect of antiviral therapy in nondividing hepatocyte cultures on the closed circular DNA of woodchuck hepatitis virus. J Virol 1997;71:9392-9399.

Moss B. Genetically engineered poxviruses for recombinant gene expression, vaccination, and safety. Proc Natl Acad Sci U S A 1996;93:11341-11348.

Mowat AM. Anatomical basis of tolerance and immunity to intestinal antigens. Nat Rev Immunol 2003;3:331-341.

Mueller DL. Mechanisms maintaining peripheral tolerance. Nat Immunol 2010;11:21-27.

Murphy KP, Travers P, Walport M, Mowat A, Weaver CT. Janeway's Immunology. 8th ed. New York: Garland Science, 2011.

Mutwiri G, Benjamin P, Soita H, Babiuk LA. Co-administration of polyphosphazenes with CpG oligodeoxynucleotides strongly enhances immune responses in mice immunized with Hepatitis B virus surface antigen. Vaccine 2008;26:2680-2688.

Mutwiri G, Benjamin P, Soita H, Townsend H, Yost R, Roberts B, Andrianov AK, et al. Poly[di(sodium carboxylatoethylphenoxy)phosphazene] (PCEP) is a potent enhancer of mixed Th1/Th2 immune responses in mice immunized with influenza virus antigens. Vaccine 2007;25:1204-1213.

Nafa S, Ahmed S, Tavan D, Pichoud C, Berby F, Stuyver L, Johnson M, et al. Early detection of viral resistance by determination of hepatitis B virus polymerase mutations in patients treated by lamivudine for chronic hepatitis B. Hepatology 2000;32:1078-1088.

Nassal M. Hepatitis B viruses: reverse transcription a different way. Virus Res 2008;134:235-249.

Nayersina R, Fowler P, Guilhot S, Missale G, Cerny A, Schlicht HJ, Vitiello A, et al. HLA A2 restricted cytotoxic T lymphocyte responses to multiple hepatitis B surface antigen epitopes during hepatitis B virus infection. J Immunol 1993;150:4659-4671.

Nemazee D, Russell D, Arnold B, Haemmerling G, Allison J, Miller JF, Morahan G, et al. Clonal deletion of autospecific B lymphocytes. Immunol Rev 1991;122:117-132.

Newman KD, Elamanchili P, Kwon GS, Samuel J. Uptake of poly(D,L-lactic-co-glycolic acid) microspheres by antigen-presenting cells in vivo. J Biomed Mater Res 2002;60:480-486.

Nishimura H, Agata Y, Kawasaki A, Sato M, Imamura S, Minato N, Yagita H, et al. Developmentally regulated expression of the PD-1 protein on the surface of double-negative (CD4-CD8-) thymocytes. Int Immunol 1996;8:773-780.

Nurieva R, Thomas S, Nguyen T, Martin-Orozco N, Wang Y, Kaja MK, Yu XZ, et al. T-cell tolerance or function is determined by combinatorial costimulatory signals. EMBO J 2006;25:2623-2633.

Osmond DG. B cell development in the bone marrow. Semin Immunol 1990;2:173-180.

Park SG, Kim Y, Park E, Ryu HM, Jung G. Fidelity of hepatitis B virus polymerase. Eur J Biochem 2003;270:2929-2936.

Parker DC. T cell-dependent B cell activation. Annu Rev Immunol 1993;11:331-360.

Payne LG, Andrianov AK. Protein release from polyphosphazene matrices. Adv Drug Deliv Rev 1998;31:185-196.

Payne LG, Van Nest G, Barchfeld GL, Siber GR, Gupta RK, Jenkins SA. PCPP as a parenteral adjuvant for diverse antigens. Dev Biol Stand 1998;92:79-87.

Pichoud C, Seigneres B, Wang Z, Trepo C, Zoulim F. Transient selection of a hepatitis B virus polymerase gene mutant associated with a decreased replication capacity and famciclovir resistance. Hepatology 1999;29:230-237.

Rabe B, Glebe D, Kann M. Lipid-mediated introduction of hepatitis B virus capsids into nonsusceptible cells allows highly efficient replication and facilitates the study of early infection events. J Virol 2006;80:5465-5473.

Ramirez JC, Gherardi MM, Esteban M. Biology of attenuated modified vaccinia virus Ankara recombinant vector in mice: virus fate and activation of B- and T-cell immune responses in comparison with the Western Reserve strain and advantages as a vaccine. J Virol 2000;74:923-933.

Ramlau R, Quoix E, Rolski J, Pless M, Lena H, Levy E, Krzakowski M, et al. A phase II study of Tg4010 (Mva-Muc1-Il2) in association with chemotherapy in patients with stage III/IV Non-small cell lung cancer. J Thorac Oncol 2008;3:735-744.

Ramshaw IA, Ramsay AJ. The prime-boost strategy: exciting prospects for improved vaccination. Immunol Today 2000;21:163-165.

Rantala M, van de Laar MJ. Surveillance and epidemiology of hepatitis B and C in Europe - a review. Euro Surveill 2008;13.

Redmond WL, Sherman LA. Peripheral tolerance of CD8 T lymphocytes. Immunity 2005;22:275-284.

Rehermann B, Nascimbeni M. Immunology of hepatitis B virus and hepatitis C virus infection. 2005;5:215-229.

Rehermann B, Nascimbeni M. Immunology of hepatitis B virus and hepatitis C virus infection. Nat Rev Immunol 2005;5:215-229.

Rippin SJ, Hagenbuch B, Meier PJ, Stieger B. Cholestatic expression pattern of sinusoidal and canalicular organic anion transport systems in primary cultured rat hepatocytes. Hepatology 2001;33:776-782.

Rouse BT, Sarangi PP, Suvas S. Regulatory T cells in virus infections. Immunol Rev 2006;212:272-286.

Russell JH, Ley TJ. Lymphocyte-mediated cytotoxicity. Annu Rev Immunol 2002;20:323-370.

Schaefer S. Hepatitis B virus taxonomy and hepatitis B virus genotypes. World J Gastroenterol 2007;13:14-21.

Schietinger A, Delrow JJ, Basom RS, Blattman JN, Greenberg PD. Rescued tolerant CD8 T cells are preprogrammed to reestablish the tolerant state. Science 2012;335:723-727.

Schildgen O, Roggendorf M, Lu M. Identification of a glycosylation site in the woodchuck hepatitis virus preS2 protein and its role in protein trafficking. J Gen Virol 2004;85:787-793.

Schirmbeck R, Bohm W, Fissolo N, Melber K, Reimann J. Different immunogenicity of H-2 Kb-restricted epitopes in natural variants of the hepatitis B surface antigen. Eur J Immunol 2003;33:2429-2438.

Schmitt S, Glebe D, Tolle TK, Lochnit G, Linder D, Geyer R, Gerlich WH. Structure of pre-S2 N- and O-linked glycans in surface proteins from different genotypes of hepatitis B virus. J Gen Virol 2004;85:2045-2053.

Schmitz A, Schwarz A, Foss M, Zhou L, Rabe B, Hoellenriegel J, Stoeber M, et al. Nucleoporin 153 arrests the nuclear import of hepatitis B virus capsids in the nuclear basket. PLoS Pathog 2010;6:e1000741.

Schulze A, Gripon P, Urban S. Hepatitis B virus infection initiates with a large surface protein-dependent binding to heparan sulfate proteoglycans. Hepatology 2007;46:1759-1768.

Schulze A, Mills K, Weiss TS, Urban S. Hepatocyte polarization is essential for the productive entry of the hepatitis B virus. Hepatology 2012;55:373-383.

Schulze A, Schieck A, Ni Y, Mier W, Urban S. Fine mapping of pre-S sequence requirements for hepatitis B virus large envelope protein-mediated receptor interaction. J Virol 2010;84:1989-2000.

Seeger C, Ganem D, Varmus HE. Biochemical and genetic evidence for the hepatitis B virus replication strategy. Science 1986;232:477-484.

Seeger C, Mason WS. Hepatitis B virus biology. Microbiol Mol Biol Rev 2000;64:51-68.

Seigneres B, Pichoud C, Ahmed SS, Hantz O, Trepo C, Zoulim F. Evolution of hepatitis B virus polymerase gene sequence during famciclovir therapy for chronic hepatitis B. J Infect Dis 2000;181:1221-1233.

Sparwasser T, Koch ES, Vabulas RM, Heeg K, Lipford GB, Ellwart JW, Wagner H. Bacterial DNA and immunostimulatory CpG oligonucleotides trigger maturation and activation of murine dendritic cells. Eur J Immunol 1998;28:2045-2054.

Sprinzl MF, Oberwinkler H, Schaller H, Protzer U. Transfer of hepatitis B virus genome by adenovirus vectors into cultured cells and mice: crossing the species barrier. J Virol 2001;75:5108-5118.

Stacey KJ, Sweet MJ, Hume DA. Macrophages ingest and are activated by bacterial DNA. J Immunol 1996;157:2116-2122.

Staib C, Sutter G. Live viral vectors: vaccinia virus. Methods Mol Med 2003;87:51-68.

Steinman RM, Hawiger D, Nussenzweig MC. Tolerogenic dendritic cells. Annu Rev Immunol 2003;21:685-711.

Stieger B, Hagenbuch B, Landmann L, Hochli M, Schroeder A, Meier PJ. In situ localization of the hepatocytic Na+/Taurocholate cotransporting polypeptide in rat liver. Gastroenterology 1994;107:1781-1787.

Summers J. The replication cycle of hepatitis B viruses. Cancer 1988;61:1957-1962.

Summers J, Smolec JM, Snyder R. A virus similar to human hepatitis B virus associated with hepatitis and hepatoma in woodchucks. Proc Natl Acad Sci U S A 1978;75:4533-4537.

Sun S, Zhang X, Tough DF, Sprent J. Type I interferon-mediated stimulation of T cells by CpG DNA. J Exp Med 1998;188:2335-2342.

Suspene R, Guetard D, Henry M, Sommer P, Wain-Hobson S, Vartanian JP. Extensive editing of both hepatitis B virus DNA strands by APOBEC3 cytidine deaminases in vitro and in vivo. Proc Natl Acad Sci U S A 2005;102:8321-8326.

Sutter G, Moss B. Nonreplicating vaccinia vector efficiently expresses recombinant genes. Proc Natl Acad Sci U S A 1992;89:10847-10851.

Takeda K, Akira S. Toll-like receptors. Curr Protoc Immunol 2007;Chapter 14:Unit 14 12.

Takeuchi O, Akira S. Pattern recognition receptors and inflammation. Cell 2010;140:805-820.

Tassopoulos NC, Koutelou MG, Polychronaki H, Paraloglou-Ioannides M, Hadziyannis SJ. Recombinant interferon-alpha therapy for acute hepatitis B: a randomized, double-blind, placebo-controlled trial. J Viral Hepat 1997;4:387-394.

Thomson AW, Knolle PA. Antigen-presenting cell function in the tolerogenic liver environment. Nat Rev Immunol 2010;10:753-766.

Trinchieri G, Sher A. Cooperation of Toll-like receptor signals in innate immune defence. Nat Rev Immunol 2007;7:179-190.

Tscharke DC, Karupiah G, Zhou J, Palmore T, Irvine KR, Haeryfar SM, Williams S, et al. Identification of poxvirus CD8+ T cell determinants to enable rational design and characterization of smallpox vaccines. J Exp Med 2005;201:95-104.

Turelli P, Liagre-Quazzola A, Mangeat B, Verp S, Jost S, Trono D. APOBEC3-independent interferon-induced viral clearance in hepatitis B virus transgenic mice. J Virol 2008;82:6585-6590.

Urban S, Schulze A, Dandri M, Petersen J. The replication cycle of hepatitis B virus. J Hepatol 2010;52:282-284.

Vandepapeliere P, Lau GK, Leroux-Roels G, Horsmans Y, Gane E, Tawandee T, Merican MI, et al. Therapeutic vaccination of chronic hepatitis B patients with virus suppression by antiviral therapy: a randomized, controlled study of co-administration of HBsAg/AS02 candidate vaccine and lamivudine. Vaccine 2007;25:8585-8597.

Vanlandschoot P, Leroux-Roels G. The role of heparan sulfate and TLR2 in cytokine induction by hepatitis B virus capsids. J Immunol 2005;175:6253; author reply 6253-6255.

Vartanian JP, Henry M, Marchio A, Suspene R, Aynaud MM, Guetard D, Cervantes-Gonzalez M, et al. Massive APOBEC3 editing of hepatitis B viral DNA in cirrhosis. PLoS Pathog 2010;6:e1000928.

Vignali DA, Collison LW, Workman CJ. How regulatory T cells work. Nat Rev Immunol 2008;8:523-532.

Visvanathan K, Lewin SR. Immunopathogenesis: role of innate and adaptive immune responses. Semin Liver Dis 2006;26:104-115.

von Boehmer H. Developmental biology of T cells in T cell-receptor transgenic mice. Annu Rev Immunol 1990;8:531-556.

von Boehmer H. Mechanisms of suppression by suppressor T cells. Nat Immunol 2005;6:338-344.

von Freyend MJ, Untergasser A, Arzberger S, Oberwinkler H, Drebber U, Schirmacher P, Protzer U. Sequential control of hepatitis B virus in a mouse model of acute, self-resolving hepatitis B. J Viral Hepat 2011;18:216-226.

Westland CE, Yang H, Delaney WEt, Gibbs CS, Miller MD, Wulfsohn M, Fry J, et al. Week 48 resistance surveillance in two phase 3 clinical studies of adefovir dipivoxil for chronic hepatitis B. Hepatology 2003;38:96-103.

Wong DK, Cheung AM, O'Rourke K, Naylor CD, Detsky AS, Heathcote J. Effect of alpha-interferon treatment in patients with hepatitis B e antigen-positive chronic hepatitis B. A meta-analysis. Ann Intern Med 1993;119:312-323.

Woodland DL. Jump-starting the immune system: prime-boosting comes of age. Trends Immunol 2004;25:98-104.

Wu JY, Wade WF, Taylor RK. Evaluation of cholera vaccines formulated with toxin-coregulated pilin peptide plus polymer adjuvant in mice. Infect Immun 2001;69:7695-7702.

Wyatt LS, Earl PL, Eller LA, Moss B. Highly attenuated smallpox vaccine protects mice with and without immune deficiencies against pathogenic vaccinia virus challenge. Proc Natl Acad Sci U S A 2004;101:4590-4595.

Xu DZ, Wang XY, Shen XL, Gong GZ, Ren H, Guo LM, Sun AM, et al. Results of a phase III clinical trial with an HBsAg-HBIG immunogenic complex therapeutic vaccine for chronic hepatitis B patients: experiences and findings. J Hepatol 2013;59:450-456.

Xu R, Zhang X, Zhang W, Fang Y, Zheng S, Yu XF. Association of human APOBEC3 cytidine deaminases with the generation of hepatitis virus B x antigen mutants and hepatocellular carcinoma. Hepatology 2007;46:1810-1820.

Yamazaki T, Akiba H, Iwai H, Matsuda H, Aoki M, Tanno Y, Shin T, et al. Expression of programmed death 1 ligands by murine T cells and APC. J Immunol 2002;169:5538-5545.

Yan H, Zhong G, Xu G, He W, Jing Z, Gao Z, Huang Y, et al. Sodium taurocholate cotransporting polypeptide is a functional receptor for human hepatitis B and D virus. Elife 2012;1:e00049.

Yang PL, Althage A, Chung J, Chisari FV. Hydrodynamic injection of viral DNA: a mouse model of acute hepatitis B virus infection. Proc Natl Acad Sci U S A 2002;99:13825-13830.

Yotsuyanagi H, Yasuda K, Iino S, Moriya K, Shintani Y, Fujie H, Tsutsumi T, et al. Persistent viremia after recovery from self-limited acute hepatitis B. Hepatology 1998;27:1377-1382.

Yu JW, Sun LJ, Zhao YH, Kang P, Li SC. The study of efficacy of lamivudine in patients with severe acute hepatitis B. Dig Dis Sci 2010;55:775-783.

Zehn D, Bevan MJ. T cells with low avidity for a tissue-restricted antigen routinely evade central and peripheral tolerance and cause autoimmunity. Immunity 2006;25:261-270.

Zhang X, Zoulim F, Habersetzer F, Xiong S, Trepo C. Analysis of hepatitis B virus genotypes and pre-core region variability during interferon treatment of HBe antigen negative chronic hepatitis B. J Med Virol 1996;48:8-16.

Zhang Y, Li S, Shan M, Pan X, Zhuang K, He L, Gould K, et al. Hepatitis B virus core antigen epitopes presented by HLA-A2 single-chain trimers induce functional epitope-specific CD8+ T-cell responses in HLA-A2.1/Kb transgenic mice. Immunology 2007;121:105-112.

Zhang Z, Zhang JY, Wang LF, Wang FS. Immunopathogenesis and prognostic immune markers of chronic hepatitis B virus infection. J Gastroenterol Hepatol 2012;27:223-230.

Zhong X, Tumang JR, Gao W, Bai C, Rothstein TL. PD-L2 expression extends beyond dendritic cells/macrophages to B1 cells enriched for V(H)11/V(H)12 and phosphatidylcholine binding. Eur J Immunol 2007;37:2405-2410.

Zoulim F. Mechanism of viral persistence and resistance to nucleoside and nucleotide analogs in chronic hepatitis B virus infection. Antiviral Res 2004;64:1-15.

Zoulim F, Saputelli J, Seeger C. Woodchuck hepatitis virus X protein is required for viral infection in vivo. J Virol 1994;68:2026-2030.

Zoulim F, Seeger C. Reverse transcription in hepatitis B viruses is primed by a tyrosine residue of the polymerase. J Virol 1994;68:6-13.

Danksagung

- Mein besonderer Dank gilt Frau Prof. Dr. Ulrike Protzer für die Möglichkeit von der Pflanzenphysiologie in die Virologie zu wechseln um an diesem spannenden Thema zu arbeiten. Das entgegengebrachte Vertrauen und die Freiheiten bei der Entwicklung des Projektes haben mir es leicht gemacht, mich bei der Arbeit wohl zu fühlen. Darüber hinaus möchte ich mich für die anregenden Diskussionen und die Unterstützung zur Teilnahme an internationalen Kongressen bedanken. Mir haben die gemeinsamen Aktivitäten wie Skifahren, die Teilnahme an den Drachenbootrennen oder Wanderungen sehr viel Spaß gemacht. Des Weiteren bedanke ich mich für die finanzielle Unterstützung unserer Fußballmannschaft „Virogoal“, die in den letzten Jahren einige Pokale an das Institut gebracht hat.

- Ich bedanke mich bei Herrn Prof. Dr. Jörg Durner für die offizielle Begutachtung meiner Arbeit und die angenehmen Diskussionen im Rahmen des „Thesis Committee Meetings“.

- Mein Dank geht auch an Frau Dr. Tanja Bauer für ihren Beitrag als Mitglied meines „Thesis Committes“ und für die Zusammenarbeit speziell bei der Erstellung des Tierversuchsantrags.

- Großer Dank gilt auch meinem Kooperationspartner Herr Dr. George Mutwiri für die Bereitstellung und Informationen über das Adjuvans PCEP, welches dieser Arbeit gerade zu Beginn einen entscheidenden Impuls gegeben hat.

- Ein ganz großes Dankeschön geht an meine Arbeitskollegen und Freunde in den Arbeitsgruppen von Frau Prof. Ulrike Protzer, Herrn Prof. Dr. Ingo Drexler, Herrn Prof. Dr. Mathias Heikenwälder und des Immunmonitorings für die tolle Unterstützung und die super Arbeitsatmosphäre.

- Im Besonderen möchte ich hier Frau Dr. Simone Backes für all ihre Hilfe und Expertise danken. Ohne den zweimonatigen Crashkurs in immunologischen Methoden bei meiner Ankunft, die hervorragende Arbeit und den Aufwand der in das Projekt gesteckt wurde sowie die gute Zusammenarbeit bei der Erstellung des Manuskripts, wäre es mir nicht möglich gewesen diese Erfolge zu feiern.

❖ Ein spezieller Dank geht auch an Frau Dr. Claudia Dembek, für die angenehme Zusammenarbeit (Rheinbio haben wir gerockt), die Korrektur dieser Arbeit und die lustigen Gespräche nicht nur im Labor. An Herrn Andreas Muschaweckh, für all die Diskussionen und Gespräche, die privaten Aktionen (FC Blutgrätscher), aber auch die Hilfe insbesondere am Anfang im Labor und die Korrektur dieser Dissertation. Unser Büro war schon sehr cool! Herrn. Dr. Martin Mück-Häusl möchte ich auch sehr danken für die gute Zeit im Labor, die Korrektur dieses Schriftstücks trotz Umzugs und Vorbereitung auf das Vatersein und in Verbindung mit Dr. Frank Thiele für die Sessions am Kicker. War immer sehr lustig! An Herrn Dr. Marc Ringelhan und Herrn Dr. Thomas Michler für ihre Hilfe vor allem mit den Transportfahrten. Für den letzten Schubs und vieles Weitere möchte ich mich herzlich bei Frau Dr. Katrin Singethan bedanken.

❖ Nicht zuletzt möchte ich mich ganz herzlich bei meinen Freunden und meiner Familie bedanken. Viel Arbeit erfordert auch einen guten Ausgleich und Ablenkung, die ich dank euch zu jederzeit haben konnte. Meinen Eltern möchte ich hier zusätzlich ganz besonders für all die bedingungslose Unterstützung und ihr Vertrauen in mich danken. Ihr seid die Besten!